ICIP2018

International Conference on Ionizing Processes

July 22-27, 2018
Loews Annapolis Hotel

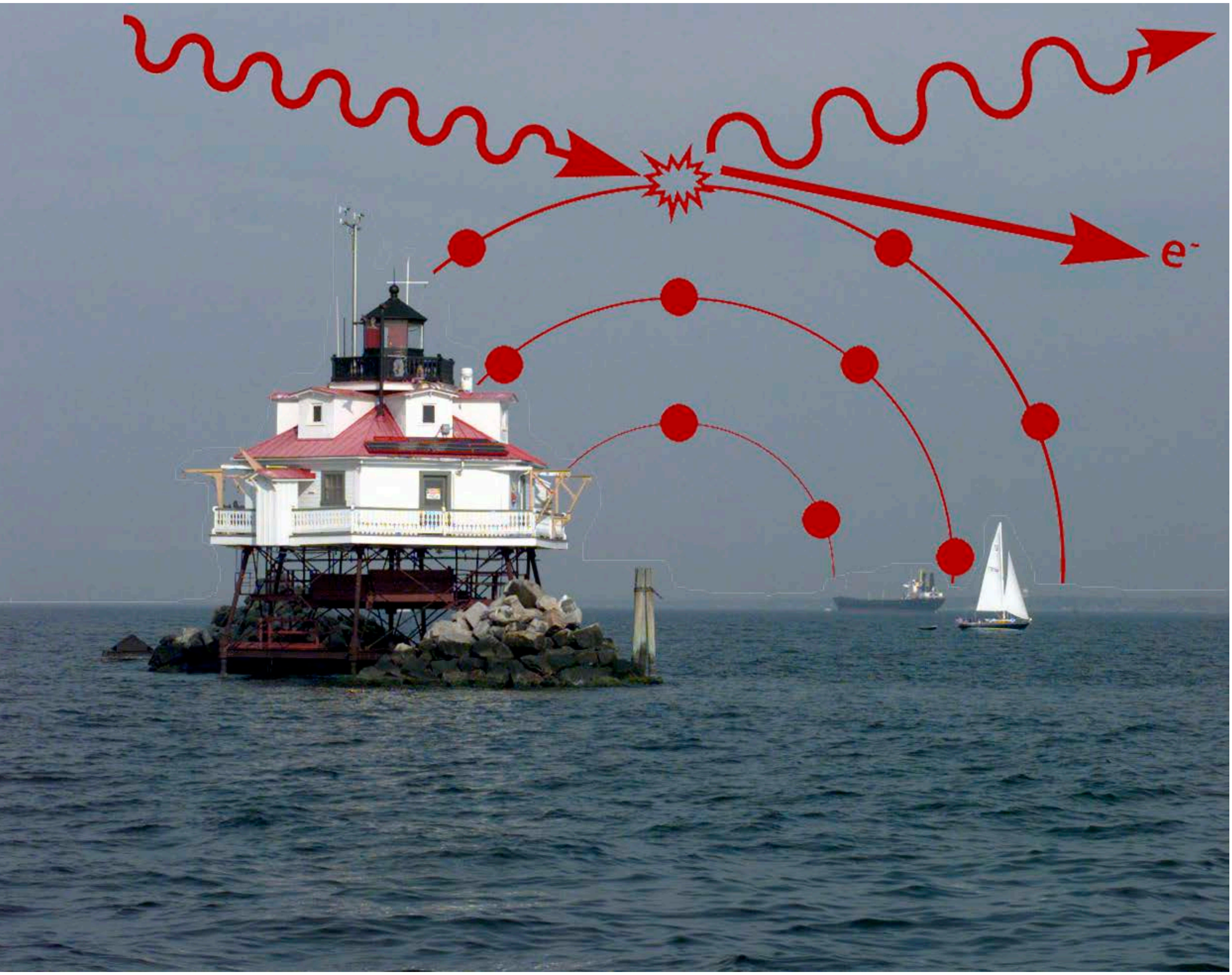

UNIVERSITY OF
MARYLAND

2nd International Conference on Ionizing Processes

ICIP-2018

July 22-27, 2018

University of Maryland, College Park, Maryland and Loews Annapolis Hotel, Annapolis, Maryland

Mohamad Al-Sheikhly, Chair

Contents

Information.. 5
Condensed Schedule 6
Conference Schedule Outline 9
List of Posters 10
Talk Abstracts 13
Poster Abstracts... 83
List of Participants 112

Website: https://icip2018.umd.edu

Organizing Committee

Mohamad Al-Sheikhly, Chair	Dianne Poster
Lisa Press	Jay LaVerne
Travis Dietz	Ileana Pazos
James Wishart	Mark Driscoll

Acknowledgements

The organizers would like to thank the members of the Local Organizing Committee and the staff of the University of Maryland Conferences and Visitor Services, including Kelly Marie Hedgepeth for her assistance in setting up the registration website. They would also like to thank the staff of the Loews Annapolis Hotel.

The organizers would finally like to extend their thanks to the U.S. Department of Energy for their staunch support of the ICIP2018 young investigator awards, as well as to Abbott Vascular, Johnson & Johnson, Nordion Inc., and the Bruker Corporation for their financial support of ICIP2018.

2nd International Conference on
Ionizing Processes
ICIP 2018

Annapolis, Maryland, USA
July 22 – 27, 2018

Steering Committee Members

James Wishart - Chair
Brookhaven National Laboratory
Mohamad Al-Sheikhly
University of Maryland (UMD) -
Chair ICIP 2018
David Bartels
University of Notre Dame
Anthony Berejka
Ionicorp
Ian Carmichael
University of Notre Dame
Jay LaVerne
University of Notre Dame (UND)
John Miller
Department of Energy
Dianne Poster
National Institute of Standards and Technology (NIST)
Christian Schöneich
University of Kansas

Organizing Committee

Mohamad Al-Sheikhly
UMD
Mark Driscoll
State University of New York
Jay LaVerne
UND
Dianne Poster
NIST
Ileana Pazos
NIST
James Wishart
Brookhaven National Laboratory

LABORATORY FOR RADIATION AND POLYMER SCIENCE
DEPARTMENT OF MATERIALS SCIENCE AND ENGINEERING
A. J. CLARK SCHOOL OF ENGINEERING
UNIVERSITY OF MARYLAND
COLLEGE PARK, MD 20742-2115
TEL: (301) 405-5214
FAX: (301) 314-2029

July 16th, 2018

Dear Participants,

On behalf of the organizing and steering committees, and the University of Maryland, it is my honor and pleasure to welcome you to the 2nd International Conference on Ionizing Processes, ICIP2018. For the next five days, we will be learning and discussing challenges and advanced topics in radiation chemistry and its applications. ICIP provides a great opportunity for our radiation chemistry community to build strong ties between the fundamentals of radiation chemistry and its applications in medicine, space, nuclear, and advanced technologies.

It is always good to remind ourselves that the essential ingredient of success is continuity. With this in mind, ICIP2018 is a continuation of the first ICIP, which was held in 2016 in Brookhaven National Laboratory (BNL). ICIP2016 was indeed a great success organized by my colleague and friend Dr. James Wishart of BNL. In this spirit of continuity in the field of radiation chemistry, we have awarded 26 young investigator awards to candidates from all over the world who represent the bright future of our field.

Together we will learn about new findings and theories on radiation chemistry from 52 invited talks. The topics of these talks range from the fundamental radiation chemistry of the kinetics of formation and decay of anions, cations, and free radicals, to the applications of radiation in nano-synthesis, modification of polymers, and environmental remediation. The talks also include presentations on nuclear systems and the radiation chemistry of biological systems.

On behalf of the organizing and steering committees, I would like to express my thanks and appreciation to Dr. Christopher Fecko of the United States Department of Energy for his staunch support of the ICIP2018 young investigator awards.

I would also like to take the opportunity to thank my colleagues who dedicated themselves from the beginning to ensuring the scientific success of ICIP2018. I am especially indebted to Dr. Travis Dietz of University of Maryland. Dr. Dietz has worked tirelessly on every aspect of the conference. I am also indebted to Dr. Jay LaVerne of Notre Dame Radiation Laboratory for his outstanding leadership on the young investigator awards and the DOE proposal to support ICIP2018. Special thanks should also go to Dr. James Wishart and Professor Mark Driscoll. I would also like to thank my friends and colleagues Dr. Byron Lambert and Mr. John Logar for their financial sponsorships of ICIP2018 through Abbott Vascular and Johnson & Johnson, respectively. Thanks, are also due to Nordion and Bruker for their financial support to ICIP2018. Last but certainly not least, I would like to thank Ms. Lisa Press of University of Maryland for her outstanding administrative care and hard work on the logistics of the conference.

Finally, I wish you all a pleasant and wonderful time over the next five days in one of the first capital cities of the United States, the beautiful Annapolis.

Sincerely,

Alsheikhly

Mohamad Al-Sheikhly
Professor
Department of Materials Science and Engineering
University of Maryland
Chair, ICIP 2018
Member, ICIP Steering Committee

Information

Registration Check-in
A check-in desk for meeting registration and other details will be available at the Loews Annapolis Hotel in the Atrium of the Loews Annapolis Hotel.

Invited Talks
All presenters are kindly reminded to respect the 25 minute presentation time + 5 minutes for questions. A computer will be available in the conference room. The authors are invited to prepare their talk as a pdf format, when possible, to avoid formatting errors. All invited talks will be presented in Salon AB in the Loews Annapolis Hotel.

Poster Sessions
Three poster sessions are scheduled, on Tuesday, July 24th at 2 pm, Wednesday, July 25th at 3:45 pm, and Thursday, July 26th at 4 pm. Each poster should be displayed on a poster board. All poster sessions will be hosted in Salon C in the Loews Annapolis Hotel.

Lunches
The lunches are no-host. The BAROAK Cookhouse & Taproom is located in the hotel and will be offering lunch and dinner. There are also a number of restaurants located in downtown Annapolis available for dining.

Dinners
All dinners are no-host, excluding the Welcome Reception on Sunday, July 22nd at 6 pm which will offer a selection of food stations and the Banquet Dinner on Thursday, July 26th at 6 pm at Buddy's Crabs & Ribs.

Evening conviviality
The BAROAK Cookhouse & Taproom is located in the hotel. The bar is open until midnight during all nights of the conference.

2nd International Conference on Ionizing Processes (ICIP-2018)

Loews Annapolis Hotel, Annapolis, Maryland

July 22-27, 2018

Condensed Schedule

Sunday:	12:00pm	Airport Shuttle will depart local airports (Baltimore-Washington International Thurgood Marshall Airport, Washington Dulles International Airport, Ronald Reagan Washington National Airport) (IAD,DCA,BWI)[1]
	3:00pm	Airport Shuttle will depart local airports (Baltimore-Washington International Thurgood Marshall Airport, Washington Dulles International Airport, Ronald Reagan Washington National Airport) (IAD,DCA,BWI) [1]
	3:00pm-8:00pm	Registration
	6:00pm-8:00pm	Welcome Reception
	8:00pm-9:00pm	Lecture Session: 25 min. presentations with 5 min. discussion – **Session 1: Fundamental Processes (1)**
Monday:	7:00am-8:00am	Breakfast
	8:00am-10:00am	Lecture Session: 25 min. presentations with 5 min. discussion – **Session 2: Fundamental Processes (2)**
	10:00am-10:15am	Break
	10:15am-12:15pm	Lecture Session: 25 min. presentations with 5 min. discussion – **Session 3: Fundamental Processes (3)**
	12:15pm-2:00pm	Lunch on your own
	2:00pm-3:30pm	Free Time
	3:30pm-3:45pm	Break
	3:45pm-6:00pm	Lecture Session: 25 min. presentations with 5 min. discussion – **Session 4: Interfaces and Nuclear Applications**
	6:00pm-8:00pm	Dinner on your own
Tuesday:	7:00am-8:00am	Breakfast
	8:00am-10:00am	Lecture Session: 25 min. presentations with 5 min. discussion – **Session 5: Radiation Chemistry in Service of Energy Applications**
	10:00am-10:15am	Break
	10:15am-12:15pm	Lecture Session: 25 min. presentations with 5 min. discussion – **Session 6: Consequences of Highly Mobile Transient Species**

---

[1] Details with pickup locations will be provided to attendees who register for the airport shuttles.

	12:15pm-2:00pm	Lunch on your own
	2:00pm-3:30pm	Poster Session
	3:30pm-3:45pm	Break
	3:45pm-6:00pm	Young Investigators Presentations: 15 min. Presentation with 5min. discussion
	6:00pm-8:00pm	Dinner on your own

Wednesday:	7:00am-8:00am	Breakfast
	8:00am-10:00am	Lecture Session: 25 min. presentations with 5 min. discussion – **Session 7: Synthesis of Materials With Radiation**
	10:00am-10:15am	Break
	10:15am-12:15pm	Young Investigators Presentations: 15 min. Presentation with 5min. discussion
	12:15pm-2:00pm	Lunch on your own
	2:00pm-3:30pm	Lecture Session: 25 min. presentations with 5 min. discussion – **Session 8: Advances in Methods and their Applications (1)**
	3:30pm-3:45pm	Break
	3:45pm-6:00pm	Poster Session
	6:00pm-8:00pm	Dinner on your own

Thursday:	7:00am-8:00am	Breakfast
	8:00am-10:00am	Lecture Session: 25 min. presentations with 5 min. discussion – **Session 9: Advances in Methods and their Applications (2)**
	10:00am-10:15am	Break
	10:15am-12:15pm	Lecture Session: 25 min. presentations with 5 min. discussion – **Session 10: Advances in Methods and their Applications (3)**
	12:15pm-2:00pm	Lunch on your own
	2:00pm-4:00pm	Lecture Session: 25 min. presentations with 5 min. discussion – **Session 11: Radiation Effects on Biological Systems (1)**
	4:00pm-5:40pm	Break and Poster Session
	4:15pm-4:45pm	ICIP Business Meeting
	5:40pm-6:00pm	Proceed to Buddy's for the Banquet
	6:00pm-8:00pm	Banquet Dinner (provided)

Friday:	8:00am-9:00am	Breakfast
	9:00am-10:00am	Lecture Session: 25 min. presentations with 5 min. discussion – **Session 12: Radiation Effects on Biological Systems (2)**
	10:00am-10:15am	Break
	10:15am-12:15pm	**Closing Remarks**

1:00pm	Airport shuttle departs to Washington Dulles International Airport (IAD)
1:15pm	Airport shuttle departs to Ronald Reagan Washington National Airport (DCA)
1:30pm	Airport shuttle departs to Baltimore-Washington International Thurgood Marshall Airport (BWI)
3:00pm	Airport shuttle departs to Washington Dulles International Airport (IAD)
3:15pm	Airport shuttle departs to Ronald Reagan Washington National Airport (DCA)
3:30pm	Airport shuttle departs to Baltimore-Washington International Thurgood Marshall Airport (BWI)

Conference Schedule Outline

	Sunday, July 22nd	Monday, July 23rd	Tuesday, July 24th	Wednesday, July 25th	Thursday, July 26th	Friday, July 27th
07:00		Breakfast	Breakfast	Breakfast	Breakfast	
07:15						
07:30						
07:45						
08:00		S. Mezyk (p.18)	M.E. Toimil-Molares (p.33)	D. Demaree (p.50)	A. Chmielewski (p.64)	Breakfast
08:15						
08:30		B. Dromey (p.20)	D. Guldi (p.34)	M. Nasef (p.51)	C. Howard (p.66)	
08:45						
09:00		S. Le Caër (p.21)	G. Horne (p.35)	J. Rojas (p.53)	J. Robertson (p.67)	K. Bobrowski (p.79)
09:15						
09:30		D. Meyerstein (p.23)	D. Grills (p.37)		T. Woehl (p.68)	A. Adhikary (p.81)
09:45						
10:00		Coffee break	Coffee break	Coffee break	Coffee break	Coffee break
10:15		X. Coqueret (p.24)	J. Miller (p.39)	Young Investigator Presentations 2 (p.55-61)	K. Morehouse (p.69)	Closing Remarks
10:30						
10:45		G. Varca (p. 26)	Y. Yoshida (p.41)		F. Bateman (p.70)	
11:00						
11:15		B. Schwartz (p.27)	S. Goldstein (p.42)		D. Peterman (p.71)	
11:30						
11:45			F. Currell (p.43)		M. Bird (p.72)	
12:00						
12:15		Lunch on your own	Lunch on your own	Lunch on your own	Lunch on your own	
12:30						
12:45						
13:00						Airport Shuttle Departs for IAD
13:15						Airport Shuttle Departs for DCA
13:30						Airport Shuttle Departs for BWI
13:45						
14:00		Free Time	Poster Session (p.84-110)	R. Livingston (p.62)	C. Schoneich (p.73)	
14:15						
14:30				F. Tang	D. Becker (p.74)	
14:45						
15:00	Registration (will be open through Monday)			R. Tosh (p.63)	Y. Berlin (p.76)	Airport Shuttle Departs for IAD
15:15						Airport Shuttle Departs for DCA
15:30		Coffee break	Coffee break	Coffee break	M. Mostafavi (p.77)	Airport Shuttle Departs for BWI
15:45		S. Maloy (p.28)	Young Investigator Presentations 1 (p.44-49)	Poster Session (p.84-110)		
16:00					Coffee break	
16:15		J. Weaver (p.29)			ICIP Business Meeting	
16:30						
16:45		E. Karim (p.30)			Poster Session (p.84-110)	
17:00						
17:15		N. Guardala (p.31)				
17:30					Proceed to Buddy's for the Banquet	
17:45						
18:00	Welcome Reception	Dinner on your own	Dinner on your own	Dinner on your own	Banquet Dinner at Buddy's (provided)	
18:15						
18:30						
18:45						
19:00						
19:15						
19:30						
19:45						
20:00	D. Bartels (p.14)					
20:15						
20:30	A. Forster (p.16)					
20:45						

Fundamental Processes	Radiation Chemistry in Service of Energy Applications	Synthesis of Materials with Radiation	Radiation Effects on Biological Systems
Interfaces and Nuclear Applications	Consequences of Highly Mobile Transient Species	Advances in Methods and their Applications	

List of Posters

1 **5-Azido-Modified Pyrimidine Nucleosides: Electron Mediated Formation Of Π-Type Aminyl Radical And Its Conversion To Σ-Type Iminyl Radical**
Zhiwei Wen, Jufang Peng, Paloma Tuttle, Dipra Debnath, Sunny Rishi, Cameron Hanson, Samuel Ward, Yaou Ren, Carol Garcia, Yuan Liu, Yanfeng Liu, Weixi Zhao, Peter M. Glazer, Anil Kumar, Michael D. Sevilla, Stanislaw F. Wnuk, and Amitava Adhikary

2 **Radiolytic Degradation Of 2,4-Dichlorophenol And Chemical Oxygen Demand Determination**
Guadalupe Albarrán and Edith Mendoza

3 **ESR Studies Of Gamma Radiation And Microwave Sterilized Grafts For Periodontological Applications**
Saharnaz Bargh, Mine Silindir-Gunay, A. Yekta Ozer, Seyda Colak , Burak Kutlu, and Rahime Nohutcu

4 **Ionizing-Radiation Induced Synthesis Of Poly(Vinylpyrrolidone) Nanohydrogels As Drug Delivery Systems And The Implementation Of MRI Contrast Agents**
Devyn Catterton, Zois Tsinas, Dianne L. Poster, David Grills, James Wishart, and Mohamad Al-Sheikhly

5 **Excited States And Electronic Coupling Explored By Pulse Radiolysis**
Andrew R. Cook, Anthony Grimonti, Paiboon Sreearunothai, Sada Asaoka, Michal Valášek, Alison M. Funston, Pavel Poliakov, Josef Michl, J. R. Miller

6 **Ion Induced Structural Changes In Graphite**
Lenore S. Miller, John Derek Demaree, Kristopher D Behler,, Weigang Lu, Zhiping Luo, and Daryush Ila

7 **Azo Functionalized, Hydrophilic Fabrics For The Extraction Of Uranium From Seawater**
Travis C. Dietz, ZoisTsinas, Ileana M. Pazos, Eli Fastow, Weixing Li, Fred Bateman, Dianne Poster, David Grills, Mohammad Adel-Hadadi, Aaron Barkatt, James Wishart, and Mohamad Al-Shiekhly

8 **Understanding Generation Of Multifunctional Nanogels In Chemical-Free Ebeam Irradiation Synthesis**
Lorena Anna Ditta, Björn Dahlgren, Maria Antonietta Sabatino, Mats Jonsson, Clelia Dispenza

9 New Experiments: Neutron/Proton Radiolysis Of Water Up To 350 °C
G. L. Draper, A. Baidak, S. M. Shubeita, H. E. Sims, R. M. Orr

10 Radiolysis Of Wood Saccharides, Oligosaccharides, Polysaccharides And Lignin
Mark S. Driscoll, Jay LaVerne, Mohamad Al-Sheikhly, Dianne Poster

11 Increased Highway Life Via Electron Beam Initiated Polymer Modification
Slavica Grdanovska, Charlie Cooper, Ben C. Cox

12 Radiolysis Of Hydrogen Peroxide Associated With Aluminum Oxide
Kazuhiro Iwamatsu, Jay A. LaVerne

13 The Role Of Surface-Bound Hydroxyl Radicals In Radiation Induced Dissolution Of UO$_2$
Alexandre Barreiro Fidalgo, Yuta Kumagai, Björn Dahlgren and Mats Jonsson

14 Novel System For Pulse Radiolysis With Multiangle Light Scattering Detection (Pr-Malls)
S. Kadłubowski, P. Sawicki, S. Sowiński, J.M. Rosiak, P. Ulański

15 Radiation Grafting Of Ionic Liquids To Synthesize Polymer Electrolyte Membranes For Fuel Cell Operation Above 100°C
Kevin Mecadon, Mohamad Al-Shiekhly, Fred Bateman, and Joseph Robertson

16 Ion Induced Structural Changes In Graphite
Lenore S. Miller, John Derek Demaree, Kristopher D Behler, Weigang Lu, Zhiping Luo, Daryush Ila

17 Au@TiO$_2$ Fabricated Through X-Ray Radiolysis And Their Application As Potential Radiosensitizers
M.C. Molina Higgins

18 Dose Rate Effect On The Depolymerization Of Cellulose
Lisa Paulsen, Mark S. Driscoll, Arthur J. Stipanovic, Fred B. Bateman and Ileana Posaz

19 Effect Of β-Diketo Group Modification Of Curcumin On Antioxidant Activity And Free Radical Reactions: Correlated With Computational Studies
Shaukat Ali M. Shaikh, Beena G. Singh, Atanu Barik, Gottumukkala V. Subbaraju, Devidas B. Naik, K. Indira Priyadarsini

20 Radical Processes Involving Quinoxalin-2-One Derivatives Relevant To Their Pharmacological Applications

K. Skotnicki, K. Bobrowski, J. De la Fuente, A. Cañete

21 **Dextran-Based Hydrogels For Biomedical Applications – Radiation-Initiated Synthesis And Characterization**
Kamila J. Szafulera, Radoslaw A. Wach, Piotr Ulanski

22 **Spectral Shift Of Solvated Electrons In A Mixture Of Ionic Liquids At Low Temperatures**
Kenji Takahashi, Surajdevprakash B. Dhiman, Koji Osawa, and James F. Wishart

23 **Gamma Radiation For The Development Of Microstructured Pva/Gelatin Based Scaffolds For Controlled Release Of Platelet Rich Plasma**
Justine P. R. O. Varca, André Ferrari, Caroline S. A. de Lima, Kamila M. Nogueira, Gustavo H. C. Varca, Monica B. Mathor, Ademar B. Lugão

24 **Reactions Induced On The Radiation In Tributyl Phosphate Studied By Picosecond Pulse Radiolysis**
Furong Wang, Gregory P. Horne, Pascal Pernot, Pierre Archirel and Mehran Mostafavi

25 **Radiolytichydrogen Production From The Water Radiolysis In CSH**
YIN, C., DANNOUX-PAPIN, A., HAAS, J., NGONO-RAVACHE, Y., RENAULT, J-P.

26 **High Resolution Dosimetry For Sterilization Of Sensitive Electronics**
Vu Le, Byron Lambert, Johnathan Manion, Dom Patel, Scott Dalton

ABSTRACTS of INVITED LECTURES

(in order of presentation)

FIXING THE WATER RADIOLYSIS MECHANISM

David M. Bartels[1] and Marcin Sterniczuk[1]

[1]*Notre Dame Radiation Laboratory, Notre Dame, IN 46556*

A kinetic model to describe the free radical chemistry in high temperature irradiated water has been compiled by numerous workers over many years, and is widely applied in the nuclear industry to predict "corrosion potential" in various parts of power reactor cooling loops. In the last three years we have tested the predictions of the 2008 Elliot and Bartels review model[1] against steady state H_2 and O_2 production measured in high temperature continuous electron radiolysis experiments, with dose rates (.5-10 kGy/s) similar to a power reactor. We are able to correctly model the results at room temperature at pH =5, 7, 9, and 11. In neutral and acidic water above 200^{o}C, we can reproduce the results simply by adjusting upward the reaction rate for $H + H_2O => H_2 + OH$, in agreement with measurements in other laboratories.

A very significant discrepancy remains for the H_2 production in the 100-200^{o}C range. The poorly known reactions which might cause model failure generally involve the HO_2/O_2- radicals. Oxidation of these radicals by OH was re-evaluated from the transient absorption pulse radiolysis data of Buxton and Elliot[2], using yields, reaction rates, and extinction coefficients consistent with the Elliot and Bartels review. The reaction rates become lower, making our H_2 predictions worse.

Measurements of the reduction reaction[3] $H+ HO_2=> H_2O_2$ up to 150^{o}C were also re-evaluated, but it has been noted that the preferred gas phase reaction path produces 2 OH radicals, and this product channel was "invisible" to the experiments previously carried out. Including the latter channel improves the fit of our H_2 data for pH 5. The more important reaction of H with O_2- has never been reported. If we assume the product of the latter reaction is HO_2-, we cannot explain our data. However, on theoretical grounds it is quite reasonable that reaction of H atom with O_2- is actually an electron transfer oxidation, producing O_2 , H_2 and OH-. In this case we can reproduce our steady state measurements of H_2 in neutral water over the full temperature range.

Major discrepancy remains for experiments carried out in presence of .001m NaOH above room temperature. The measured H_2 is ca. 10x larger than the prediction over the full range of temperature. We have investigated the rate and product for the reaction of $(e\text{-})_{aq}$ with O_2-, which is only reported at room temperature. Based on multiple-pulse radiolysis experiments that successively convert dissolved O_2 to O_2-, the reaction rate of $(e\text{-})_{aq}$ with O_2- is similar to its reaction rate with O_2 up to 100^{o}C. The product of the reaction seems to be HO_2- + OH- as expected. At this time we are forced to conclude that some other reaction(s) that have been "reliably" measured under alkaline conditions are incorrectly evaluated, and investigations continue.

References

(1) Elliot, A. J.; Bartels, D. M. "The Reaction Set, Rate Constants and g-Values for the Simulation of the Radiolysis of Light Water over the Range 20° to 350°C Based on Information Available in 2008", report AECL 153-127160-450-001, Atomic Energy of Canada, Ltd., 2009.

(2) Elliot, A. J.; Buxton, G. V. Temperature dependence of the reactions OH + O_2- and OH + HO_2 in water up to 200 °C. *J. Chem. Soc., Faraday Trans.* **1992**, *88*, 2465-2470.

(3) Lundstrom, T.; Christensen, H.; Sehested, K. Reactions of the HO_2 radical with OH, H, Fe^{2+} and Cu^{2+} at elevated temperatures. *Radiat. Phys. Chem.* **2004**, *69*, 211-216.

LONG-LIVED POLYENYL RADICALS IN IRRADIATED HIGHLY CRYSTALLINE UHMMPE FIBERS

Amanda L. Forster[1], Zois Tsinas[1,2], and Mohamad Al-Sheikhly[1,2]

[1]*National Institute of Standards and Technology, Gaithersburg, MD USA.*
[2]*University of Maryland College Park, College Park, MD USA*

To improve properties such as thermal conductivity, low temperature thermal strain, and creep resistance of UHMMPE fibers, several researchers have undertaken efforts to crosslink these fibers using radiation. Ionizing radiation is commonly used to crosslink bulk UHMMPE in other applications, such as artificial joints. However, UHMMPE fibers differ from bulk UHMMPE in that they have a higher crystallinity (approximately 85 % to 90 % crystalline) and are very highly oriented during manufacture through a process known as “superdrawing”, in which the fibers are stretched 50 to 100 times their original length. Thus, the amorphous fraction of the UHMMPE fibers is also highly ordered. Several experiments were conducted to crosslink the UHMMPE fibers using both low dose rate (gamma) and high dose rate (electron beam) irradiation, all in the absence of oxygen to minimize the probability of oxidation. In all cases, the tensile strength was greatly reduced by the irradiation. Oxidation index was also measured for the irradiated samples, and oxidation was not found to play a major role in the reduction of tensile strength in the fibers after irradiation. Chain scission is highly catastrophic in a high molecular weight system, and available crosslink sites are saturated at low dose due to the low amorphous content of these fibers. After the crosslink sites are saturated, chain scission becomes dominant in the fiber, greatly reducing its mechanical properties, likely due to preferential scission of the “taut tie molecules” that connect crystalline regions in the fiber. While this work did not achieve the desired result of improving the mechanical properties of the UHMMPE fiber, a surprising result was found. Several authors have previously examined the effect of irradiation on the physical properties of UHMMPE fibers, however no work could be found that examined the free radicals formed in the fibers after irradiation. Accordingly, the EPR spectrum of the UHMMPE fibers was measured shortly after irradiation, and alkyl radicals were detected, as expected. The irradiated samples were stored in dark ambient conditions for at least five years, then then reexamined using EPR for free radicals. Surprisingly, the gamma-irradiated samples showed clear evidence of long-lived polyenyl radicals. The alkyl radicals formed immediately after irradiation would be expected to react quickly to form polyenyl radicals. One possible explanation for the presence of these polyenyl radicals so long after irradiation is the high crystallinity of these UHMMPE as compared to typical bulk polyethylene. Typically, these polyenyl radicals would be expected to eventually migrate to the surface of the crystalline domain and be eliminated in the amorphous region. However, we suspect that due to the high crystallinity and large anisotropy of the highly drawn UHMMPE fiber, the polyenyl radicals were unable to eliminate and were trapped in the crystal. An experiment was performed to test this hypothesis, by which a sample of the irradiated fibers were heated to temperatures above the alpha relaxation for polyethylene, and EPR measurements showed that the polyenyl radical signal persisted. Then, the fibers were heated to temperatures above the melting point of the polymer, and EPR signals showed that the polyenyl signal was rapidly eliminated. These experiments support the hypothesis that the long-lived polyenyl radicals were trapped in the crystalline region of the polyethylene fibers.

KINETICS OF THE RADIATION-INDUCED DEGRADATION OF METAL-EXTRACTION LIGANDS IN THE ORGANIC PHASE

Stephen P. Mezyk[1], Gregory P. Horne[2], Andrew R. Cook[3]

[1]*California State University at Long Beach, Long Beach, CA 90840 USA*
[2]*Idaho National Laboratory, Idaho Falls, Idaho*
[3]*Brookhaven National Laboratory, Upton, New York*

The solvent-based reprocessing of used nuclear fuel is typically based upon mixed-phase extraction techniques, and utilizes designer ligands dissolved in an organic phase to extract ligand-complexed lanthanide/actinide metal ions from a highly acidic aqueous phase. However, these extractions occur in a highly radioactive environment, and therefore an understanding of the radiation chemistry of these complexants and their diluents is vital in determining process extraction efficiency, separation factors, and solvent-recycle longevity. Among the species produced in the aqueous phase are the reactive products of water and nitric acid radiolysis, notably the hydroxyl ($HO^{\bullet}$) and nitrate ($^{\bullet}NO_3$) radicals.[1,2] However, little fundamental kinetic and mechanistic data has been reported for the degradation of extraction ligands in the organic phase. The radiolysis of organic diluents[3] (dodecane, TPH, kerosene) produces radical cations ($R^{\bullet+}$), carbon-centered radicals ($R^{\bullet}$), organic solvated electrons (e^{-}_{solv}), and molecular products such as hydrogen (H_2). Typically, the radical species react with dissolved oxygen to produce less-reactive peroxyl radicals, leaving the alkane radical cation species, $R^{\bullet+}$, as the major radiolytically-produced species that can react with, and degrade, extraction agents in this phase.

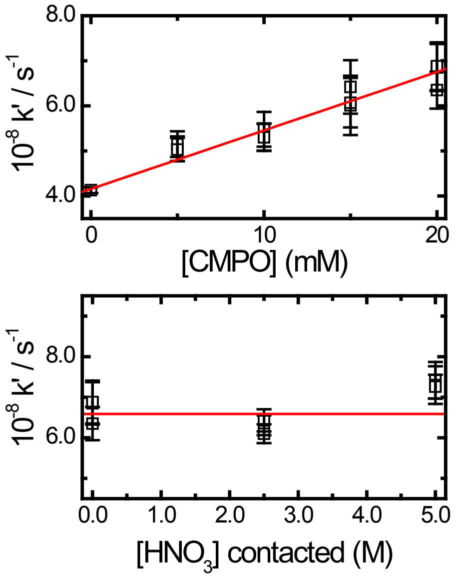

Figure 1. Top: Second-order rate constant plot for reaction of dodecane radical cation ($R^{+\bullet}$) with CMPO in dodecane/0.10 M CH_2Cl_2 at 295K. Individual data points and error bars are the average of 3 individual measurements for each CMPO concentration. Solid line is weighted linear fit, corresponding to a slope of $k_8 = (1.30 \pm 0.11) \times 10^{10}\ M^{-1}\ s^{-1}$, ($R^2 = 0.96$). Bottom: Measured rate constants for 20 mM CMPO in aerated dodecane/0.10 M CH_2Cl_2 contacted with different nitric acid concentrations showing no significant increase in reactivity.

Here we report on our kinetic studies for organic radical cation reactions with various nitrogen- and phosphorus-containing ligands (CMPO, TODGA, TBP, etc.), both free and complexed with lanthanide metal ions. Typical data for CMPO are shown in Figure 1. Fast reaction rate constants were measured, stressing the importance of this mechanistic pathway. The ultimate goal is to combine these data with the known acidic aqueous phase chemistry to allow a full, fundamental, understanding of the impact of radiation on solvent extraction based separation processes.

References

(1) Buxton G.V.; Greenstock C.L.; Helman W.P.; Ross A.B., (1988) J. Phys. Chem. Ref. Data, 17, 513-886.

(2) Jiang P.Y.; Nagaishi R.; Yotsuyanagi T.; Katsamura Y.; Ishiguri K*.,* (1994) J. Chem. Soc. Faraday Trans., 90, 93-95.
(3) Spinks J.W.T.; Woods R.J., (1991) *An Introduction to Radiation Chemistry, 3rd Ed* John Wiley and Sons, Hobokken, NJ

PICOSECOND SCALE ELECTRON SOLVATION DYNAMICS IN H_2O DURING ULTRAFAST PULSED ION RADIOLYSIS

B. Dromey[1], L. Senje[2], M. Coughlan[1], H. Donnelly, N. Breslin, G. Nersisyan[1], C. L. S. Lewis[1], F. Currell[1], C.-G. Wahlström[2], M. Zepf[1,3]

[1]School of Mathematics and Physics, Queens University Belfast, Belfast BT7 1NN, United Kingdom
[2]Department of Physics, Lund University, P. O. Box 118, S-221 00 Lund, Sweden
[3]Helmholtz-Institut Jena, D-07743 Jena, Germany
**b.dromey@qub.ac.uk*

Beams of energetic ions are finding application in multiple cutting edge technologies ranging from hadrontherapy to semiconductor device manufacture/metrology. To date, however, ion interactions in matter have been dealt with in a manner similar to those of electrons/photons, with attention primarily being paid to the energy, E, lost over path length, dx, giving the stopping power $S(E) = - dE/dx$. The obvious distinction is of course that ion stopping in matter exhibits a Bragg peak. In both scenarios the expected cell death or material damage are then generally extrapolated from empirical studies of dose deposition. For ions it is not immediately clear that this is the correct approach as it masks a critical phase of the interaction. When ions are incident on matter they generate dense tracks of ionisation that rapidly evolve. Exactly how this evolution, which occurs on femtosecond and picosecond times, determines the nascent radiation chemistry is still largely unknown.

Recently we have demonstrated that laser driven ion accelerators can provide an ultrafast tool for studying this inherently multiscale regime with temporal resolution < 0.5 ps.[1,2] Here we present novel results that show a marked difference in the solvation time of electrons generated due to the passage of fast electrons/X-rays and protons (~3 MeV) in water. The solvation time is shown to dramatically increase from < 5 ps for a < 1 ps pulse of fast electrons/X-rays to > 190 ps for a 22 ± 3 ps (Fig 1 a, b) pulse of protons. We discuss the role of nano-cavitation during ion radiolysis in H_2O and how this can lead to the increased time for the solvation of the electron.

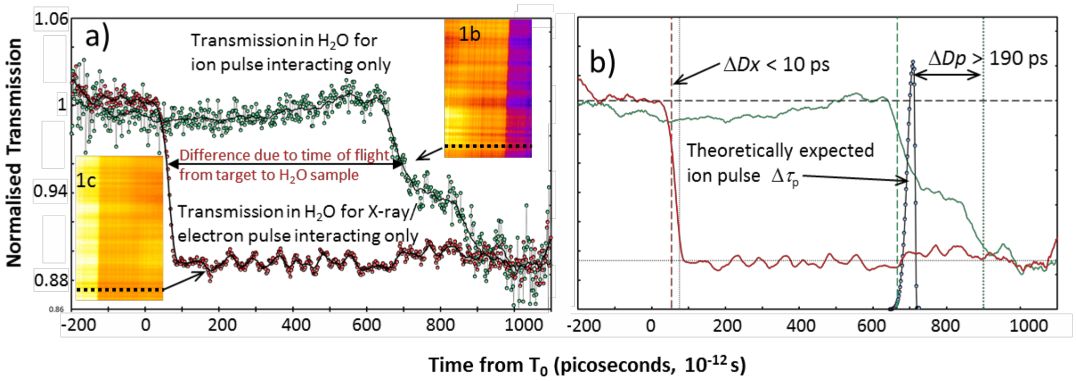

Figure 1 - Ultrafast solvation dynamics of the electron for pulse ion radiolysis in H_2O

References

(1) B. Dromey, et al., *Nat.Comms.*,**4**, 1763 (2013)
(2) L. Senje, et al., App. Phys. Letts., 110, 104102 (2017)

RADIOLYSIS IN 2D- AND 1D- CONFINING MATERIALS

Sophie Le Caër[1]

[1]*LIONS, NIMBE, UMR 3685, CEA, CNRS, Université Paris-Saclay, CEA Saclay, F-91191 Gif-sur-Yvette Cedex, France. Email: sophie.le-caer@cea.fr*

The influence of ionizing radiation on clay minerals is poorly known, in spite of their use as a major component of the engineered barrier in High Level Nuclear Waste Repositories (HLNWR).[1] In this context, the production of H_2 by clay minerals under ionizing radiation could be a real issue. It can, e.g., lead to the loss of radionuclide retention properties by creating cracks in the engineered barrier. It is thus important to determine H_2 formation reaction mechanisms and to understand the role of several parameters on this production, such as the water amount, the presence of impurities and the nature of the clay mineral.

Moreover, clay minerals provide a unique and very interesting system to study radiolysis in a model 2D-confining material. Indeed, clay minerals are hydrous silicates of aluminum, magnesium, or iron displaying a layered structure. In the sheets, TO_4 tetrahedral (T) sites usually occupied by Si^{4+}, Al^{3+}, or Fe^{3+} cations interconnected by three vertices, combine themselves into pseudo-hexagons $(TO_4)_6$ linked to a sheet of octahedral (O) sites, usually occupied by Al^{3+}, Fe^{3+}, Mg^{2+}, or Fe^{2+} cations and form 2D sheets (Figures 1a and 1b). By changing the nature of the atoms which are present, the amount of water can be tuned: in talc, no water is present (Figure 1a) whereas its amount can be varied in swelling clays such as montmorillonite or saponite for example (Figure 1b) due to the presence of cations in the interlayer space. We have shown that under irradiation by accelerated electrons, the dihydrogen production in synthetic talc, which is solely due to structure hydroxyl groups, is of the same order of magnitude as the one obtained in liquid water.[2] This yield is divided by 30 in the case of natural talc from Luzenac, evidencing the importance of the impurities as scavengers of the precursors of dihydrogen. In the case of synthetic montmorillonite and saponite, the radiolysis of water confined in the interlayer space, that has a thickness of a few Å, leads to H_2 yields which are two to three times higher than the one measured in water.[3] Moreover, these yields are similar for montmorillonite and saponite, evidencing that the charge location only plays a minor role in the H_2 production.

Layered double hydroxides (LDH) are analogous of clay minerals (Figure 1c). They are also a layered material, where the positive charges of the sheets are compensated by the presence of anions in the interlamellar space. In this case, the anion can play a role in the radiation chemistry, contrary to the case of clay minerals for which the cation (Na^+ in the present work) is inert towards ionizing radiation. We have shown that the nature of the anion controls the H_2 production in LDHs.

A last system of interest is imogolite[4] (Figure 1d) which is an aluminosilicate nanotube. It enables understanding the radiation chemistry of water confined in an 1D geometry.

Parallel to the H_2 production measurements, other characterization techniques such as electron paramagnetic experiments have enabled proposing reaction schemes. Reaction mechanisms accounting for H_2 production in confined media will be proposed and discussed according to the nature of the confining matrix, the amount of water…. All these results are of interest in the context of the disposal of radioactive waste.

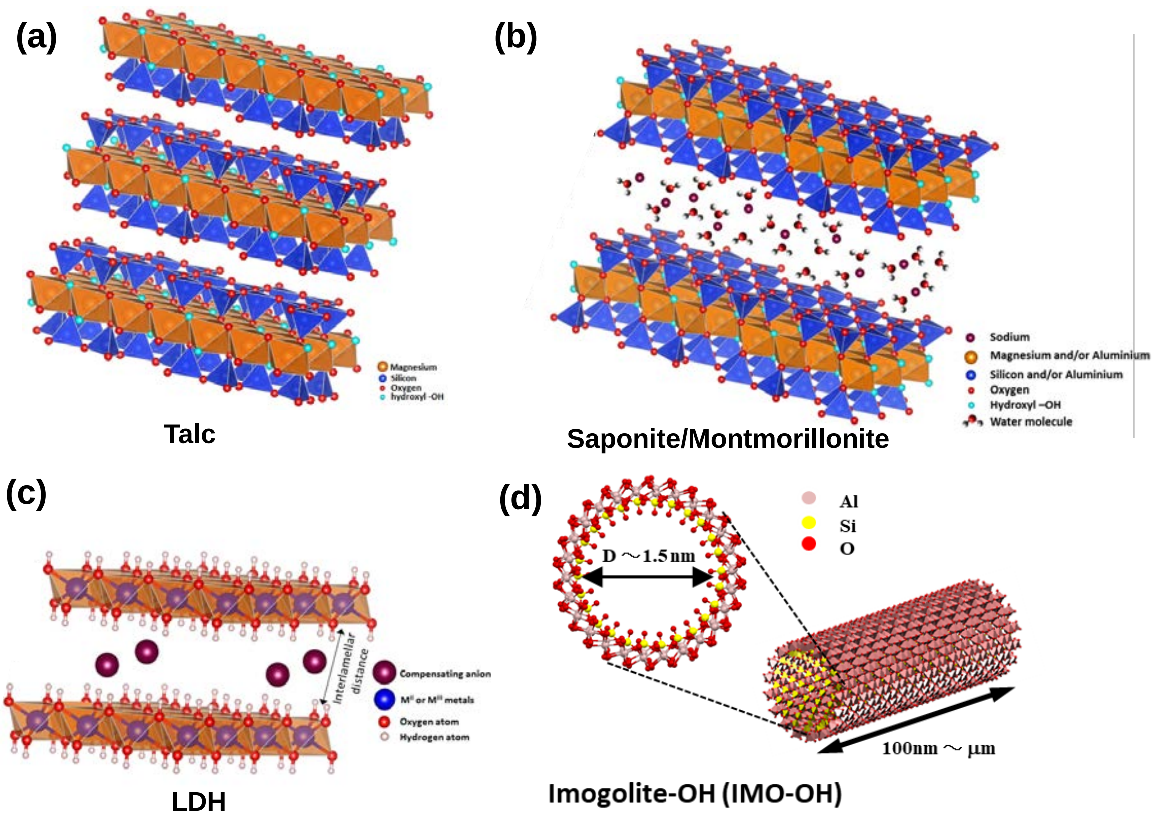

Figure 1 - Different confining materials under study. 2D geometries: a) talc; b) swelling clays (saponite and montmorillonite); c) Layered Double Hydroxides (LDH). 1D geometry: d) imogolite.

References

(1) Fourdrin, C.; Aarrachi, H.; Latrille, C.; Esnouf, S.; Bergaya, F.; Le Caër, S. Water radiolysis in exchanged-montmorillonites: the H_2 production mechanisms. *Environ. Sci. Technol.* **2013**, *47*, 9530-9537.

(2) Lainé, M.; Balan, E. A., Th. ; Martin, F.; von Bardeleben, H.-J.; Robert, J.-L.; Le Caër, S. Reaction mechanisms in talc under ionizing radiation: evidence of a high stability of $H^{\bullet}$ atoms. *J. Phys. Chem. C* **2016**, *120*, 2087-2095.

(3) Lainé, M.; Balan, E.; Allard, T.; Paineau, E.; Jeunesse, P. M., M.; Robert, J.-L.; Le Caër, S. Reaction mechanisms in swelling clays under ionizing radiation: influence of the water amount and of the nature of the clay mineral. *RSC Adv.* **2017**, *526*, 526-534.

(4) Liao, Y.; Picot, P.; Brubach, J.-B.; Roy, P.; Le Caër, S.; Thill, A. Self-supporting thin films of imogolite and imogolite-like nanotubes for infrared spectroscopy. *App. Clay Sci.* **2017**, https://doi.org/10.1016/j.clay.2017.1006.1005.

ON THE RADIOLYSIS OF AQUEOUS SOLUTIONS OF $(CH_3)_2SO$

Ana Lerner,[1,2] Israel Zilbermann,[1,2] Magal Saphier,[2] Guy Yardeni,[2] Dan Meyerstein.[3,1]

[1] *Chemistry Dept., Ben-Gurion University, Beer-Sheva, Israel.*
[2] *Nuclear Research Centre Negev, Beer-Sheva, Israel.*
[3] *Chemical Sciences Dept., Ariel University, Ariel, Israel.*

The radiolysis of N_2O saturated aqueous solutions containing $(CH_3)_2SO$ is commonly used to produce methyl radicals. In the absence of other solutes the following reactions are usually considered:

(1) $H_2O \xrightarrow{e^-,\gamma} e^-_{aq}$ (2.65); $OH^{\cdot}$ (2.65); $H^{\cdot}$ (0.60); H_2O_2 (0.75).
(2) $e^-_{aq} + N_2O \rightarrow OH^{\cdot} + N_2 + OH^-$
(3) $(CH_3)_2SO + OH^{\cdot} \rightarrow (CH_3)_2S(O)OH^{\cdot}$
(4) $(CH_3)_2S(O)OH^{\cdot} \rightarrow CH_3^{\cdot} + (CH_3)S(O)OH$
(5) $CH_3^{\cdot} + (CH_3)_2SO \rightarrow CH_4 + (CH_2)(CH_3)SO^{\cdot}$
(6) $2CH_3^{\cdot} \rightarrow C_2H_6$

According to these equations one expects $G(CH_3^{\cdot}) = 6.0$ and $G(CH_3\ \text{total}) = G(CH_4) + 2G(C_2H_6) = 6.0$. These values are indeed often observed within the accuracy of the measurements. This is somewhat surprising as the reaction

(7) $CH_3^{\cdot} + (CH_2)(CH_3)SO^{\cdot} \rightarrow (C_2H_5)(CH_3)SO$

Is expected to decrease $G(CH_3\ \text{total})$ to a value significantly below 6.0.

Experiments at low dose rates point out that the following thre reactions contribute to the reaction mechanism:

(8) $CH_3^{\cdot} + (CH_3)_2SO \rightarrow C_2H_6 + (CH_3)SO^{\cdot}$
(9) $(CH_2)(CH_3)SO^{\cdot} + (CH_3)_2SO \rightarrow (CH_3)_2S(O)\text{-}CH_2(CH_3)SO^{\cdot}$
(10) $(CH_3)_2S(O)\text{-}CH_2(CH_3)SO^{\cdot} \rightarrow CH_3^{\cdot} + (CH_3)S(O)\text{-}CH_2(CH_3)SO$

These reactions clearly increase the observed $G(CH_3\ \text{total}) = G(CH_4) + 2G(C_2H_6)$, and seem to balance under many conditions the effect of reaction (7). However at low dose rates and high $[(CH_3)_2SO]$ $G(CH_3\ \text{total}) \sim 10$ is obtained.

It is pointed out that reactions (7) – (10) have always to be considered.

KINETIC AND MECHANISTIC FEATURES OF RADIATION-INITIATED CROSSLINKING-POLYMERIZATION: THE ASSETS OF RADIATION PROCESSING FOR THE FABRICATION OF HIGH PERFORMANCE COMPOSITES

Mickael Krzeminski,[1,2] Arnaud Martin,[1,2] Gabriela Tataru,[1] Guillaume Ranoux,[1]
Christelle Kowandy,[1] Brigitte Defoort,[2] Alexandre Berquand,[3]
Michael Molinari[3] and Xavier Coqueret[1]

[1] *Institut de Chimie Moléculaire de Reims, CNRS UMR 7312, Université de Reims Champagne-Ardenne, 51687 Reims, France*
[2] *Ariane Group, BP 11, 33165 Saint Médard en Jalles, France*
[3] *Laboratoire de Recherche en Nanosciences,* Université de Reims Champagne-Ardenne, *51685 Reims, France*

The potentialities of electron beam- (EB) or X-ray-initiated crosslinking polymerization have been recognized during the mid 1980's. Since then, the technological features of this novel curing process were explored as a very attractive alternative for the production of high performance composite materials. High energy radiation processing indeed offers several advantages over thermosetting technology, essentially for the fast and out-of-autoclave curing operation as well as for the ability to manufacture complex and large structures at low costs.

Compared to conventional thermoset-based technology, radiation-induced cross-linking polymerization is based on relatively new chemistry, commonly used for coatings and in the graphic arts, but not for large and thick parts with specific and demanding requirements in terms of use properties.

The mechanistic and kinetic aspects of radiation-initiated polymerization of acrylate and epoxy monomers will be reviewed in this presentation, with emphasis on the influence of chemical composition as well as on processing factors such as dose rate and thermal effects. Free radical and cationic polymerization exhibit specific features which will be discussed in some detail: need for initiator, post-irradiation effects, sensitivity to various inhibitors, impact of transfer reactions, vitrification).

Among the identified limitations associated with the fast elaboration of polymer matrices by chain polymerization, the brittleness of networks and the weak interactions between fibers and matrix have kindled advanced investigations and new approches to formulation design. Both the free radical and cationic chemistries were found to yield nanoheterogeneous networks which can be finely characterized by various thermophysical and imaging methods. A common global scenario is proposed accordingly to describe the formation of monolithic glassy materials from the liquid compositions.

In order to improve composite damage tolerance, we are currently progressing in the development of formulations including a high Tg thermoplastic toughener. Starting from very fluid and homogeneous formulations, the fast polymerization process induces phase separation of particles rich in thermoplastic toughening agent. A detailed investigation of composition and curing parameters on both morphological aspects and on mechanical properties allowed for defining composition and processing parameters yielding materials with outstanding mechanical properties. The kinetic and thermal conditions of radiation-initiated polymerization were confirmed as key assets for achieving high performance mechanical properties in the cured composites.

RADIATION TECHNOLOGIES FOR THE DEVELOPMENT OF NANOCARRIERS FOR RADIO AND CHEMOTHERAPEUTICS

Gustavo H. C. Varca[1], Gabriela N. Fazolin[1], Aryel H. Ferreira[1], Justine P. R. O. Varca[1], Jorge G.S. Batista[1], Lucas F. de Freitas[1], Fabio L. N. Marques[2], Ademar B. Lugão[1]

[1]Nuclear and Energy Research Institute – IPEN-CNEN/SP, Brazil.

[2] Faculdade de Medicina FMUSP, Universidade de São Paulo, São Paulo, SP, BR.

The use of ionizing radiation for the development or improvement of materials is widely recognized worldwide. Advantages of the technology rely on the possibility to combine multiple processes simultaneously. When it comes to nanotechnology, radiation may be successfully applied towards nanoparticles formation with simultaneous sterilization in a single step and without the need for toxic reagents or chemical crosslinkers. The present work reports the synthesis of protein-based nanoparticles – albumin or papain, inorganic nanoparticles such as gold nanoparticles, and hybrid systems, involving albumin and papain functionalized gold nanoparticles, all synthesized using ionizing radiation. The synthesis of protein-based nanocarriers has become an important area of study due to their ability to improve drug retention times as well as to promote biocompatibility, among other biopharmaceutical advantages. Papain, a proteolytic enzyme, and albumin, a globular protein, are examples of widely applied biomolecules in the biomedical and pharmaceutical area with strong and recognized potential in drug delivery. Nanogold, on the other hand, has been extensively used for a plethora of biomedical applications, i.e. diagnostics, treatment or theranostics. The functionalization onto gold nanoparticles is performed to provide site specific delivery, improve tumor/cell uptake, among other properties. Protein crosslinking onto gold nanoparticles using radiation is also reported in this work. Proofs of concept of the technology will also be addressed in this talk, including biodistribution aspects, drug loading, radiolabeling with technetium and other aspects.

THE HYDRATED ELECTRON: CAVITY, NON-CAVITY OR SOMETHING IN BETWEEN?

Benjamin J. Schwartz[1], Erik P. Farr, Chen-Chen Zho

[1]*University of California, Los Angeles, Department of Chemistry and Biochemistry, Los Angeles 90095*

Despite intense investigation, it is still unclear whether the structure of an excess electron in liquid water is best thought of as a quasi-halide ion, where most of the electron resides in a solvent cavity, as a non-cavity object, with many water molecules packed within the electron's wavefunction, or something in between. To address this question, we performed a series of mixed quantum/classical simulations with the goal of connecting the structure of simulated hydrated electrons with experiment. We find that traditional cavity models are unable to predict the temperature dependence of the hydrated electron's excited-state lifetime, whereas a non-cavity model provides good qualitative agreement with experiment. Cavity models also fail to reproduce features of both static and time-resolved photoelectron spectroscopy (TRPES) experiments, including the fact that hydrated electrons are not found near the air/water interface, that solvation dynamics lower the excited-state energy prior to internal conversion, and that solvation of the ground-state is significantly slower than the excited-state lifetime, features that are all well captured with a non-cavity model. We are able to rationalize these observations by comparing free energies of cavity and non-cavity model hydrated electrons. We find that cavity hydrated electrons behave effectively as hard spheres, with large free energy penalties for any incursion of water into the electron's interior. In contrast, there is only a small free energy penalty to remove water molecules from the interior of non-cavity electrons, so that non-cavity electrons have a highly fluxional structure that are non-cavity on average but vary continuously between cavity and non-cavity. The driving force for placing water molecules into the non-cavity electron's interior is entirely entropy-driven, so that non-cavity electrons become more cavity-like on average as the temperature decreases, explaining the experimentally-observed temperature dependence of the hydrated electron's transient absorption spectroscopy (performed in our group) and various features of the previous TRPES experiments.

RADIATION TOLERANT MATERIALS FOR ADVANCED REACTOR CLADDING APPLICATIONS

S.A. Maloy[1], E. Aydogan[1], B. Eftink[1], T.A. Saleh[1], M. Toloczko[2], T.S. Byun[2], C. Lavender[2],
G.R. Odette[3], M.E. Alam[3], S. Pal[3], D.T. Hoelzer[4]

[1]Los Alamos National Laboratory, Los Alamos, NM 87545, USA
[2]Pacific Northwest National Laboratory, Richland, WA 99352, USA
[3]University of California, Santa Barbara, Santa Barbara, CA 93106 USA
[4]Oak Ridge National Laboratory, Oak Ridge, TN 37831, USA

The Nuclear Technology R&D program is investigating options to transmute minor actinides. To achieve this goal, new fuels and cladding materials must be developed and tested to high burnup levels (e.g. >20%) requiring cladding to withstand very high doses (greater than 200 dpa) while in contact with the coolant and the fuel. Thus, these materials must withstand radiation effects that promote low temperature embrittlement, high temperature helium embrittlement, swelling, accelerated creep, corrosion with the coolant, and chemical interaction with the fuel (FCCI). One of the most promising materials for this demanding applications are ferritic alloys. New ferritic/martensitic and ferritic Oxide Dispersion Strengthened (ODS) alloys are being developed with improved radiation tolerance. The ferritic/martensitic alloys include slight variations in the composition of HT-9 to improve resistance to low temperature embrittlement and void swelling. In addition, ferritic ODS alloys are being developed and tested. These materials are ferritic alloys with high chrome (9-14Cr) with a high density ($>10^{23}/m^3$), fine distribution of nanosized (~2 nm) oxide particles and a fine grain size (<0.5 micron). This fine microstructure provides an alloy with high strength at high temperatures and excellent radiation tolerance (e.g. reduced void swelling and ductility retention at low temperatures) but also increases the difficulty of producing engineering parts (e.g. thin walled tubes) from these advanced materials. Thus, significant research is underway to process alloys into tube form and test them for future nuclear applications. Recent progress in high dose irradiated materials testing and materials development will be presented.

NATURAL ALTERATION OF NEUTRON SHIELDING GLASS

Jamie Weaver[1] and Danyal Turkoglu[1]

[1]*National Institute of Standards and Technology, Materials Measurement Laboratory,*
Gaithersburg, MD 20899

The long-term service potential of a neutron shielding material is in part dependent on its chemical durability. However, many shielding materials, including ^{6}Li neutron shielding glass, have not been assessed for their chemical stability under natural conditions and within operational timescales (years). To address this gap a study has been conducted at the NIST Center for Neutron Research (NCNR) on a ^{6}Li doped neutron shielding glass that has been exposed to natural conditions for variable timeframes (3 years, 2 months, and 0 month). Prompt Gamma Activation Analysis (PGAA), Neutron Depth Profiling (NDP), and complimentary X-ray and Electron analyses were executed on the samples. Results of the studies on the 3 years exposed, 2 months exposed, and unaltered (0 month) samples of glass found that the glass had both chemical and physical signatures of alteration within 2 months, and that the ^{6}Li distribution was vary within the alteration layer as a function of age (2 months vs. 3 years). The ^{6}Li depletion in the alteration layer relative to the bulk glass as determined by NDP for the 2 months exposed glass was ≈ 47%, and for the 3 years exposed sample was between ≈ 47% and ≈ 75%. When the alteration layer on the 3 years sample was removed, the H content (as measured by PGAA) of the glass's surface was nearly eliminated. From these findings it was concluded that the depletion of Li from the glass's surface did not affect its neutron shielding properties. However, the increase H content in the alteration layer may lead to increase neutron scattering and may make this glass an inappropriate material for the lining of certain neutron analysis instruments.

ELUCIDATION OF THE MECHANISMS OF PROTONS AND ALPHA PARTICLES-INDUCED DAMAGES ON THE SURFACE REGION OF 4H SILICON CARBIDE

Eaman Karim[1], John Derek Demaree[2], Noel Guardala[3], and Mohamad Al-Sheikhly[1]

[1] *Department of Materials Science and Engineering, University of Maryland, Collage Park, MD, USA*

[2] *US Army RDECOM, US Army Research Laboratory, APG, MD, USA*

[3] *The George Washington University, NW Washington, DC, USA*

Silicon carbide (SiC) has received a considerable attention as a cladding engineering material for nuclear fuel and inner canister material for a long-term nuclear waste disposal. Owing this to its distinguishable properties such as high temperature resistance, low neutron cross section, remarkable stability under corrosion and oxidation, good thermal conductivity and low thermal expansion. In nuclear applications, SiC is usually subjected to extreme conditions of high temperature and radiation. Irradiation with high linear energy transfer (LET) such as alpha particles, neutron, and protons as well as low LET such as gamma rays and beta particles induce degradation in the SiC crystal structure and rapture in the Si-C covalent bonds.

In this research project, we have been working on elucidating the mechanisms of protons and alpha particles induced-damages on 4H-SiC by using several experimental techniques such as Raman spectroscopy, Scanning Electron Microscope (SEM), X-ray Photoelectron spectroscopy (XPS), Fourier-Transform Infrared spectroscopy (FTIR). In addition, the computational modeling such as the Stopping and Range of Ions in Matter (SRIM) has been used to model the ranges of these charged particles inside SiC. The findings obtained from these techniques demonstrate decreases in the degree of crystallinity of 4H-SiC, increase in the short-range ordering, and the enhancement of homonuclear band intensity of silicon and carbon. The oxidation due to the rapture of SiC covalent bonds followed by the radiotically produce free radical molecular oxygen is also observed from the XPS technique. Additionally, SEM images have demonstrated the effects of the irradiation on the surface morphology of SiC, as can be seen from Fig. 1.

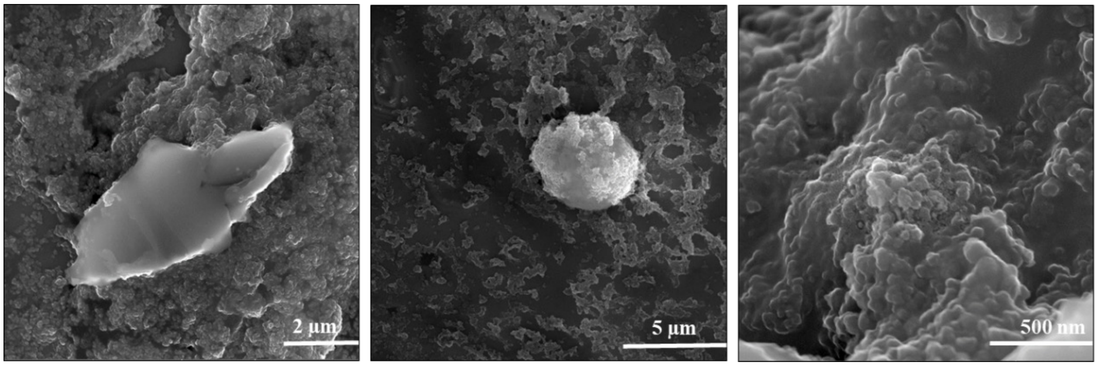

Figure 1 - SEM images demonstrate the effects of the irradiation on the surface morphology of SiC

ENHANCED EFFECTS OF RESONANT ELASTIC SCATTERING OF FAST NEUTRONS, PROTONS AND ALPHA PARTICLES ON INDUCED DAMAGE IN MATERIALS USED IN NUCLEAR APPLICATIONS

Noel A. Guardala[1], Jeffry A. Vanhoy[2], Derek Demaree[3]

[1]Department of Physics, George Washington Univ., Corcoran Hall, Washington D.C 20052
[2]Department of Physics, US Naval Academy, Chauvenet Hall, Annapolis, MD 21402
[3]Army Research Lab, Weapons and Materials Directorate, Rodman Materials Lab, Aberdeen, Proving Ground, Havre de Grace, MD 21078

The study of particle and radiation-induced damage to a number of advanced materials intended to be employed in new and advanced nuclear reactor designs with the intention to improve a number of operational parameters related to performance, reliability, reactor stability, thermal management, anti-corrosion properties, resistance to hydrolytic reactions etc.[1] It is highly desirable to introduce these kind of materials into the fuel rod assembly which would add to the functioning of various reactor designs both presently operational and being considered for new construction and installation on the national power grid. In addition these same materials are also being considered for their various capabilities to make storage of reactor waste more efficient, safe and cost effective.

We have investigated the enhancement of induced damage by the irradiation with energetic neutrons, protons and alpha particles on a number of these proposed materials such as: SiC, CVD Diamond, GaN, BN etc. Simulation programs for neutron-induced damage such as: NJOY,[2] MCNP-X, GEANT-4 etc. track only the incident particle's track and energy deposition producing information about those parameters related only to the incident particle and a single recoiling nucleus for each particular nuclear interaction. In the case of elastic scattering processes which is the dominant interaction for neutrons of all energies as well as showing up strongly at specific particle energies in the case of ions like: protons and alpha particles in the form of these isolated nuclear elastic scattering resonances the overwhelming amount of induced damage is not from the initial recoiling energetic atom, the primary displacement or "*primary knockout atom*" referred to as PKA but from the cascade of lower-energy atoms which greatly magnifies the amount of displacement and disorder damage.[3]

In the case of fast neutron-induced damage there have been attempts to improve on the accuracy of damage simulations from codes like NJOY by coupling the PKA values to the subsequent cascade formation using a charged-particle transport code like SRIM. It has been demonstrated that by inclusion of these low-energy cascade effects the amount of damage from fast neutrons is increased dramatically such that in SiC a single 2 MeV neutron can produce up to 2000 displacements.[4] However, another subtle contribution must be considered on the basis of nuclear kinematics related directly to the amount of induced damage from fast neutrons is that at elastic scattering resonances the distribution of the scattered neutron is significantly altered from the case for non-resonant scattering. That means that there is an increase in the number of energetic recoils i.e recoiling ions in the forward direction at the resonant scattering energies compared to the non-resonant condition. This effect has been termed now by some neutron scattering researchers as a '*focusing effect*'[5] in terms of the increase in the number of energetic recoils which leads to more displacement and disorder than predicted for non-resonant energies even when the cascade effects are included via a code like SRIM.[6]

A closely related phenomenon exists for the nuclear elastic scattering of both protons and alpha particles. Just as is the case for neutrons these particles also exhibit large the scattering amplitudes over what would be predicted solely from Coulomb scattering.[7] These resonances have a similar effect on altering of the momentum transfer probabilities from the projectile to a target nucleus by also increasing dramatically the amount of energy transferred to recoiling atoms which will subsequently produce larger than predicted damage values using a code like SRIM which does not include nuclear scattering amplitudes and kinematics.

We will demonstrate these enhanced damage effects at nuclear elastic scattering resonance both in simulations by coupling the nuclear probabilities including kinematics effects to the predicted damage values from both SRIM in the case of ions and for NJOY in the case of fast neutrons and from results of induced damage from proton and alpha particle irradiations both on and off resonance for various nuclei of interest such as: ^{12}C, ^{28}Si, ^{14}N etc.

References

(1) Deck C. P., Jacobsen G. M., Sheeder J., Gutierrez, O., Zhang J., Stone J.,Khalifa H. E., and Back C. A., Journal of Nuclear Materials, **2015**, 455, 667-681.

(2) MacFarlane R. E., and Kahler A. C., Methods for Processing ENDF/B-VII with NJOY, Nuclear Data Sheets, **2010,** 111, 2739- 2890.

(3) Heinisch H. L., Greenwood L. R., Weber W. J., and Williford R. E., Journal of Nuclear Materials **2004**, 327, 175–181.

(4) Chang J., Cho J-Y, Gil C-S., and Lee W-J., Nuclear Engineering and Technology, **2014,** 46, 475-480.

(5) Chadwick M. B. et al., ENDF/B-VII.1, Nuclear Data for Science and Technology: Cross Sections, Covariances, Fission Product Yields, and Decay Data, Nucl. Data Sheets, **2011**, 112(12) 2887-
2996.

(6) Zeigler, J. F., SRIM-2000, Code and manuals available on http://www.srim.org/ (2001, 2013).

(7) IBANDL, Ion Beam Analysis Nuclear Data Library, https://www-nds.iaea.org/exfor/ibandl.htm

SEMICONDUCTOR-BASED NANOSTRUCTURES FABRICATED BY ION-TRACK NANOTECHNOLOGY AND ELECTRODEPOSITION

M.E. Toimil-Molares[1]

[1]*GSI Helmholtz Center for Heavy Ion Research, Darmstadt, Germany*

Semiconductor nanowires and nanotubes can be potentially implemented in catalysis, sensing, and energy conversion. Their successful application requires not only an excellent control on geometry, crystallinity and composition of the individual nanostructures, but also its successful assembly into 2-D and 3-D architectures. Nanowire ensembles offer important advantages compared to planar films including e.g. larger surface area, larger surface to volume ratio, and better crystalline quality.

Ion-track nanotechnology is a powerful technique to create templates for the controlled synthesis of such 3-D nanowire architectures. Etched ion-track membranes are fabricated in two separate process steps: (i) sequential irradiation of polymer foils from one or various directions with swift heavy ions resulting in the creation of tracks; (ii) converting the ion tracks into nanochannels by selective chemical etching. Channel density and orientation, as well as diameter and geometry are adjusted by the irradiation and etching conditions, respectively. Afterwards, by electrodeposition in the nanochannels and subsequent removal of the polymer template 3-D assemblies of nanowires are synthesized. Since the nanowires adopt the exact shape of the host etched ion-track, their diameter can be adjusted between ~15 nm and few μm, and their length between ~1 and several tens of μm.

In this talk, I will show recent examples illustrating how the unique combination of electrochemical deposition and etched ion-track membranes provides an excellent platform for (i) controlling semiconductor nanowire growth, (ii) synthesizing 3-D nanowire assemblies, and (iii) investigating their size-dependent properties. The implementation of the nanowire assemblies in photoelectrochemical and thermoelectric devices will be also discussed.

ADVANCED NANOCARBON MATERIALS FOR SOLAR ENERGY CONVERSION SCHEMES

Dirk M. Guldi[1]

[1]*Department of Chemistry and Pharmacy 7 Interdisciplinary Center for Molecular Materials (ICMM), Friedrich-Alexander-Universitaet Erlangen-Nuernberg, Egerlandstr. 3, 91058 Erlangen, Germany*

Carbon is the key to many technological applications that have become indispensable in our daily life. Altering the periodic binding motifs in networks of sp^3-, sp^2-, and sp-hybridized C-atoms is the conceptual starting point for a wide palette of carbon allotropes. To this end, the past two decades have served as a test-bed for measuring the physico-chemical properties of low-dimensional carbon with the advent of fullerenes (0D), followed in chronological order by carbon nanotubes (1D), carbon nanohorns, and, most recently, by graphene (2D). These species are now poised for use in catalysis.

Expanding global needs for energy have led to a significant effort to develop alternatives to fossil fuels. While alternative sources for energy are already in use, they comprise a small percentage of the energy demands needed to carry us through the 21st century. No single source will solve the global needs, but the development of photocatalysis has vast potential as a point-of-use power source.

I report on our efforts regarding a unifying strategy to use the unprecedented charge transfer chemistry of 0D fullerenes, the ballistic conductance of 1D carbon nanotubes, and the high mobility of charge carriers in 2D graphene, together in a groundbreaking approach to solving a far-reaching challenge, that is, the efficient use of the abundant light energy around us. For example, hybrid materials based on nanocarbons and metaloxides are the ideal design for realizing breakthroughs in high photon conversion efficiencies suitable for the catalysis of water.

MULTIVALENT (III, IV, V, AND VI) AMERICIUM SELF-RADIOLYSIS

Gregory P. Horne[1], Travis S. Grimes[1], Christopher J. Dares[2], Simon M. Pimblott[1], Stephen P. Mezyk[3], and Bruce J. Mincher[1]

[1]Idaho National Laboratory, 1955 N. Fremont Ave., Idaho Falls, Idaho 83415, United States
[2]Department of Chemistry, Florida International University, Miami, FL 33199, USA.
[3]Department of Chemistry and Biochemistry, California State University, Long Beach, CA 90804, USA.

The efficient separation of americium (Am) from nuclear waste fission products is one of the key challenges in the design of advanced spent nuclear fuel (SNF) reprocessing strategies. The difficulty in Am separation arises from the predominance of its' trivalent oxidation (Am(III)) state, which exhibits similar chemical properties to the trivalent lanthanides. One approach to effect this separation is to oxidise Am(III) to its higher americyl oxidation states (AmO_2^{n+})[1,2] and then extract using traditional SNF reprocessing solvent system formulations, e.g. 30% tributyl-phosphate in dodecane contacted with concentrated aqueous nitric acid (HNO_3).

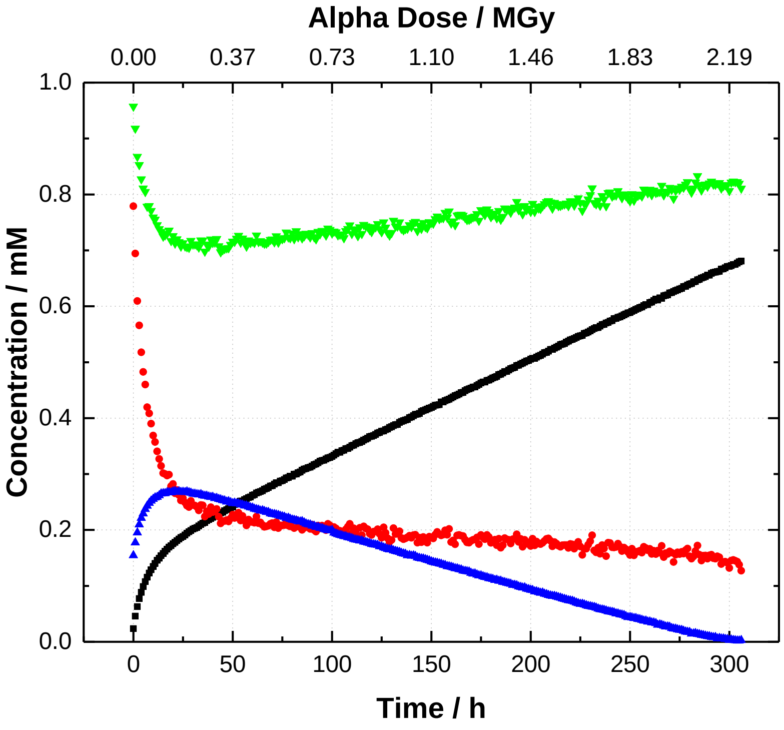

Figure 1 - Concentration of Am(III)(■), Am(V)(●), Am(VI)(▲), and Am Mass Balance (▼) for the autoreduction of 0.96 mM ^{243}Am in 6.5 mol dm^{-3} HNO_3.

The limitation of this methodology is the lifetimes of the americyl states, the chemistries of which are less well-understood, but have recently been demonstrated to be influenced by the radiolysis products of HNO_3.[3] The significance of these findings is that under process conditions, a SNF reprocessing solvent system is subjected to an intense multi-component radiation field (γ-rays, α-particles, β-particles, neutrons, and fission fragments). Consequently, fully understanding the fundamental radiation induced redox chemistry of americium's oxidation states is pertinent to the design of effective SNF reprocessing strategies.

Here we present a complete multi-scale mechanistic understanding of the complex radiation chemistry of multi-valent (III, IV, V, and VI) americium in irradiated aqueous HNO_3 (1, 3, 6.5, and 9 mol dm^{-3}), induced by self-radiolysis (alpha irradiation from ^{243}Am radioactive decay). Further, we report indirect evidence for the steady-state existence of Am(IV), a species long considered as a highly oxidizing transient (E^o = 2.62 V vs. SCE), stable under harsh, complexing conditions.[4-7]

References

(1) Dares, C. J.; Lapides, A. M.; Mincher, B. J.; Meyer, T. J., Electrochemical Oxidation of ^{243}Am(III) in Nitric Acid by a Terpyridyl-Derivatized Electrode. *Science*, **2015**, *350*, 652-655.

(2) Runde, W. H.; Mincher, B. J., Higher Oxidation States of Americium: Preparation, Characterization and Use for Separations. *Chem. Rev.*, **2011**, *111*, 5723-5741.

(3) Grimes, T. S., Horne, G. P., Dares, C. J., Pimblott, S. M., Mezyk, S. P., Mincher, B. J., Kinetics of the Reduction of Hexavalent Americium in Aqueous Nitric Acid. *Inorg. Chem.*, **2017**, *56*, 8295-8301.

(4) Asprey, L. B.; Penneman, R. A. Preparation and Properties of Aqueous Tetravalent Americium. *Inorg. Chem.*, **1962**, 1, 134-136.

(5) Myasoedov, B. F.; Lebedew, I. A.; Milyukova, M. S.; Production and Properties of Americium and Other Elements in Highest States of Oxidation in Phosphoric Acid Solutions. *Revne de Chimie Minerale*, **1977**, 14, 160-171.

(6) Picart, S.; Chartier, D.; Donnet, L.; Adnet, J. M. Electrochemical Oxidation of Americium in Nitric Acid: Study of Reaction Mechanisms. *Scientific Report*, **1999**, 1-7.

(7) Yanir, E.; Givon, M.; Marcus. Y. Direct Determination of the Formal Potential of the Am(IV), Am(III), and Am(VI)-Am(V) Couples in Phosphoric Acid. *Inorg. Nucl. Chem. Lett.*, **1970**, 6, 415-419.

FROM THE FUNDAMENTAL RADIATION CHEMISTRY OF ACETONITRILE TO MECHANISTIC PULSE RADIOLYSIS STUDIES OF CATALYTIC CO_2 REDUCTION

David C. Grills[1], Sergei V. Lymar, James T. Muckerman, Dmitry E. Polyansky, and Etsuko Fujita

[1]*Chemistry Division, Brookhaven National Laboratory, Upton, NY 11973-5000, USA*

Our research seeks a fundamental understanding of the processes involved in the capture and chemical conversion of solar energy, often using transition metal complexes as catalysts. Since these processes can involve multiple redox states, many of which are transient in nature, pulse radiolysis is a powerful method for their rapid production and subsequent interrogation by time-resolved spectroscopic methods.[1] While UV-vis transient absorption is an important technique for monitoring radiolytically-generated intermediates, we have coupled nanosecond time-resolved infrared detection with pulse radiolysis (PR-TRIR), targeting improved characterization to gain a better mechanistic understanding of energy-related processes.[2]

We are applying PR-TRIR to a diverse range of systems, including fundamental studies of the radiation chemistry of non-aqueous solvents, and the investigation of other physical processes that underpin energy conversion, such as ion pairing and charge delocalization. In addition to these fundamental investigations, we are using PR-TRIR to characterize specific intermediates involved in artificial photosynthetic processes, such as metal-hydrides and metal-CO_2 adducts, and to reveal mechanistic details of CO_2 reduction, not only in organic solvents but also in aqueous solution.[1]

Radiolytic Formation of the Carbon Dioxide Radical Anion in Acetonitrile

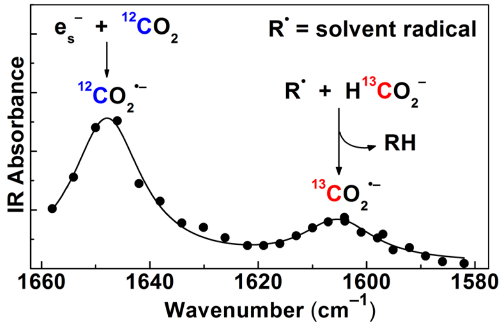

Fig. 1 - TRIR spectrum recorded 60 ns after PR of CD_3CN containing 28 mM $^{12}CO_2$ and 50 mM $H^{13}CO_2^-$.[3]

The carbon dioxide radical anion ($CO_2^{\bullet-}$) is often used as a versatile reductant ($E°(CO_2/CO_2^{\bullet-})$ = –1.90 V vs SHE) for mechanistic pulse radiolysis studies in water, where $CO_2^{\bullet-}$ can be generated through both the reduction of dissolved CO_2 by the solvated electrons (e_s^-), and the oxidation of added formate ion (HCO_2^-) via H-atom transfer scavenging of the radiolytically-generated radicals, $OH^\bullet$ and $H^\bullet$. While water is a heavily-used solvent, a large number of energy-related catalytic processes, e.g., CO_2 reduction, are carried out in organic solvents such as acetonitrile (CH_3CN). Unfortunately, the fundamental radiation chemistry of CH_3CN and the radiolytic production of $CO_2^{\bullet-}$ in this solvent are not well understood, limiting its use as a medium for pulse radiolysis. The properties and reactivity of $CO_2^{\bullet-}$ in CH_3CN are also of importance for understanding electrochemical CO_2 reduction in polar aprotic solvents. In this work, we have used PR-TRIR to unambiguously identify $CO_2^{\bullet-}$ in CH_3CN by its antisymmetric stretch at 1650 cm^{-1} following the reduction of CO_2 by e_s^- (Fig. 1).[3] In neat CH_3CN, $CO_2^{\bullet-}$ decays on a ~10 μs time scale via recombination with solvent-derived radicals ($R^\bullet$) and solvated protons. Upon addition of HCO_2^-, the radiation yield of $CO_2^{\bullet-}$ is substantially increased by H-atom transfer from HCO_2^- to $R^\bullet$ ($R^\bullet + HCO_2^- \rightarrow RH + CO_2^{\bullet-}$), which occurs in two kinetically separated steps due to the different H-atom abstracting abilities of the various $R^\bullet$

(Fig. 1 shows the initial step with isotopically-labeled $H^{13}CO_2^-$). The removal of solvent radicals by HCO_2^- also results in over a hundredfold increase in the $CO_2^{•-}$ lifetime. $CO_2^{•-}$ scavenging experiments suggest that at 50 mM HCO_2^-, ~60% of the solvent-derived radicals are engaged in $CO_2^{•-}$ generation. These studies open up the possibility of CH_3CN becoming a standard solvent for pulse radiolysis. Work is currently under way to identify alternative radical scavengers that will further enhance the yield of reducing species from $R^•$, and also allow the production of oxidants for the investigation of oxidative processes in CH_3CN.

Mechanistic Pulse Radiolysis Investigations of CO_2 Reduction Catalysis

The use of pulse radiolysis enables the production of highly reactive transient intermediates such as metal hydride, metal–CO_2, or metal–CO species. This in turn allows the advanced stages of a catalytic cycle to be interrogated, where steady-state concentrations of intermediates are typically small. An example is our recent PR-TRIR investigation of a well-known CO_2-to-CO reduction catalyst, $[Co^{II}(HMD)]^{2+}$ (HMD = 5,7,7,12,14,14-hexamethyl-1,4,8,11-tetraazacyclotetradeca-4,11-diene), in dry CH_3CN. We have shown that the generation of the doubly reduced $[(CO_2^{2-})Co^{II}(HMD)]$ intermediate by Na/Hg chemical reduction of $[Co^{II}(HMD)]^{2+}$ followed by CO_2 addition and pulse radiolysis, leads to the formation of $[(CO)Co^{I}(HMD)]^+$ *via* an oxide transfer reaction between $[(CO_2^{2-})Co^{II}(HMD)]$ and $[(CO_2^{2-})Co^{III}(HMD)]^+$ (see Scheme above). Owing to the strong binding between the Co^I metal center and the CO ligand, the formation of $[(CO)Co^{I}(HMD)]^+$ likely represents a deactivation pathway, resulting in the relatively low activity of this catalyst in dry organic solvents. The addition of a weak Brønsted acid (AH), e.g., water, increases the catalyst's activity by shifting the mechanism towards the protonation of the $[(CO_2^{2-})Co^{II}(HMD)]$ species. This PR-TRIR study demonstrates how the intricate interplay between reaction conditions and the reactivity of catalytic intermediates can control the mechanism of a CO_2 reduction reaction.

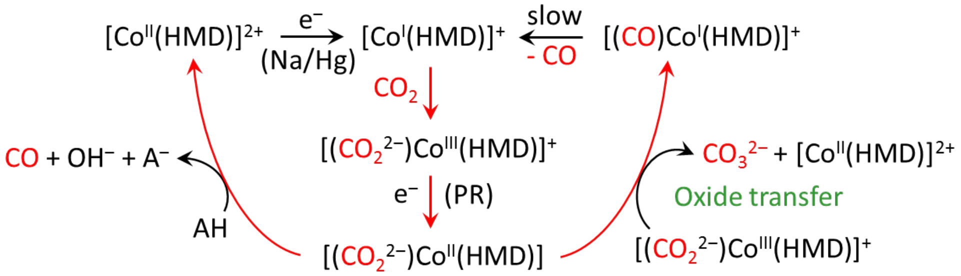

This work, and use of the BNL Accelerator Center for Energy Research, was supported by the US Department of Energy, Office of Basic Energy Sciences, under contract DE-SC0012704.

References

(1) Grills, D. C.; Polyansky, D. E.; Fujita, E. Application of Pulse Radiolysis to Mechanistic Investigations of Catalysis Relevant to Artificial Photosynthesis. *ChemSusChem* **2017**, *10*, 4359-4373.

(2) Grills, D. C.; Farrington, J. A.; Layne, B. H.; Preses, J. M.; Bernstein, H. J.; Wishart, J. F. Development of Nanosecond Time-Resolved Infrared Detection at the LEAF Pulse Radiolysis Facility. *Rev. Sci. Instrum.* **2015**, *86*, 044102.

(3) Grills, D. C.; Lymar, S. V. Radiolytic Formation of the Carbon Dioxide Radical Anion in Acetonitrile Revealed by Transient IR Spectroscopy. *Phys. Chem. Chem. Phys.* **2018**, *20*, 10011-10017.

PULSE RADIOLYSIS CREATES A REDOX LADDER TO THE TOP

Richard Marasas, Hung-Cheng Chen, Arpad Szarka and John R. Miller[1]

[1]*Chemistry Division, Brookhaven National Laboratory, Upton, NY 11973-5000, USA*

Redox potentials are widely used in chemistry to learn energetics of adding electrons or holes to molecules. They are usually measured electrochemically, most commonly by cyclic voltammetry. In the radiation chemistry of water, the redox potential for the strongest, “top” reducing agent, the hydrated electron, has long been known. This is often not true for nonaqueous media. Free energy ladders have been constructed before for oxidation of molecules in acetonitrile,[1] for reductions in the gas phase[2-4] and for triplet energies.[5] We describe here creation of a ladder for reductions in THF using methods pioneered by Dorfman[6]and used in our laboratory but for much less negative potentials.[7] The ladder connects known reduction potentials for molecules like biphenyl through a series of equilibria to the solvated electron in THF, thus determining its redox potential.

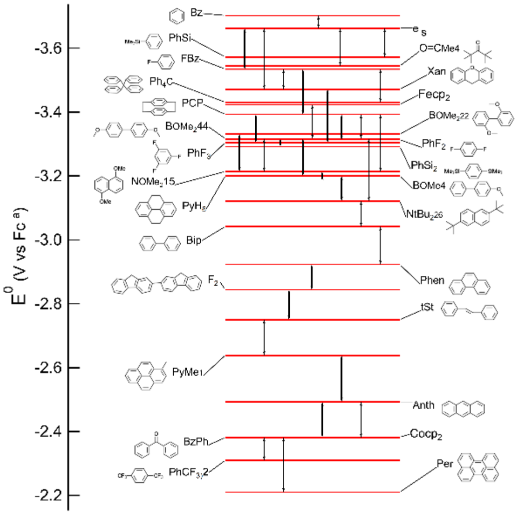

The ladder consists of free energy changes determined from equilibria of the type

$$D^{\bullet-} + A \rightleftharpoons D + A^{\bullet-} \qquad (1)$$

where the radical anion $D^{\bullet-}$ is an electron donor and A is an acceptor. The ladder enabled determination of reduction potentials for molecules which could not be measured electrochemically because the solvents or electrolytes break down at very negative potentials. Each step in the ladder was smaller than ~200 meV because equilibrium constants much larger than 1000 are difficult to determine. We did not succeed to determine a redox potential for acetone due to destruction of the radical anions by proton transfer reactions. Determination for dihydroanthracene failed for similar reasons, but succeeded for both in molecules having less acidic hydrogens.

(1) Merkel, P. B.; Luo, P.; Dinnocenzo, J. P.; Farid, S., Accurate Oxidation Potentials of Benzene and Biphenyl Derivatives Via Electron-Transfer Equilibria and Transient Kinetics. *J. Org. Chem.* **2009**, *74*, 5163-5173.
(2) Chowdhury, S.; Kishi, H.; Dillow, G. W.; Kebarle, P., Electron-Affinities of Substituted Nitrobenzenes. *Can. J. Chem.* **1989**, *67*, 603-610.
(3) Chowdhury, S.; Kebarle, P., Electron-Affinities of Dicyanoethylene and Tetracyanoethylene and Cyanobenzenes Based on Measurements of Gas-Phase Electron-Transfer Equilibria. *J. Am. Chem. Soc.* **1986**, *108*, 5453-5459.

(4) Chowdhury, S.; Heinis, T.; Kebarle, P., Radical-Anions - Electron-Affinities of Benzene, Naphthalene, and Anthracene Having the Substituents Cho, Cn, and No2. *J. Am. Chem. Soc.* **1986**, *108*, 4662-4663.

(5) Merkel, P. B.; Dinnocenzo, J. P., Thermodynamic Energies of Donor and Acceptor Triplet States. *J. Photochem. Photobiol. A* **2008**, *193*, 110-121.

(6) Arai, S.; Dorfman, L. M., Rate Constants and Equilibrium Constants for Electron Transfer Reactions of Aromatic Molecules in Solution. *Adv. Chem. Ser.* **1968**, *No. 82*, 378-86.

(7) Miller, J. R.; Calcaterra, L. T.; Closs, G. L., Intramolecular Long-Distance Electron Transfer in Radical Anions. The Effects of Free Energy and Solvent on the Reaction Rates. *J. Am. Chem. Soc.* **1984**, *106*, 3047.

PRIMARY PROCESS OF RADIATION CHEMISTRY OF LIQUID ALKANES STUDIED BY FEMTOSECOND PULSE RADIOLYSIS

Y. YOSHIDA[1]
[1]*ISIR, Osaka University, Japan*

Geminate ion recombination of electron and cation radical in liquid alkane is one of the most important process of the primary process of radiation chemistry. Recently, the precursors of the electron and the cation radical have been found in the femtosecond pulse radiolysis.

The precursor of electron showed higher mobility than the usual (thermalized) electron. That means that the geminate ion recombination occurs very rapidly in short time-region.

The precursor of the cation radical has the lifetime of several picoseconds in n-dodecane. The lifetime corresponds to the formation time of n-dodecane alkyl radical. That means the decomposition process occurs so quickly.

The primary process of radiation chemistry in liquid alkane will be reconstructed base on the recent results.

THE CHEMISTRY OF HYDROXAMIC ACIDS: DIRECT OBSERVATION OF ACYL NITROSO COMPOUNDS IN AQUEOUS SOLUTIONS

Eric Maimon[1], Amram Samuni[2], Sara Goldstein[3]

[1]*Nuclear Research Centre Negev, Beer Sheva, Israel*
[2]*Institute of Medical Research Israel-Canada, Medical School, The Hebrew University of Jerusalem, Jerusalem 91120, Israel*
[3]*Institute of Chemistry, The Accelerator Laboratory, the Hebrew University of Jerusalem, Jerusalem 91904, Israel*

Hydroxamic acids (RC(O)NHOH) form a class of compounds, which display interesting chemical and biological properties. Recent studies have highlighted their biological activities, which are associated with their ability to bind transition metal ions and to generate under oxidative stress nitroxyl (HNO) and nitric oxide (NO). The chemistry of RC(O)NHOH is associated with one- and two-electron oxidations forming the respective nitroxide radical ($RC(O)NHO^{\bullet}$) and presumably acyl nitroso (RC(O)N=O), respectively, which are relatively unstable species.

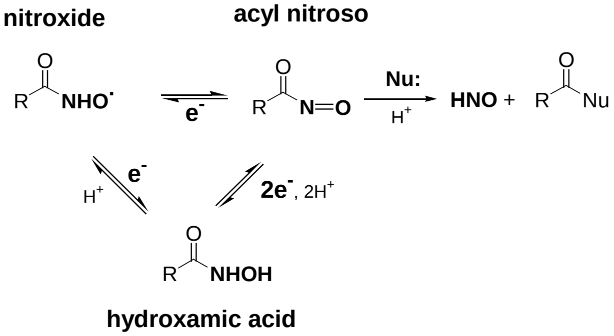

The presumed generation of acyl nitroso (nitrosocarbonyl) has been generally evidenced by trapping it with conjugated 1,3-dienes or by detection of N_2O, the product of HNO dimerization followed by dehydration. So far, the only direct evidence for acyl nitroso was provided by time-resolved infrared spectroscopy in non-aqueous solution.

Ionizing radiation was used to generate nitroxide radicals derived from various hydroxamic acids and study the kinetics of their self-decomposition as well as their oxidation by $^{\bullet}NO_2$. Both processes form a transient intermediate absorbing at 314 nm, which decays *via* a first-order reaction whose rate increases upon increasing the pH or the hydroxamic acid concentration. Transient intermediates absorbing around 314 nm are also formed upon the oxidation of the hydroxamic acids electrochemically or enzymatically by H_2O_2 and horseradish peroxidase. It is shown that HNO is formed during the decomposition of these intermediates, and therefore they are assigned to acyl nitroso compounds. This is the first direct spectrophotometric observation of acyl nitroso compounds in aqueous solutions allowing the study of their chemistry and reaction kinetics.

RADIATION PHYSICS AND CHEMISTRY OF NANOPARTICLES IN AQUEOUS MEDIA

F. Currell[1]

[1]*School of Mathematics and Physics, Queens University Belfast, Belfast BT7 1NN, United Kingdom*

Within the Centre for Advanced and Interdisciplinary Radiation Research (CAIRR) at Queen's University Belfast, one of our research focusses is the interactions of radiation with nanoparticles and the down-stream effects which take place. Our approach is inherently transdisciplinary, with both experiment and modelling approaches being used in roughly equal measure to understand systems applicable to both radiation nanomedicine and civil nuclear waste. Our modelling capabilities have been extended from our previously published work concerning the effects of energy transfer from nanoparticles into the surrounding media.[1-3] Using a multi-scale approach, we have now extended these calculations to account for systems containing clusters of nanoparticles (more than 1 million in some cases), thereby mimicking the situation typically found when nanoparticles are taken up by cells. Clinically relevant insights derived from such calculations will be presented.

Diffusive kinetics of reactive species in the aqueous phase have also been modelled in a new, quasi-analytical framework. Again, results of this modelling activity will be presented. Historical work concerning the generation of hydroxyl radicals[4] will be reviewed in the light of this modelling. Furthermore, results from new experiments will be presented concerning the radiolytic generation of hydrogen in magnox waste mimics, comprising $Mg(OH)_2$ nanoparticles in water. Here, instrumentation developments facilitate our determination of both absolute radiolytic yields and diffusivities without reference to external calibrants.

References

(1) McMahon,SJ; Hyland,WB; Muir,MF; Coulter,JA; Jain,S; Butterworth,KT; Schettino,G; Dickson,GR; Hounsell,AR; O'Sullivan,JM; Prise,KM; Hirst,DG; Currell,FJ "Clinical relevance of nanoscale energy deposition near irradiated heavy atom nanoparticles" Radiother Oncol. **100(3)**; 412-416; (2011)
([2) McMahon,SJ; Hyland,WB; Muir,MF; Coulter,JA; Jain,S; Butterworth,KT; Schettino,G; Dickson,GR; Hounsell,AR; O'Sullivan,JM; Prise,KM; Hirst,DG; Currell,FJ "Biological consequences of nanoscale energy deposition near irradiated heavy atom nanoparticles" Nature Scientific Reports, **1**, 18; (2011).
(3) Currell, F.J. and Villagomez-Bernabe, B. "Physical and Chemical Processes for Gold Nanoparticles and Ionising Radiation in Medical Contexts" (2017) in "Gold Nanoparticles for Physics, Chemistry and Biology (2nd edn)" Eds. Pluchery O. and Louis C. World Scientific ISBN: 978-1-78634-124-2
(4) Sicard-Roselli, C; Brun, E; Gilles, M; Baldacchino, G; Kelsey, C; McQuaid, H; Polin, C; Wardlow, N; Currell, FJ "A New Mechanism for Hydroxyl Radical Production in Irradiated Nanoparticle Solutions" Small **10** 3338-3346; (2014)

SELF-SUSTAINING LOW-ENERGY ELECTRON SOURCES FOR TARGETED SUB-CELLULAR DAMAGE

Benjamin P. Coughlin[1], Alex Pronschinske, Charles R. Mace, and E. Charles H. Sykes[1]

[1]*Tufts University, Department of Chemistry 62 Talbot Avenue, Medford, MA 02155*

High-energy radiation has been used for decades; however, the role of low-energy electrons (LEEs) created during irradiation has only recently begun to be appreciated. LEEs are the most important component of radiation damage in biological environments because they have subcellular ranges, interact destructively with chemical bonds, and are the most abundant product of ionizing particles in tissue. However, methods for generating them locally without external stimulation do not exist. To address this deficiency, we have synthesized one-atom-thick films of the radioactive isotope ^{125}I on gold that are stable under ambient conditions. Using a combination of surface science and microscopy, we directly observe nuclear transmutation of individual ^{125}I atoms into ^{125}Te, and explain the surprising stability of the 2D films as they underwent radioactive decay (*Nature Materials*, **2015**, 14, 904-907). Importantly, the metal interface geometry induces a 600% amplification of LEEs (<10 eV), compared with atomic ^{125}I. Moreover, our results reveal that the Auger electrons emitted during the ultrafast radioactive decay process have a kinetic energy corresponding to neutral Te. We are able to identify the reaction of newly formed Te to TeO_2 and its subsequent dimerization on the gold surface. The fact that the Te_2O_4 units stay intact during major lateral rearrangement of the monolayer illustrates their stability (*ACS Nano*, **2016**, 10, 2152-2158). We have extended these studies to targeted gold nanoparticles in cancer cells--where the same LEE enhancement exists--with the aim of creating targeted nanoemitters for cancer therapy.

A KINETIC MODEL FOR ELECTRON BEAM CONVERSION OF CO_2 / CH_4 TO COMMODITY CHEMICALS

Weiyao Gu[1] and Theodore S. Dibble[1]

[1]*Chemistry Department, State University of New York-Environmental Science and Forestry, Syracuse, NY 13210*

Electron beams may be able to transform CO_2 to commodity chemicals (methanol, acetic acid etc.) less expensively than traditional processes using high temperature and pressure. Here we present a kinetic model to describe (and, hopefully, predict) yields of products upon electron beam irradiation of a CO_2-CH_4 mixture at atmospheric pressure. The first generation of reactive species (cations and radicals) react primarily with CO_2 and CH_4, alongside with high-energy electrons. At this point, the model includes 200 chemical species and 1500 reactions. The bulk of the species in the model are radicals, cations, and anions. We have complied rate constants for reactions of three types: ion + neutral, electron + neutral, cation + anion (where thermal electrons are included among the "ions"). Our simulation shows large amounts of CO, H_2, and H_2O are generated in a short period, with accumulation of methanol, formic acid, and several hydrocarbons over time. We will present insights on the processes controlling formation of commodity chemicals. Future work will focus on validating the model against experiments that are yet to be carried out.

AU@TIO$_2$ FABRICATED THROUGH X-RAY RADIOLYSIS AND THEIR APPLICATION AS POTENTIAL RADIOSENSITIZERS

M.C. Molina Higgins[1]

[1]*Mechanical and Nuclear Engineering, Virginia Commonwealth University, 401 West Main St, Richmond, Virginia 23284-306730. molinahiggimc@vcu.edu*

Research on methods that enhance the absorbed dose in tumors are of valuable interest in radiotherapy as they may reduce the collateral damage to healthy tissue. One of these techniques is radiosensitization where nanomaterials are used to increase radiation effectiveness during treatment. This work aims to produce and evaluate gold-titania (Au@TiO$_2$) nanocomposites (NCs), for its use as potential radiosensitizers. Au@TiO$_2$ NCs were fabricated using X-rays, a method that departs from traditional synthesis and provides low by-product formation, which is fundamental for medical applications. Au NPs were supported on TiO$_2$ with either particle size distributions of 5-10 nm or 10-30 nm, using different ligands such as NaOH or urea and under different absorbed doses ranging from 0.1 KGy to 7.6 KGy, in order to determine the effects of these parameters in the final Au nanoparticle size and loading. The use of high absorbed doses (7.6 KGy) produced Au particles of 1.1 ± 0.1 nm, herein the size was not affected by the choice of ligand, meanwhile at low absorbed doses (0.72 KGy) the ligand affected the Au particle size, resulting in a size reduction of 20% when NaOH was used. The radiosensitization assessment of Au@TiO$_2$ NCs was made by monitoring the decomposition of a Methylene Blue (MB) solution under X-rays in the presence of Au@TiO$_2$ NCs. The dye containing the nanomaterial was irradiated at different operating voltages (50 KV and 225 KV) and results showed that the presence of Au@TiO$_2$ NCs increased MB decomposition rate by a factor of ~ 3.8.

EFFECTS OF RADIATION IN SLURRY SYSTEMS CONTAINING ALUMINUM (OXY)HYDROXIDES

Patricia L. Huestis[1], Josiane A. Kaddissy, Jay A. LaVerne[1]

[1]*University of Notre Dame, Notre Dame, IN 46556*

High-level waste (HLW) from legacy plutonium production is mainly stored in 177 tanks at the Hanford Washington site and the waste is difficult to handle given the hostile environment due to the ionizing radiation, extreme alkalinity, and high salt content.[1] Boehmite (γ-aluminum oxyhydroxide) and gibbsite (γ-aluminum hydroxide) are problematic solids present in the tanks and their removal is essential for final storage of the waste in glass matricies.[2] A fundamental understanding of how these solids age in the tanks is essential for safe and efficient processing of HLW.

The radiolytic stability of boehmite and gibbsite with adsorbed water was investigated using Raman spectroscopy, powder X-Ray Diffraction (pXRD), and X-ray Photoelectron Spectroscopy (XPS). Raman and pXRD revealed that the bulk structure of both boehmite and gibbsite were relatively radiation stable, even when subjected to large doses using 5 MeV He ions. However, surface sensitive techniques such as XPS revealed the reduction of Al^{3+} to aluminum metal and the formation of a currently unidentified oxygen bond in both boehmite and gibbsite.[3] The latter is thought to be an embedded displaced oxygen atom.

The completion of the baseline study provides a solid background for moving forward into slurry systems in order to understand the effects of the environment on surfaces. These slurry systems will gradually increase in complexity to mimic conditions present in the waste tanks. Current efforts are aimed at quantifying the dissolution of aluminum in environments of high nitrates and high pH using Inductively Coupled Plasma Optical Emission Spectroscopy (ICP-OES).

(1) Babad, H.; Cash, R. J.; Deichman, J. L.; Johnson, G. D., High-priority Hanford Site radioactive waste storage tank safety issues: An overview. *Journal of Hazardous Materials* **1993,** *35* (3), 427-441.
(2) Peterson, R. A.; Buck, E. C.; Chun, J.; Daniel, R. C.; Herting, D. L.; Ilton, E. S.; Lumetta, G. J.; Clark, S. B., Review of the Scientific Understanding of Radioactive Waste at the U.S. DOE Hanford Site. *Environmental Science & Technology* **2018,** *52* (2), 381-396.
(3) Huestis, P.; Pearce, C. I.; Zhang, X.; N'Diaye, A. T.; Rosso, K. M.; LaVerne, J. A., Radiolytic stability of gibbsite and boehmite with adsorbed water. *Journal of Nuclear Materials* **2018,** *501*, 224-233.

ALPHA PARTICLE IRRADIATION OF BULK AND EXFOLIATED MOS$_2$ AND WS$_2$ MEMBRANES

Liam H. Isherwood[1,2], Robyn E. Worsley[1], Cinzia Casiraghi[1], and Aliaksandr Baidak[1,2]

[1] School of Chemistry, University of Manchester, Oxford Road, Manchester, M13 9PL, United Kingdom

[2] Dalton Cumbrian Facility, University of Manchester, Westlakes Science and Technology Park, Moor Row, Cumbria, CA24 3HA, United Kingdom

2D transition metal dichalcogenide (TMDC) nanosheets are promising materials for future electronic, photonic and sensor applications. Unlike the well-known "scotch tape" method used to produce mechanically exfoliated flakes, liquid phase exfoliation (LPE) is a scalable and low-cost technique to produce few-layer nanosheets from bulk material. However, the radiation damage mechanisms in TMDC nanosheets produced by LPE haven't been studied before. This knowledge is critical for paving the way to commercialisation of 2D material based devices with intended operation in radiation fields.

We administered 1.66 MeV alpha particles to both bulk and liquid phase exfoliated MoS$_2$ and WS$_2$ membranes to two different fluences. Raman spectroscopy shows that the out- of-plane ($\boldsymbol{A_{1g}}$) and doubly degenerate in-plane ( ) $_{\boldsymbol{2g}}$ vibrational modes of bulk MoS$_2$ blueshift after irradiation whilst a reduction in the phonon lifetime is observed. He^{2+} ion irradiation induces a blueshift and mean peak-width decrease of the 2LA(M) phonon mode of bulk WS$_2$ with increasing fluence. Interestingly, the invariance of the Raman spectra of exfoliated TMDCs suggests they are more radiation stable than their bulk counterparts.

Raman spectroscopy, in agreement with energy dispersive x-ray spectroscopy, shows that amorphous carbon is present in the exfoliated membranes after irradiation. It is suggested that this material is formed by radiolytic amorphisation of residual solvent (N-methyl-2-pyrrolidone) retained within the ripplocations of the nanosheets during LPE. The relative radiation stability of the liquid phase exfoliated nanosheets is expected to arise from attenuation and dissipation of the ion beam energy by the residual solvent and the amorphous carbon subsequently produced.

References:

(1) L.H. Isherwood, R.E. Worsley, C. Casiraghi and A. Baidak, *Nucl. Instrum. Meth. Phys. Res. B*, 2018, (DOI: 10.1016/j.nimb.2018.01.018)

DIRECT OBSERVATION OF DISSOCIATIVE RIOSETHYMIDINE RADICAL ANION GENERATED FROM ELECTRON ATTACHMENT IN COMPETITION WITH ELECTRON SOLVATION

Jun MA[1], Shinichi Yamashita, Yusa Muroya, Shu Seki.

[1]*Department of Molecular Engineering, Kyoto University, Japan*

In the action of slowing down the secondary electrons (SEs) in radiation biology, low-energy electrons (LEEs; 0-20 eV) can induce DNA strand breaks via dissociative electron attachment (DEG). The end point of SEs is fully trapped as the solvated electron, which only forms a stable anion radicals with DNA nucleotide without leading to subsequent bond dissociation. It is not clear yet whether the presolvated electron dissociates DNA components.

Previous pulse radiolysis studies of presolvated electron scavenging have been based on the observation of the decreasing of initial yield / absorbance of solvated electron on by rising the concentration of scavengers. (Hunt *et al*, Jonah *et al* and LaVerne *et al*.). The detail mechanism the electron reactivity at the multiply stage of solvation has been missing for decades due to a severe limitation of the time resolution in currently-available high-energy pulse radiolysis techniques to typically sub-picosecond time scales.

In this work using picosecond pulse radiolysis, we resolved the solvation of electrons in diethylene glycol and investigated the reactions of presolvated electron with DNA models (ribothymidine) in real time. It shows only high-lying states of electron dissociate DNA.

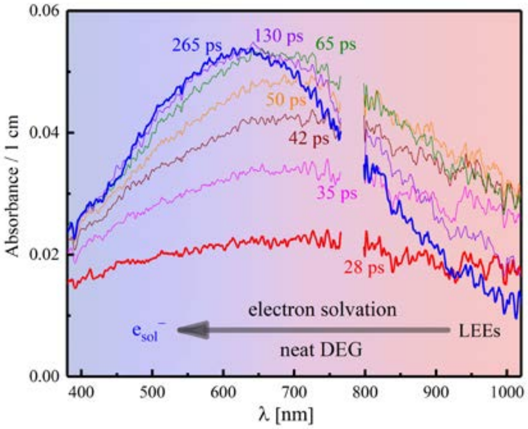

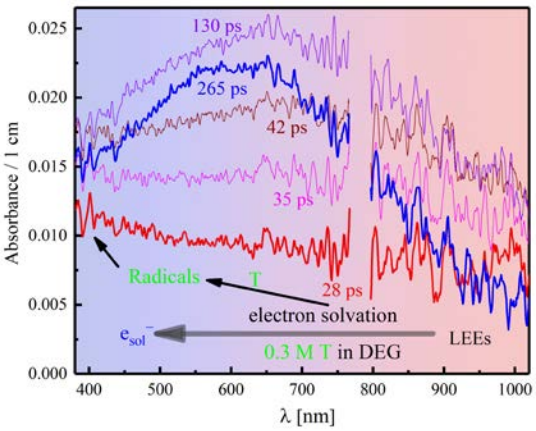

SEQUENTIAL MEV IMPLANTATION EFFECT ON THE REFRACTIVE INDEX AND NANOPARTICLE NUCLEATION IN SILICA

J. D. Demaree[1], C. Umerah[2], Z. Luo[3], and D. ILA[3]

[1]*US Army Research Laboratory, Aberdeen Proving Ground, MD 21005*

[2]*Department of Materials Science and Engineering, Tuskegee University, Tuskegee, AL 36088*

[3]*Department of Chemistry and Physics, Fayetteville State University, Fayetteville, NC 28301*

In this work we have studied changes in the optical properties of Infrasil (Heraeus high-purity optical quality fused quartz silica) before and after the sequential implantation of 1.450 MeV Au and 0.785 MeV Ag ions using a National Electrostatics 5SDH-2 tandem accelerator. An area several millimeters in size was uniformly implanted using a step-by-step method in which the sample was moved stepwise in horizontal and vertical directions in submillimeter increments. Samples were prepared using two processing sequences: 1) a Au-implanted sample was annealed to form Au nanoparticles before subsequent Ag implantation and a final annealing step, and 2) a Au-implanted sample was immediately implanted with Ag, and then annealed to form metallic nanoparticles.

The samples were studied using optical absorption photo spectrometry after each annealing step to assess the nucleation and characteristic absorption of metallic nanoparticles. Rutherford Backscattering Spectrometry (RBS) was used to confirm the implantation dose and the uniformity of the implanted area. Changes in the refractive index of the implanted substrate were observed using a 3D optical profilometer.

We have observed that the defects induced by a second round of heavy ion bombardment facilitates subsequent substrate healing during annealing and nanocluster formation, returning the matrix index of refraction to the value for a pristine substrate. Under some conditions studied, however, a localized regimented change in the index of refraction was noted using a 3D optical profilometer, on length scale corresponding to the lateral steps used in the implantation method, perhaps from the enhanced production of nucleation sites or diffusion traps in heavily bombarded regions during the second-stage heavy ion implantation. Recent findings on these observations will be discussed, including polarization phenomena observed in the 3D optical profilometer.

AN INTEGRATED STRATEGY FOR PREPARATION OF NANOFIBROUS ADSORBENT FOR CO_2 CAPTURE BY ELECTROSPINNING AND RADIATION INDUCED GRAFTING

Ali Abbasi,[1] Mohamed Mahmoud Nasef,[2,3] Ebrahim Abouzari,[1] and Arshad Ahmad[1]

[1]Center of Hydrogen Energy, Universiti Teknologi Malaysia, Kuala Lumpur, Malaysia.
[2]Chemical Engineering Department, Universiti Teknologi PETRONAS, Seri Iskandar, Perak, Malaysia.
[3]Malaysia-Japan International Institute of Technology, Universiti Teknologi Malaysia, Kuala Lumpur, Malaysia.

The growing concern over the increase of CO_2 emissions resulting mainly from burning fossil fuel is reaching a critical level that is calling for an intervention to find a solution for the climate change and global warming. Various technologies have been proposed for CO_2 capture including absorption with chemical solutions and adsorption. The former method is challenged by high operational cost and environmental concerns whereas the latter is challenged by issues pertaining CO_2 adsorption rate and capacity, regeneration energy and cost of the adsorbent.[1] Radiation induced grafting (RIG) is an attractive technique allowing modification of polymeric substrates into functional materials for environmental remediation. The presence of substrates in nanofibrous form imparts an enhanced separation properties caused by high surface area and eliminates diffusion limitations existing in their corresponding commercial microporous ionic resins.[2] Thus, integration of electrospinning and RIG is likely to provide a powerful technique for preparation of appealing adsorbent materials for CO_2 capture.

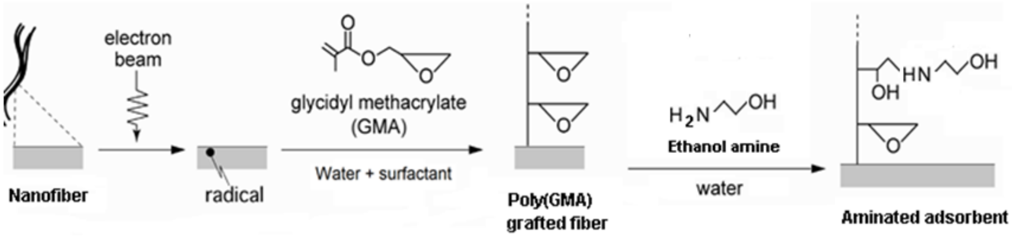

Fig. 1 - Schematic diagram for prepare of nanofibrous adsorbent containing amine group.

In this contribution, we report an integrated strategy for preparation of a new amine-containing nanofibrous adsorbent for CO_2 capture at ambient conditions. It involves electrospinning of syndiotactic polypropylene (s-PP), irradiation of the s-PP nanofibrous substrate with an electron beam (EB) followed by RIG of glycidyl methacrylate (GMA) onto the nanofibrous substrate and subsequent amination with enthanol amine as shown in Fig. 1. The parameters in every stage (electrospinning, grafting and amine treatment) were optimized. The physico-chemical properties of the obtained adsorbent were investigated using various techniques including scanning electron microscope (SEM), differential scanning calorimetry (DSC), thermogravimetric analysis (TGA), Fourier transform infrared spectroscopy (FTIR), and Brunauer–Emmett–Teller porosity analysis (BET). The adsorbent affinity to CO_2 was evaluated in a fixed bed column using a binary mixture of CO_2/N_2 containing 10% CO_2. The breakthrough curves were established at different temperatures. The adsorption and desorption cycles were also evaluated.

The s-PP was successfully dissolved in a three-solvent mixture composed of decalin, acetone and dimethylformamide at a weight ratio of 80:10:10. The fiber diameter and morphology of electrospun s-PP nanofibers were found to be dependent on electrospinning parameters such as polymer solution concentration, applied voltage, flow rate and needle tip to collector distance.

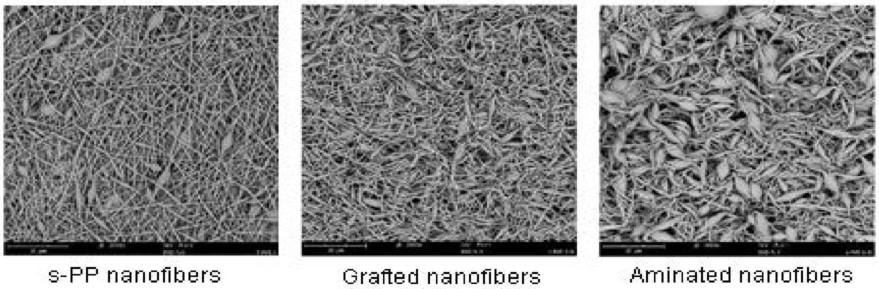
s-PP nanofibers
Grafted nanofibers
Aminated nanofibers

Fig. 2 - SEM images of pristine s-PP nanofibers and its crossponding grafted and aminated samples.

The degree of grafting (DG) of GMA on s-PP nanofiber was found to be a function of absorbed dose, monomer concentration, temperature and time. The amine density on the obtained adsorbent was found to be dependent on the amine agent concentration, temperature and reaction time. The fibers diameters were increased by incorporation of poly(GMA) and subsequent amination with beads left on the fibers as depicted from SEM images in Fig. 2.

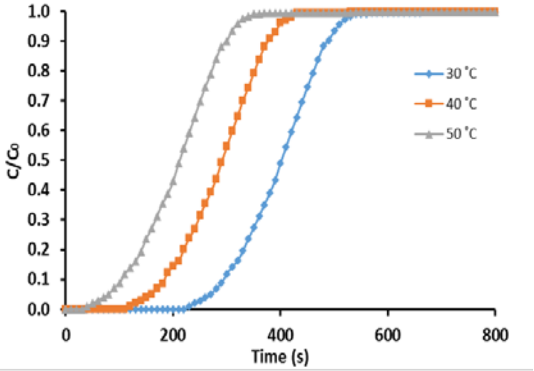

Fig. 3 - Breakthrough curves for CO_2 adsorption at different temperatures (CO_2 conc. = 10 %, pressure = 1 bar, flow rate = 50 ml/min; DG = 300%; DA = 94% and RH = 80%).

The aminated adsorbent showed a maximum CO_2 adsorption capacity of 2.57 mmol/g-adsorbent for a sample with DG of 300% and degree of amination (DA) of 94%. Higher temperatures reduced the breakthrough time without altering the adsorption dynamics suggesting higher mass transfer with the temperature increase. The regeneration of the CO_2 saturated adsorbent was carried out at 80°C during 15 minutes. The adsorbent showed adsorption consistency during 4 adsorption/desorption cycles suggesting a potential for CO_2 capture at ambient condition.

References

(1) Lee, S.-Y.; Park, S.-J. A review on solid adsorbents for carbon dioxide capture. J. Ind. Eng. Chem. 2015, 23, 1–11.
(2) Nasef, M. M.; Ting, T. M.; Abbasi, A.; Layeghi-moghaddam, A., Alinezhad, S. S.; Hashim, K. Radiation grafted adsorbents for newly emerging environmental applications. Rad. Phys. Chem. 2016, 118, 55–60.

SUPPORTED TRANSITION METAL NANOMATERIALS: RADIATION SYNTHESIS AND THEIR USE IN MEDICAL AND ENVIRONMENTAL APPLICATIONS

Jessika Rojas[1]

[1]*Virginia Commonwealth University, Department of Mechanical and Nuclear Engineering, Richmond, VA 23284*

With the current trends in nanotechnology, there is a need for revolutionary methods in nanomaterial synthesis that drastically improves control of physical properties coupled with scalability and simplicity. Special attention is given to those techniques whose implementation of the manufacturing process are considerably easier than current ones. For example, methods that do not require the use of harsh chemicals nor the use of high temperatures and pressures are desirable. On this effort, radiation chemistry has demonstrated a huge advancement in nanoparticle synthesis.[1-4] The interaction of high energy ionizing radiation, such gamma rays and X-rays, with aqueous solutions leads to the generation of randomly distributed reducing and oxidizing agents having large redox potentials. Through the use of appropriate scavengers, such as secondary alcohols, the environment in the reaction solution will generate an increased reducing agent concentration. These reductive species readily react with solvated metal ions and reduce their oxidation state.[6] Subsequently, metallic atoms obtained in solution move towards the nucleation and growth process. This synthesis method represents an environmentally benign approach that eliminates the need for excessive reducing agents that compromise the nanomaterial performance. Moreover, radiolytic syntheses are carried out under desirable conditions for a large number of applications (i.e. catalysis, drug delivery) such as aqueous media and ambient temperature and pressure.

Particle growth is controlled by addition of surfactants, polymers or various substrates, otherwise referred to as supports, which enhance the formation of well dispersed nanoparticles. Furthermore, the combination of nanoparticles with supports can offer desirable synergisms not solely presented by the substrate or nanoparticles.[7] Thus, supported nanoparticles offer a huge diversity of applications. Given the advantages of ionizing radiation methods to synthesize nanomaterials and modify their characteristics, this work focuses on the progress of morphological control and distribution of particle size by judiciously varying parameters including absorbed dose, dose rate, concentration of metal precursor, and stabilizing agents. In addition, the opportunities to develop and exploit other accessible ionizing radiation sources such as X-rays are discussed. Results on metal nanoparticles on carbon supports and oxides are shown below.

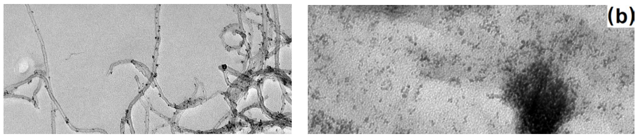

Figure 1 - TEM images of a)Ru nanoparticles onto carbon nanotubes[2] and b)Ir nanoparticles on graphene oxide synthesized through gamma irradiation[3]

Carbon supports such as nanotubes and graphene have evidenced useful thermal and chemical stability properties making them an advantageous choice for nanoparticle supports. Figure 1 shows ruthenium and iridium nanoparticles synthesized using gamma irradiation with an absorbed dose of 60 kGy at a dose rate of ~7 kGy/h (0.7

Mrad/h). This process leads to homogeneously distributed nanoparticles with an average size ~2 nm.

Oxide-supported metal nanoparticles open a wide variety of applications in several medical and engineering fields such as drug delivery, nanoelectronics, optics, and catalysis. Among them, Au decorated on TiO2 (anatase) has received significant attention due to their unique physical and chemical properties, which are controlled by the particles' characteristics. X-ray irradiation has been successfully implemented to synthesize Au on TiO_2 having particle sizes from 6 nm down to 2nm by varying the absorbed dose. Our results indicate that high radiation doses lead to smaller Au NPs on the surface of the support.

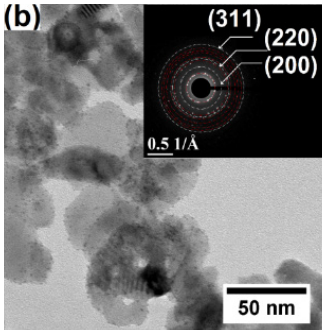

Figure 2 - TEMs of Au@TiO2(10-30nm), with inset of SAED pattern showing Au and TiO_2 (anatase) reflections[5]

Figure 2 shows a TEM image of TiO_2 decorated with Au nanoparticles using X-ray irradiation. Au nanoparticles have an average size of 1.3nm

Oxide-supported metal nanoparticles hold promise as radiosensitizers. Radiosensitizers are materials that amplify the radiation dose in the region where they are located, thus increasing the radiation damage. We will review the radiosensitization mechanisms in the basis of interaction of radiation with matter and radiation chemistry. Results obtained with Au@TiO_2 will be presented and their potential use in applications such as targeted radiation therapy and accelerated decomposition of dyes will be discussed.

References

(1) Belloni, J.; Mostafavi, M., Radiation Chemistry of Nanocolloids and Clusters. In *Radiation Chemistry: Present Status and Future Trends*, Jonah, C. D.; Rao, B. S. M., Eds. Elsevier: 2001; pp 411-452.

(2) Rojas, J. V.; Toro-Gonzalez, M.; Molina-Higgins, M. C.; Castano, C. E., Facile Radiolytic Synthesis of Ruthenium Nanoparticles on Graphene Oxide and Carbon Nanotubes. *Materials Science and Engineering: B* **2016**, *205*, 28-35.

(3) Rojas, J. V.; Molina Higgins, M. C.; Toro Gonzalez, M.; Castano, C. E., Single Step Radiolytic Synthesis of Iridium Nanoparticles onto Graphene Oxide. *Applied Surface Science* **2015**, *357*, 2087-2093.

(4) Rojas, J. V.; Castano, C. H., Production of Metal Nanoparticles on Carbon Nanotubes by Gamma Irradiation. In *Radiation Synthesis of Materials and Compounds*, Kharisov, B. I.; Kharissova, O. V.; Mendez, U. O., Eds. CRC Press: 2013; pp 491-503.

(5) Molina Higgins, M. C.; Clifford, D. M.; Rojas, J. V., Au@Tio 2 Nanocomposites Synthesized by X-Ray Radiolysis as Potential Radiosensitizers. *Applied Surface Science* **2018**, *427*, 702-710.

(6) Belloni, J., Nucleation, Growth and Properties of Nanoclusters Studied by Radiation Chemistry. *Catal Today* **2006**, *113*, 141-156.

(7) Campelo, J. M.; Luna, D.; Luque, R.; Marinas, J. M.; Romero, A. A., Sustainable Preparation of Supported Metal Nanoparticles and Their Applications in Catalysis. *ChemSusChem* **2009**, *2*, 18-45.

IONIC-IMPRINTED POLYESTERS OF PYROMELLITATE-ALLYL ALCOHOL POLYMERIZED BY GAMMA RADIATION FOR SELECTIVE EXTRACTION OF URANYL IONS (UO_2^{2+})

A. Ramos-Ballesteros[1], E. Bucio

[1]*Departamento de Química de Radiaciones y Radioquímica, Instituto de Ciencias Nucleares, Universidad Nacional Autónoma de México, Circuito Exterior, Ciudad Universitaria, CDMX 04510, México.*

Among the main reasons why non-conventional uranium extraction sources are not the most used, is due to the high extraction costs associated with low concentrations and chemical forms that require extra purification processes (Romero Guzmán et al., 1995). Therefore, efforts should focus on cheaper extraction processes, develop more and better solid phase extraction materials and highlight the environmental benefits represented by the extraction of uranium from phosphate rocks and bodies of water. The main characteristics that must be met by materials designed for the extraction of uranium in water bodies are high extraction capacity, reversible interactions with the analyte, selectivity, resistance to environmental conditions and stability against ionizing radiation (Ahmadi et al., 2010).

Taking humic acids as an example; which are aromatic compounds of natural occurrence with a high density of carboxyl groups (Wei et al., 2007); ionic-imprinted resins were synthesized for the selective extraction of uranyl ions in aqueous solution, using polyesters of pyromellitic acid-allyl alcohol polymerized by gamma radiation as based material. On the one hand, Pyromellitic acid (benzen-1,2,4,5-tetracarboxylic acid) has the characteristic extraction capacities of humic compounds thanks to the presence of carboxyl groups (Barkleit et al., 2011), and, on the other hand, the existence of an aromatic ring in its structure confers resistance against gamma radiation, which extends to chains attached to the ring and even to different molecules present in the solution (LaVerne and Dowling-Medley, 2015).

Esters were synthesized from pyromellitic acid and allyl alcohol by condensation reactions to generate 2,5-bis((allyloxy)carbonyl)terephthalic acid; 4,6-bis((allyloxy)carbonyl)isophthalic acid and 4,5-bis((allyloxy)carbonyl)phthalic acid monomers. Then, resins were polymerized under different irradiation doses and the effect of ionic imprinting on the selectivity of uranium was compared. The extraction capacity (Q) of the resins obtained was evaluated by varying parameters such as pH, temperature, extraction time and ionic strength. Final materials were characterized by FTIR, NMR-H, UV-Vis, SEM and TGA.

RADICAL PROCESSES INVOLVING QUINOXALIN-2-ONE DERIVATIVES RELEVANT TO THEIR PHARMACOLOGICAL APPLICATIONS

K. Skotnicki[1], K. Bobrowski[1], J. De la Fuente[2], A. Cañete[3]

[1]*Institute of Nuclear Chemistry and Technology, Warsaw, Poland*
[2]*Universidad de Chile, Santiago de Chile, Chile*
[3]*Pontificia Universidad Católica de Chile, Chile*

Quinoxaline derivatives gained a great deal of attention, mostly due to their biological activity. They are concerned as a potential anticancer, antimicrobial, antifungal and anxiolytic drugs as well as inhibitors of enzymes activity.

In the first stage, spectral and kinetic properties of quinoxalin-2-one one-electron oxidation and reduction products have been characterized. In the context of potential quinoxalin-2-one interactions with protein receptors the second stage of research have focused on elucidation of radical processes involving quinoxalin-2-ones and selected amino acids. I have confirmed that tryptophan and tyrosine can be oxidized by products of quinoxalin-2-ones $N_3^{\bullet}$ oxidation products, yielding tryptophyl and tyrosyl radicals respectively. On the other hand 3-methylquinoxalin-2-one can be reduced by α-aminoalkyl radicals produced by means of $^{\bullet}OH$ oxidation of methionine. Second order reaction rates have been measured for aforementioned reactions with several C7-substituted quinoxalin-2-one derivatives.

In the final stage I have for the first time characterized spectral and kinetic properties of caroverine hydrochloride derived radicals. What is more, second-order rate constants have been measured for their reactions with Trp and Tyr. I have also confirmed the possibility of caroverine hydrochloride reduction by α-aminoalkyl radicals from Met.

In this work I have utilize pulse radiolysis technique based on linear electron accelerator, combined with UV-Vis spectrophotometry.

STRUCTURE OF LOW ENERGY ELECTRON SPURS IN WATER

Marisa E. Smith[1], Nicholas J.B. Green[2] & Simon M. Pimblott[1,3]

[1] School of Chemistry and Dalton Cumbrian Facility, The University of Manchester, U.K.
[2] Department of Chemistry, University of Oxford, U.K.
[3] Nuclear Science User Facilities, Idaho National Laboratory, U.S.A.

Monte Carlo simulation using experimentally based collision cross sections for low energy electrons (1- 100eV) in gaseous and amorphous ice water has been use to model and understand the physical and implicitly the chemical processes underpinning the attenuation of electrons in water.

The gamma radiolysis of water has a G-value yield of 0.45 molecules of H_2 per 100eV energy deposited. However, the experimental studies for radiolytic yields of H_2 from certain water-oxide systems can be two to three orders of magnitude larger. The mechanism for the excess production is unclear, and there is no current experimental evidence for excess production of oxidant, O_2 or H_2O_2. A current theory is that the increased yield is due to the transport of energy via low energy electrons from the solid oxide into the liquid water phase.

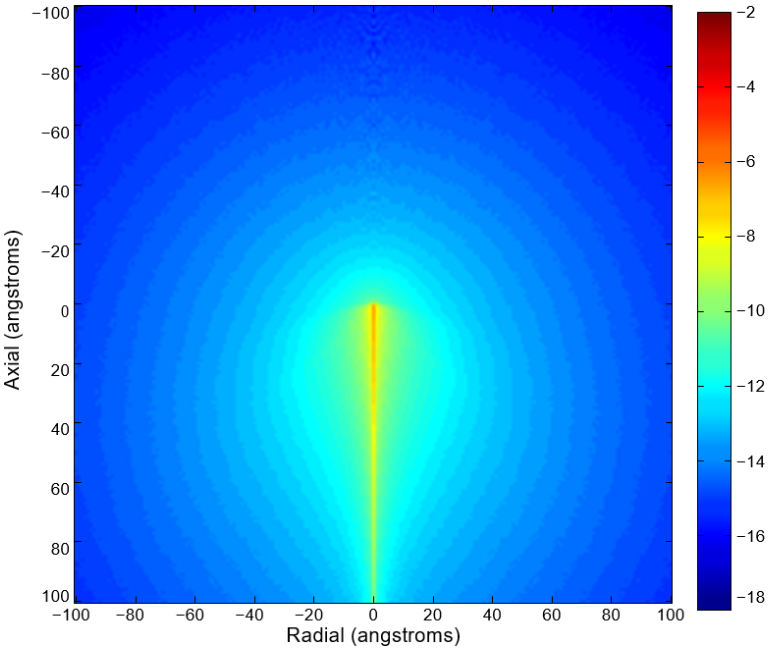

Figure 1 - The dose distribution of a 25 eV electron in amorphous solid water

The spur in water has always assumed to be spherical based on the premise that the effects of elastic collisions dominated those of inelastic collisions. Our simulations of the dose distribution derived from the energy attenuation of low energy electrons in condensed water suggest this assumption is not valid and the inelastic interactions dominate the electron track structure. For example, Figure 1 shows the spatial distribution of dose for 25 eV electrons in water.

The data presented will provide insight into the structure of low energy electron tracks in water. Specific comparisons will include the axial and radial components of the penetration and the distribution of the dose as a function of electron energy. The results will be explained by examining the average frequencies at which elastic and inelastic events occur in an electron track as a function of initial electron energy.

Acknowledgement. MES was a Presidential PhD Scholar at The University of Manchester. The research described is supported by the Dalton Cumbrian Facility Project, a joint initiative of The Nuclear Decommissioning Authority and The University of Manchester

PULSE RADIOLYSIS STUDY OF TYROSINE PEPTIDES – H$^+$ INFLUENCE ON PHENOXYL RADICALS FORMATION

Sebastian Sowinski[1], Slawomir Kadlubowski, Piotr Ulanski[1]

[1]Institute of Applied Radiation Chemistry, Lodz University of Technology, Lodz, Poland.

Oxidative stress induces changes in the structure of protein molecules that can influence their functionality, therefore study of amino acids and oligopeptides reactions with water radiolysis products (such as hydroxyl radicals) is relevant both in terms of naturally occurring radical processes and in controlled site-specific modifications that could possibly be used in medical and industrial applications (i.e. tyrosine cross-linking in synthesis of protein nanoparticles).
Two peptides, H-Gly-Tyr-Gly-OH and (H-Cys-Tyr-OH)$_2$, have been chosen as low-molecular-weight model particles that could possibly simulate behavior of tyrosine in more complex protein systems and its potentially protective activity towards disulfide bridge. Pulse radiolysis with spectrophotometric detection was a method of choice in this study. The research concentrated on the reactions of selected peptides with hydroxyl radicals and the modifications of the reaction environment that promotes the formation of phenoxyl radicals. Measurements were conducted on a wide range of aqueous solutions, also at low pH and/or with phosphate buffer addition in order to determine the influence of H$^+$ concentration on the formation of phenoxyl radicals on tyrosine residues. Peptide solutions in phosphate buffer were also investigated considering possible interaction between phosphate radicals and amino acid residues. Experimentally obtained reaction rate constants were double-checked using stochastic calculations in Kinetiscope software package.

Acknowledgments
The work has been partially financed by the National Science Centre, Poland, 2017/25/B/ST4/01110

UTILIZING RADIATION CHEMISTRY TO INVESTIGATE NUCLEATION AND GROWTH KINETICS OF METALLIC NANOCRYTALS

Mei Wang[1] and Taylor J. Woehl[1]

[1]Department of Chemical and Biomolecular Engineering, University of Maryland, College Park, MD, USA

Nucleation and subsequent growth mechanisms that control the shape and size of colloidal nanocrystals are still poorly understood due to the lack of experimental approaches capable of directly probing these processes. With the advent of in-situ liquid cell electron microscopy (LCEM), nucleation and growth process can be observed in real time at nanometer scale resolution. In liquid cell experiments, the electron beam serves as both the stimulus to induce nanocrystal formation and the imaging tool. In these experiments, water radiolysis stimulated by the imaging electron beam creates both oxidizing and reducing radicals. Among these species, aqueous electrons and hydrogen radicals are strong reducing species that can reduce precursor metal ions to metal atoms. However, oxidizing species ($\mathrm{OH}^{\cdot}, OO_2$) are produced at the same time, which oxidize metal atoms back to higher valences. Because of these multiple forward and backward reactions, which have not been considered previously, kinetics of nucleation and growth are poorly controlled during LCEM. Here we show that silver nanoparticles can be synthesized under strict kinetic control by adding tertiary-butanol, a typical $\mathrm{OH}^{\cdot}$ and OO_2 scavenger, and utilizing a microfluidic system. Various microscopy parameters were changed to systematically vary the dose rate and radical concentration by varying electron flux; numerical simulations were used to quantify the radical concentrations. In situ movies of nanocrystal nucleation and growth are converted to kinetic data using advanced image analysis and particle tracking. Our results demonstrate the effects of reaction rate on formation kinetics of silver nanocrystals and develop a new approach for investigating quantitative kinetics of nanoparticle formation.

RADIOLYTIC HYDROGEN PRODUCTION FROM THE WATER RADIOLYSIS IN CSH

YIN, C.[1], DANNOUX-PAPIN, A.[1], HAAS, J.[1], NGONO-RAVACHE, Y.[2], RENAULT, J-P.[3]

[1]CEA, DEN, MAR, DE2D, SEAD, Laboratoire d'études des Ciments et Bitumes pour le Conditionnement, 30207 Bagnols sur Cèze Cedex, France
[2]CIMAP, UMR CEA-CNRS-ENSICAEN-USBN, BP5133, 14070 Caen Cedex 5, France,
[3]CEA, DRF, IRAMIS, NIMBE, Université Paris Saclay, 91191 Gif-sur-Yvette Cedex, France

Water radiolysis is one of the consequences of the interaction between a cementitious matrix and low or intermediate-level radioactive wastes that are encapsulated within this matrix.[1] Thus, for safety assessment, the hydrogen released from the cementitious packages must be limited and quantified.

Up to now, the hydrogen production was thought to arise solely from the water trapped in the cement porous network.[3,4] However, recent experimental and theoretical indication suggest that the cement paste itself can play a significant role in H2 production.[2]

Calcium silicate hydrate (C-S-H) is the main hydrate (70%) of Portland cement. This present work is focused on the interactions between water and C-S-H, a nanocrystallized product with a layered chemical structure. The aim of this study is to understand the radiolytic mechanisms of the hydrogen production in hydrated C-S-H.

Therefore, after characterization by several techniques (nitrogen gas adsorption-desorption, X-ray diffraction, thermogravimetric analysis, infrared and Raman spectroscopies, small-angle X-ray scattering), C-S-H with different chemical composition and cured at different controlled relative humidities were submitted to gamma radiation and heavy ions beams to determine their H_2 radiolytic yield, $G(H_2)$[i]. The results show the H_2 production is strongly modified in highly confined system in comparison to the bulk water.

The EPR spectroscopy experiments using trapping molecules are in progress to reveal the reaction mechanisms involved. The present work would help us to understand the radiation effects in confined media and particularly in cements.

References

(1) Spinks, J. W. T.; Woods, R. J., An introduction to radiation chemistry. **1990**.

(2) Le Caër, S.; Dezerald, L.; Boukari, K.; Lainé, M.; Taupin, S.; Kavanagh, R. M.; Johnston, C. S. N.; Foy, E.; Charpentier, T.; Krakowiak, K. J.; Pellenq, R. J. M.; Ulm, F. J.; Tribello, G. A.; Kohanoff, J.; Saúl, A., Production of H2 by water radiolysis in cement paste under electron irradiation: A joint experimental and theoretical study. *Cement and Concrete Research* **2017,** *100* (Supplement C), 110-118;

(3) Bouniol, P.; Bjergbakke, E., A comprehensive model to describe radiolytic processes in cement medium. *Journal of Nuclear Materials* **2008,** *372* (1), 1-15;

(4) Bouniol, P.; Muzeau, B.; Dauvois, V., Experimental evidence of the influence of iron on pore water radiolysis in cement-based materials. *Journal of Nuclear Materials* **2013,** *437* (1), 208-215.

---

[i] *$G(H_2)$ represents the amount of H_2 produced per energy unit deposited in the system. It is expressed in mol.J^{-1}.*

A STANDARD-FREE PORTABLE X-RAY FLUORESCENCE MEASUREMENT METHOD OF THICKNESS OF THIN MANGANESE-RICH LAYERS ON SANDSTONE BUILDINGS

Richard A. Livingston[1], Carol A. Grissom[2], Gwénaëlle Kavich[2], and Nicole C. Little[2]

[1]*Dept. of Materials Science and Engineering, University of Maryland, College Park, MD*
[2]*Museum Conservation Institute, Smithsonian Institution, Washington, DC*

Black surface layers on the order of a few µm in thickness have been observed on the Smithsonian Castle and other sandstone buildings in the Washington DC area.[1] Nondestructive elemental analysis of the layers using a portable X-ray fluorescence (pXRF) instrument found that the crust was significantly enriched in manganese (Mn). This is a characteristic feature of desert varnish, which is found growing on rocks in arid climates and which is thought to be of microbial origin. In order to calculate the growth rate of these layers an estimate of the layer thickness is required. However, it was not possible to make such an estimate directly from the Mn XRF K_α peak in the absence of an Mn reference thickness standard for calibration of the instrument.

An alternative standard-free approach to calculating the layer thickness has been developed based on the attenuation of the iron (Fe) XRF peaks generated by the significant iron content of the underlying sandstone. This takes advantage of the unique relationship between the Fe K_α and K_β peaks and the Mn X-ray attenuation factor. The Fe K_α and Fe K_β peaks bracket the K absorption edge for Mn at 6.539 keV, which results in a nearly six fold difference in the mass attenuation factor between the two Fe K peaks.

In practice, the ratio of the Fe K peaks, instead of the individual peaks themselves, was used to estimate the layer thickness. This approach eliminates many of the factors of uncertainty such as surface roughness or X-ray beam variability. The estimated crust thickness is 4 ± 1 µm, assuming that it consists of pure manganese dioxide. This is consistent with the measured thickness of 5.4 ± 1.5 µm obtained by X-ray transmission scanning microscope on a cross-section of a sample of the layer.[2] Given the age of the Castle of 155 years this corresponds to an average growth rate of 26 ± 6 nm/yr. This falls in the middle of the range of 1- 40 nm/yr. observed in desert varnish samples.

References

(1) Livingston, R. A.; Grissom, C.; Vicenzi, E. P.; Weldon-Yochim, Z. A.; Little , N. C.; Douglas, J. G.; Fowler, A.J.; Santelli, C. M.; Macholdt, D. S.; Ortiz-Montalvo, D. L.; Watson, S. S., Investigation of Urban Rock Varnish on the Sandstone of the Smithsonian Castle. In *Science and Art: A Future for Stone Proceedings of the 13th International Congress on the Deterioration and Conservation of Stone*, Hughes, J. J.; Howind, T., Eds. University of the West of Scotland,: Paisley, Scotland, 2016; Vol. II, pp 399-406.

(2) Macholdt, D. S.; Jochum, K. P.; Pöhlker, C.; Arangio, A.; Förster, J. D.; Stoll, B.; Weis, U.; Weber, B.; Müller, M.; Kappl, M.; Shiraiwa, M.; Kilcoyne, A. L. D.; Weigand, M.; Scholz, D.; Haug, G. H.; Al-Amri, A.; Andreae, M. O., Characterization and differentiation of rock varnish types from different environments by microanalytical techniques. *Chemical Geology* **2017,** *459*, 91-118.

NEW DIRECTIONS FOR CALORIMETRY-BASED DOSIMETRY

Ronald E. Tosh[1]

[1] *National Institute of Standards and Technology, Gaithersburg, MD USA.*

Traceability to national absorbed-dose standards within the US can take a variety of pathways, depending on the type of incident radiation (photon, particle), its energy spectrum and the magnitude of dose one would like to measure. The variety of paths owes its existence to the ingenuity of scientists who have developed reliable metrological tools out of diverse materials – air, graphite, aqueous solutions, radiochromic gels and film, and alanine, to name a few – suitable for radiation modalities and applications of interest. Remarkably, all such paths converge upon a single national primary standard for realizing the gray (Gy), a water calorimeter in a Co-60 reference beam maintained at NIST.

Such a traceability scheme is advantageous from the point of view of simplicity – what could be simpler than traceability that terminates, regardless of application or radiation modality, at a single point, of reference beam and instrument? However, the simplicity belies a highly complicated web of industry-specific protocols involving secondary measurements and computational corrections to make it work. The overall scheme has done remarkably well for many years, with a huge and growing variety of applications for which traceability to this one primary standard has been achieved.

However, while this traceability scheme has proven robust to many of the demands placed upon it by industry, it has also been stubbornly unresponsive to needs arising in what is arguably the fastest growing area of technology: nanoscience. This talk will detail steps NIST is taking to address this shortcoming, with new sensors and imaging capabilities that would enable absolute dosimetry at the micron scale and, eventually, at the nano scale, where the concept of "dose" itself becomes problematic due to limitations of thermodynamics and quantum mechanics.

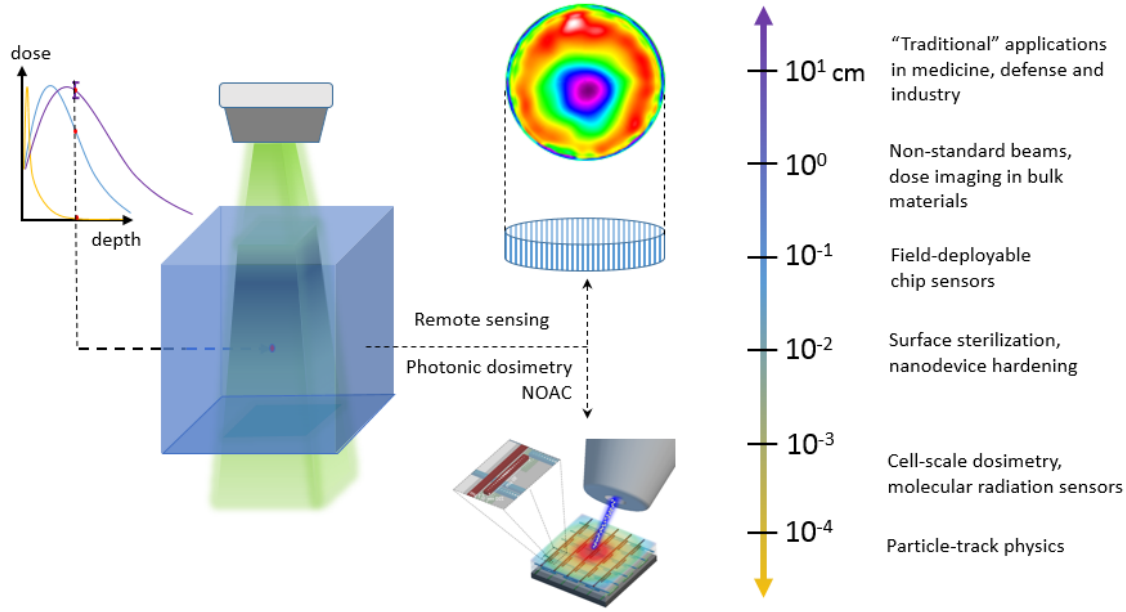

RADIATION CHEMISTRY REACTIONS SCHEME IS JUST A STARTING POINT FOR THE INDUSTRIAL PROCESS DEVELOPMENT

Andrzej G. Chmielewski[1], Yongxia Sun[1], Ewa Zwolińska[1]

[1]Institute of Nuclear Chemistry and Technology, Warsaw, Poland

Radiation chemistry is a branch of physical chemistry, like photo-chemistry, plasma chemistry, ultrasonic chemistry, etc. Shortwave high-energy electromagnetic radiation (gamma radiation or X-rays) and high-penetration corpuscular (electrons) radiation transfer energy into continuous, even high density, matter.[1] The collision of a photon with a molecule usually causes an electron to be ejected via the Compton effect. Thus, nearly all of the physical and chemical changes in the system are produced by the energetic electron and not by the initial photon. The kinetics of reactions induced by high-energy photons are therefore similar to those obtained if high-energy electrons are used as the primary radiation. Therefore, there is no big difference in the effects caused by these different forms of radiation. Depending to the energy transferred, molecules can undergo ionization, excitation, or thermal transfer. Interaction with matter can be divided by time scale into the following stages: initial physical processes, pre-chemical reactions, chemical reactions, and, finally, radical diffusion. Following primary events, the ions, secondary electrons, and excited molecules undergo further transformations, exchanging charges and energy and reacting with the surrounding molecules, thereby producing free radicals and other reactive species which finally evolve into new stable products. Reaction mechanisms are step-by-step descriptions of what occurs on a molecular level in chemical reactions. Collectively, an overall reaction and a reaction mechanism consist of multiple elementary processes. These elementary steps are the basic building blocks of a complex reaction, and cannot be broken down any further.The initial task in approaching the description of a chemically reacting system is to understand the answer to the question what changes are expected to occur by elucidating the thermodynamics of the process. The knowledge of radiation chemistry is not enough to describe the reacting system when is tailored to producing marketable product or used in the existing industrial conditions (like purification of gaseous or liquid effluents). The main constraints placed on a reacting system by thermodynamics depends on the parameters of state (e.g. temperature, volume, pressure). The mechanism of a chemical reaction is the sequence of events that take place as reactant molecules are converted into products. The study of kinetics of these reactions includes very complex and sophisticated reactions that cannot be analyzed without a proposed mechanism, a series of steps that a reaction takes before reaching the final products.

On the basis of the of the chemistry description in the systems having a possible practical applications further steps are undertaken. These concern process engineering with selection of the unit operation, mass and heat balances, separation techniques etc. The very important in the industrial process development based on the radiation technology is the proper ionizing radiation source selection.Three main sources of radiation are applied for radiation processing. These are electron accelerators,[2] gamma sources,[3] and X-ray units based on the e^-/X conversion process.[4] Accelerators are available supplying electron beams in the energy range up to 10 MeV and sources of the radionuclides Co-60 and Cs-137 emitting gamma rays at 1.17/1.33 and 0.662 MeV, respectively. The introduction of new X-ray (Bremsstrahlung) powerful radiation sources opens new, until now unexplored, fields, as well.

Electron beams are corpuscular radiation and are characterized by limited penetration in solid state objects and liquids. The whole energy of high energy electrons is deposited in relatively thin layers of material. An exemption are gases having three orders of magnitude lower density. In the case of X-rays and gamma rays, ionizing radiation is provided by photons which have no mass and are thus able to penetrate deeper into materials. The process up scaling methodology is similar in most of the cases, like sterilization,[5] polymer processing[6] and other materials treatment.[7] However in this paper the discussion of the subject will be limited to the examples related to the flue gas treatment.[8] The examples will be based on the theoretical and experimental evaluation of the processes for electron beam flue gas treatment; from coal and oil fired power plants,[9] gases containing organic pollutants like municipal waste incinerators[10] and diesel engines off-gases.[11] The all stages of process development from theory, through laboratory experiment up to process design are discussed in the paper.

Acknowledgements: This work was financed partly by Tango 2 Project (TANGO2/ 341079/NCBR/2017) entitled "Plasma technology to remove NOx from off-gases" and partly by H2020 ARIES project and co-financed by the Polish Ministry of Science and Higher Education, project 3697/H2020/2017/2.

References:

(1) Chmielewski A.G. Practical Applications of Radiation Chemistry. *Russian Journal of Physical Chemistry A*, **2007**, 81 (9) 1488–1492

(2) Gamma Irradiators for Radiation Processing **2005**, IAEA, Vienna http://www-naweb.iaea.org/napc/iachem/Brochgammairradd.pdf

(3) Zimek Z, Chmielewski A.G. Present Tendencies In Construction Of Industrial Electron Accelerators Applied In Radiation Processing. *Nukleonika* **1993**, 38 (2) 3 – 21

(4) Chmielewski A.G. Worldwide Developments In The Field Of Radiation Processing Of Materials In The Dawn Of 21st Century. *Nukleonika*, **2006**, 51(Supplement 1):S3−S9

(5) Chmielewski A.G., Berejka A.J. Radiation Sterilization Centers Worldwide, in Trends in Radiation Sterilization of Health Care Products, IAEA, Vienna, Austria, **2008**, 49 – 61

(6) Chmielewski A.G., Al-Sheikhly M., Berejka A.J., Cleland M.R., Antoniak M. Recent developments in the application of electron accelerators for polymer processing *Radiation Physics and Chemistry*, **2014**, 94,147–150

(7) Sun Y. & Chmielewski A. G. (eds). Applications Of Ionizing Radiation In Materials Processing INCT, Warsaw, **2017** ISBN 978-83-933935-8-9 http://www.ichtj.waw.pl/ichtj/publ/monogr/m2017_1.htm

(8) Chmielewski, A.G. & Han, B. Electron Beam Technology for Environmental Pollution Control. *Topics in Current Chemistry (Z)* **2016**, 374: 68. https://doi.org/10.1007/s41061-016-0069-4

(9) Pawelec A., Chmielewski A.G., Licki J., Han B., Kim J., Kunnummal N., Fageeha O.I. Pilot Plant For Electron Beam Treatment Of Flue Gases From Heavy Fuel Oil Fired Boiler. *Fuel Processing Technology* **2016**, 145, 123–129

(10)Yongxia Sun, Chmielewski A.G. Organic Pollutants Treatment from Air Using Electron Beam Generated Nonthermal Plasma – Overview, in Organic Pollutants Ten Years After the Stockholm Convention – Environmental and Analytical Update, InTech, **2012** https://www.intechopen.com/books/organic-pollutants-ten-years-after-the-stockholm-convention-environmental-and-analytical-update/

(11) Chmielewski A.G., Zwolińska E., Licki J., Sun Y., Zimek Z., Bułka S. A Hybrid Plasma-Chemical System For High-NOx Flue Gas Treatment, *Radiation Physics and Chemistry*, **2018**, 144, 1–7

This project has received funding from the European Union's Horizon 2020 Research and Innovation programme under Grant Agreement No 730871

CONTINUOUS IMPROVEMENTS IN MEASURING THE GAMMA IRRADIATOR PROCESS

Chris Howard

Gamma irradiators have traditionally been used to terminally sterilize single use medical supplies to ensure safety in the healthcare industry. Due to the increasing demand for more advanced medical devices for various applications, medical device manufactures are designing more unique and challenging devices to be sterilized using the traditional gamma irradiation process.

Gamma irradiation is currently applied on a wide range of medical polymer products, tissues, pharmaceuticals, and food.

In all applications of irradiation, the dose being delivered to the product must be accurately known to ensure sterility and functionality of the product. Delivering a precise and accurate dose can be achieved using dosimetry and mathematical modelling.

This talk will outline some of Nordion's specialty irradiation configurations and conditions, as well as dosimetry capabilities using Nordion's precise small scale irradiator. It will discuss Nordion's collaboration with the National Research Council of Canada to calibrate the Nordion source as a Canadian National Standard, and Nordion's mathematical modelling capabilities for predicting dose and validating new products in gamma irradiation process.

ADVANCING THE PRODUCTION AND CHARACTERIZATION OF RADIOLYTICALLY SYNTHESIZED POLY(VINYLPYRROLIDONE) NANOGELS

Zois Tsinas,[1] Devyn Catterton,[1] Eaman Karim,[1] Joseph Robertson,[2] Dianne Poster,[2] and Mohamad Al-Sheikhly[1]

[1]University of Maryland, College Park, Maryland, USA
[2]National Institute of Standards and Technology, Gaithersburg, Maryland, USA

Nano-hydrogels (nanogels) made of bio-compatible hydrophilic polymers can be used in various medical applications such as drug delivery and imaging. Intravenously introduced hydrogel-drug conjugate (10 - 200 nm particles) can be effectively accumulated in tissues/organs by prolonged circulation and can be selectively transported into tumor tissues by the enhanced permeability and retention effect. We are investigating the radiation-induced synthesis of functionalized nanogels that can serve as targeted medicinal carriers. The latest results on the synthesis and analysis of poly(vinylpyrrolidone) (PVP) nanogels in dilute aqueous solutions using γ-rays and electron beam will be presented.

Nanogels are synthesized using ionizing radiation by first altering solution conditions to collapse the PVP chains. At temperatures above 60 °C, PVP chains start to collapse decreasing their average hydrodynamic radius, R_h –from 23 (at 20 °C) to 15.6 nm (at 80 °C) due to the disruption of polymer-water hydrogen bonds. This molecular collapse enhances the intra-molecular crosslinking reactions of the radiolytically produced free radicals leading to a further decrease in its average R_h to the value of 14 nm via steady-state radiolysis.

The nanogels were also synthesized using pulsed electron beam irradiation at high repetition rates (*e.g.*, 300 pulses per second), which give rise to a high yield of multiple intra-chain free radicals. These free radicals enhance the intra-crosslinking reactions leading to the formation of smaller nanogels with an average R_h value of 12 nm. At high pulse repetition rates, the intra-molecular crosslinking reactions of the carbon centered free radicals are preferred. In contrast, low pulse repetition rates and the extended shape of the PVP molecules favor inter-molecular crosslinking. This effect is being examined further using relatively low dose-rate irradiation and nano-porous membranes, whereby the PVP molecules are biaxially compressed.

In addition to the examining R_h values irradiated products are being examined for morphology using atomic force microscopy and electron microscopy. Synthesis conditions are also being varied to include the doping of metal ions, such as iron and cobalt, to produce nanogels with ferromagnetic properties. Polymer-metal complexes are being examined using UV-VIS and FTIR spectroscopy. An overview of the materials and methods will be presented, along with a discussion on the effects of temperature and pulse repetition rate on the crosslinking yields and the size, as described by the R_h values of the products.

HARNESSING RADIATION CHEMISTRY TO DETERMINE HETEROGENEOUS NUCLEATION MECHANISMS DURING LIQUID PHASE CRYSTALLIZATION

Taylor J. Woehl[1]

[1]*Department of Chemical and Biomolecular Engineering, University of Maryland, College Park, MD 20740*

Nucleation marks the beginning of the formation of a new material phase and underlies many important natural and synthetic processes, including ice formation in the atmosphere, mineral formation in the Earth's crust, and synthesis of engineered nanomaterials, heterogeneous catalysts, and pharmaceuticals. Crystallization of a solid from a liquid phase begins with the formation of sub-nanometer sized crystal nuclei, whose properties define the polymorph of the new crystal phase and its subsequent material properties. Our current understanding of nucleation is mainly based on a centuries old framework: classical nucleation theory (CNT). Despite decades of experimental and theoretical research showing little agreement between CNT and most material systems, little progress has been made in understanding crystal nucleation.

Current approaches to quantitatively investigate nucleation kinetics involve tracking the crystallization of liquid droplets using optical microscopy. The downside to this approach is that nuclei are not directly resolved but instead inferred to have formed only after they grow into a visible crystal. In this talk, I will outline our recent work using *in situ* liquid cell electron microscopy (LCEM) to directly resolve nucleation in real time. LCEM utilizes a microfluidic sample holder to directly visualize nucleation of metal nanocrystals from a liquid phase in a transmission electron microscope (TEM) with nanometer scale spatial resolution. The TEM electron beam both stimulates nucleation and growth *via* radiolysis-induced formation of reducing radicals and enables simultaneous observation of nucleation kinetics. Specifically, aqueous electrons and other reducing radicals formed during the experiment directly reduce metal precursor salts into zero valent metal atoms (*e.g.* silver, gold, or platinum salts), which become supersaturated in solution and nucleate and grow into nanocrystals. I will discuss our use of radical scavengers and dose rate to control the reaction and nucleation kinetics, as well as our fundamental investigation of heterogeneous nucleation kinetics on various types of surfaces, including porous catalyst supports.

IDENTIFICATION OF IRRADIATED PLANT MATERIALS COMMONLY USED AS SPICES, HERBS AND DIETARY SUPPLEMENTS BY ELECTRON PARAMAGNETIC RESONANCE AND PHOTOSTIMULATED LUMINESCENCE SPECTROSCOPY

Kim M. Morehouse[1]

[1]*Division of Analytical Chemistry, Center for Food Safety and Applied Nutrition, U.S. Food and Drug Administration, 5100 Paint Branch Parkway, College Park, MD 20740*

The Food Safety Modernization Act (FSMA) requires food facilities conduct hazard assessments and if a hazard is reasonably likely to occur they must put in place preventive measures to control the hazard. Pathogens are reasonably likely to occur in some plant materials used in the production of spices, herbs and dietary supplements. Under current regulations, manufactures can choose irradiation as a form of hazard control for numerous plant materials. Currently, there are no reliable methods to determine if a product has been irradiated for verification of compliance with the Act. The use of Electron Paramagnetic Resonance (EPR) (EN 1787:2000 Detection of irradiated food containing cellulose by ESR spectroscopy) and Photostimulated Luminescence Spectroscopy (PSL) (EN 13751:2009 Detection of irradiated food using photostimulated luminescence) to detect irradiated spices was demonstrated in the early 2000's. This presentation will give an overview of methods that can be used to identify irradiated foods, as well as data on the use of EPR and PSL for detecting irradiation treatment in a variety of plant-derived materials. Over 60 plant materials commonly used as spices, herbs and dietary supplements were purchased and portions of those were irradiated. Most of the irradiated plant materials analyzed display an EPR spectrum that is assigned to the cellulosic radical. However, some of the products, such as garlic powder and onion powder, demonstrated a more complex radical spectrum which appears to originate from other components. The EPR spectra of the irradiated products were markedly different from the non-irradiated products and this difference could be measured up to 90 days post irradiation treatment. The PSL procedure could differentiate irradiated plant materials from non-irradiated plant materials for a limited number of products. Several of the plant materials that were investigated did not generate a luminescent signal that was significantly above that from the non-irradiated control. A summary of the results will be presented providing data on the limitations of these techniques to identify irradiated plant materials.

CURRENT AND FUTURE DIRECTIONS IN NIST RADIATION PROCESSING

Fred Bateman[1]

[1]*National Institute of Standards and Technology, Gaithersburg, Maryland, USA*

NIST's Radiation Physics Division operates and maintains three electron accelerator facilities, supplying medical and industrial electron beams supporting numerous internal and external research programs. These facilities are based on direct-current and pulsed-beam accelerators, covering an energy range from 600 keV to 30 MeV, and providing high dose rates suitable for radiation processing as well as extremely low currents for detector pulse counting.

These facilities serve a broad user community and play a vital role in NIST's development of dosimetry standards and protocols in the fields of radiation processing and medical radiotherapy. The presentation will describe the electron accelerator facilities and capabilities, discuss some of the diagnostic tools used for dosimetry and quality assurance, and outline many of the applications of these accelerators. These applications include an active program in radiation hardness testing of solar cells and devices, allowing researchers to evaluate the performance of their devices under a variety of exposure conditions. This leads to the development of radiation-resistant devices, enhancing their long-term survivability in harsh radiation environments. Another area of active research involves the synthesis of advanced materials via electron beam irradiation. Some examples include the production of electroactive copolymers, radiation grafting of membranes for hydrogen fuel cells and uranium extraction, and synthesis of nanogels.

A new low-energy electron beam facility, based on a 100 keV to 300 keV laboratory e-beam unit, is currently under development with a planned installation date of January 2019. This new facility will extend NIST's beam processing capabilities into the low-energy industrial regime and will support the development of protocols and standards for low-energy electron beam dosimetry. The presentation will describe the e-beam unit itself and outline some of the applications and planned usage of the facility.

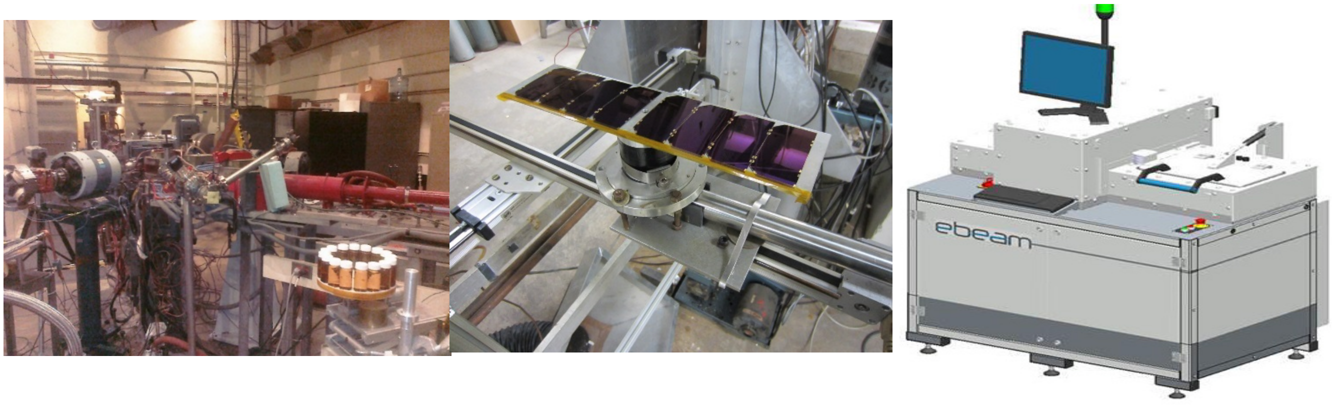

MIRF facility (left) Van de Graaff solar cell irradiation (center) Low-energy e-beam unit (right)

STUDIES OF THE IMPACTS OF GAMMA RADIOLYSIS ON ACTINIDE/LANTHANIDE SEPARATION TECHNOLOGIES

Dean R. Peterman[1]

[1]*Aqueous Separations & Radiochemistry, Idaho National Laboratory, Idaho Falls, ID 83415, USA*

The radiolysis/hydrolysis test loop, located at the Idaho National Laboratory (INL), was designed to allow the investigation of how of radiolytic and hydrolytic degradation processes may impact the efficacy of a solvent extraction process flowsheet. Recently researchers at the INL have studied the impacts of gamma radiolysis on the Actinide Lanthanide Separation (ALSEP) extraction process. The ALSEP process was developed through a joint collaboration between Argonne National Laboratory and Pacific Northwest National Laboratory.[1,2] This process uses an organic solvent consisting of a neutral extractant, *N,N,N'N'*-tetra-2-ethylhexyl-diglycolamide (T2EHDGA) and an acidic extractant 2-ethylhexylphosphonic acid mono-2-ethylhexyl ester (HEH[EHP]) dissolved in *n*-dodecane. The actinides and lanthanides are co-extracted from relatively high concentration nitric acid and the actinides are selectively stripped from the loaded organic phase using a carboxylic acid buffered aminopolycarboxylic acid solution.

The impact of gamma radiolysis upon the efficacy of the ALSEP process was previously evaluated by determining americium, europium, and cerium distribution ratios as a function of absorbed dose using samples taken test loop irradiation experiments. The measured distribution ratios demonstrated that the ALSEP solvent performance was degraded by γ-irradiation. The compositional analysis of the irradiated ALSEP solvent samples revealed that the decrease in americium, europium, and cerium distribution ratio with increasing absorbed dose is primarily attributable to the loss of the T2EHDGA extractant due to radiolytic degradation.[3] Continuing experiments have focused upon the impacts of gamma radiolytic degradation in acid-loaded and metal loaded ALSEP solvent. These similarities and difference between these irradiation conditions will be discussed.

References:

(1) Gelis, A.V.; Lumetta, G.J., (2014) Actinide Lanthanide Separation Process—ALSEP. *Industrial & Engineering Chemistry Research* **2014**, *53*, 1624-1631.

(2) Lumetta, G.J.; Gelis, A.V.; Carter, J.C.; Niver, C.M.; Smoot, M.R., The Actinide-Lanthanide Separation Concept. *Solvent Extraction and Ion Exchange* **2014,** *32*, 333-347.

(3) Peterman DR, Zarzana CA, Tillotson RD, McDowell RG, Rae C, Groenewold GS, Law JD (2018) Evaluation of the impacts of gamma radiolysis on an ALSEP process solvent. Journal of Radioanalytical and Nuclear Chemistry. doi:10.1007/s10967-018-5737-0

RADIATION-INDUCED PROCESSES IN MOLECULAR THIN FILMS

Matthew Bird[1]

[1]*Chemistry Division, Brookhaven National Laboratory, Upton, NY 11973-5000, USA*

Pulse radiolysis is most commonly performed in solution, where the yields of ions, radicals and excited states for many solvents have been well documented. For example it is known that ~25 eV of energy is deposited for every electron-hole pair created in saturated hydrocarbons. Less is known about the radiolytic products of molecular systems in the solid state, in particular 'semiconducting' molecules which have small HOMO-LUMO energy gaps of 1-3 eV such as conjugated polymers, small molecules or nanotubes. How do these narrow bandgaps affect the yield of ions? These materials can transport charges with high mobility in delocalized pi orbitals without breaking bonds; could this help reduce radiation damage by preventing scission or cross linking reactions?

We have performed pulse radiolysis (PR) on films of conjugated polymers at the Laser Electron Accelerator Facility (LEAF) at BNL. Through transient absorption measurements in the visible, and IR, we have established the radiolytic yields and decay kinetics of ions and excited states in a number of systems. A factor of ten difference in ion yields have been seen in films made from the same polymer but with different microstructure showing that the picture is more complex than in solvents. This potential control over the radiation products, coupled with the mechanical properties of these plastics may find use in a number of applications. Furthermore, PR, with transient absorption, enables new ways of studying charge transport in these materials.

ELECTRON TRANSFER MECHANISMS IN THE CHEMICAL DEGRADATION OF PEPTIDES AND PROTEIN THERAPEUTICS

Christian Schöneich[1]

[1]*Department of Pharmaceutical Chemistry, The University of Kansas, 2095 Constant Avenue, Lawrence, KS 66047*

Therapeutic proteins suffer from numerous pathways of chemical degradation, with potential consequences for potency, shelf-life and immunogenicity. The rational design of protein therapeutics greatly benefits from the mechanistic understanding of degradation pathways, which assists in the selection of appropriate formulation and storage conditions. Light-induced protein degradation remains a constant concern for various potential reasons such as (i) the co-purification of photo-sensitizers present in fermentation media, (ii) the exposure of proteins to analyzers, which utilize high intensity light, (iii) the presence of photo-catalysts in pre-filled glass syringes, and (iv) the prolonged light-exposure of proteins in i.v. bags. Specifically with respect to potential immunogenicity, it is mandatory to delineate all degradation mechanisms and products of a therapeutic protein under a given set of conditions.

Here, we report on proteomic studies designed to provide a comprehensive analysis of light-induced protein degradation, using UV as well as visible light, with focus on selected peptide and protein sequences. Light exposure of human growth hormone (hGH) resulted in the characterization of ca. 60 degradation products originating from the direct photolysis of disulfide bonds and/or photo-induced electron transfer from Trp to disulfide bonds. Electron transfer was also critical for the degradation of Tyr residues in IgG4-Fc, resulting in the cleavage of para-quinone methide, most likely from an intermediary Tyr radical cation. This mechanism was supported by product solvent isotope effects as well as specifically designed mutant proteins. Electron transfer from Met resulted in novel cross-links across peptide sequences containing His residues. Overall, there is a rich electron transfer chemistry, generating novel reaction products, which must be taken into consideration when analyzing peptide and protein formulations for chemical degradation.

A RADIATION CHEMISTRY TRACK STRUCTURE MODEL FOR ION-BEAM IRRADIATED DNA

David Becker[1], Amitava Adhikary[1], Thomas Baumann[2], Keaton Curran[1], Cameron G. Hanson[1], Taiyasa Jacobs[1], Ensa Stafa[1], Samuel Ward[1], and Michael D. Sevilla[1]

[1]Department of Chemistry, 146 Library Drive, Oakland University, Rochester, MI, 48309, [2]National Superconducting Cyclotron Laboratory, Michigan State University, 640 S. Shaw Lane, East Lansing, MI, 48824

It has long been recognized that a double strand break embedded in a clustered damage site is difficult for cellular repair[1,2] and may result in cell death[3] or mutagenesis.[4] Multiple damage sites within *ca.* 10 base pairs generally qualify as a damage cluster.[5] Because the spatial locations of damage sites are relevant to the cellular effect of the damage, we have focused on characterization of the location, in three dimensions, of the various types of damage (e.g., strand breaks, base damage) that occur in ion-beam irradiated DNA, and the radiation chemical processes that lead to them.

Experiments are performed on DNA samples hydrated to ca. 12 H_2O/nucleotide, which minimizes the effect of •OH, so direct-type effects are emphasized.[6,7] In the experiment, approximately 12 small (*ca.* 10 mm x 4 mm x 1 mm) samples are stacked in a sample packet (Scheme) and ion-beam irradiated at 77 K.

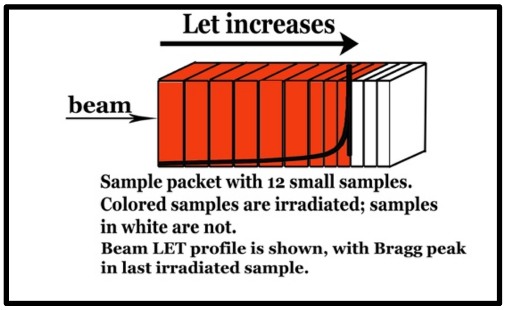

Sample packet with 12 small samples.
Colored samples are irradiated; samples in white are not.
Beam LET profile is shown, with Bragg peak in last irradiated sample.

Scheme

Each small sample is analyzed, using ESR, for trapped radicals at 77 K, and, after warming to room temperature, for unaltered base release using HPLC. Strand break formation leads directly to unaltered base release and, thus, increased unaltered base release is a good measure of strand break formation[8].

At 77 K, nine different radicals have been identified in ion-beam irradiated samples to date. These are three base radicals formed, one by one-electron oxidation/deprotonation, designated as G(–H)•, and two by one-electron reduction/protonation, C(N3)H•, $T^{\bullet-}$, four sugar radicals, C1′•, C3′•, C5′•, and $C3'^{\bullet}_{dephos}$, and two phosphorus-centered radicals, $ROPO_2^{\bullet-}$, and, the, as yet, unidentified, $P_x^{\bullet}$. In Kr-86 irradiated samples, the yield of unaltered bases is the same as the total yield of trapped sugar radicals at 77 K, indicating, as has been hypothesized earlier, that, in ion-beam irradiated DNA, sugar radicals are the precursors to strand breaks.[6,7,9] (It should be noted that in γ-irradiated DNA, the unaltered base release yield exceeds the yield of sugar radicals, indicating that a fraction of the strand breaks formed do not originate only with preformed sugar radicals.[6,7])

The radiation chemical model that results posits that the high energy density in the beam core results in a high concentration of radicals in the core, and that, even at 77 K, rapid recombination between oppositely charged free radicals due to Coulomb attractions depletes the concentration of charged radicals in the core.[9] However, neutral sugar radicals, formed by early rapid deprotonation of sugar cation radicals, survive and are trapped in the core.[6,7,9] The model also postulates that γ-irradiation-like spurs are formed in the ion-beam penumbra, and that the trapping of radicals in the penumbra mimics that which would be found in γ-irradiated DNA.[6,7,9] In addition, relative to γ-irradiated samples, there is a higher concentration of the immediate strand break radicals $C3'{\bullet}_{dephos}$, and $ROPO_2{\bullet}^-$ found in ion-beam irradiated DNA samples than found in γ-irradiated DNA samples. These likely originate with low energy electrons. Their presence implies that there are a relatively high number of strand breaks in the low core volume, which would be especially high near the Bragg peak given the high energy deposition in the "pencil down" region inherent at the Bragg peak. With the proposition that the penumbra is γ-radiation like with regard to radical trapping, the energy partition between the beam core and beam penumbra is determined.

Lastly, we have found that the percentage of unaltered guanine base release in O-16 ion-beam irradiated DNA samples is higher than that found in γ-irradiated samples.[10] Since there is a known mechanism by which excited state $G{\bullet}^+$ radicals form sugar radicals on an adjoining sugar,[6,9,11] the higher percentage of unaltered guanine suggests the occurrence of excited state reactions in the beam core.

Supported by: NIH NCI R01CA045424; Research Excellence Fund and Center for Biomedical Research at Oakland University; and The National Superconducting Cyclotron Laboratory at Michigan State University.

References:

(1) Fujimoto, H., Pinak, M., Nemoto, T., O'Neill, P., Kume, E., Saito, K., Maekawa, H. Molecular Dynamics Simulation of Clustered Damage Sites Containing 8-oxoguanine and Abasic Site. *J. Comp. Chem.* **2005,** *26*, 788-798.

(2) Rothkamm, K., Löbrich, M. Evidence for lack of DNA double-strand break repair in human cells exposed to very low X-ray doses. *Proc. Natl. Acad. Sci.* **2003,** 100, 5057–5062.

(3) Goodsell, D. The Molecular Perspective: Double-Stranded DNA Breaks. *The Oncologist* **2005**, *10*, 361-362.

(4) Rodgers, K., Mcvey, M. Error-Prone Repair of DNA Double-Strand Breaks. *J. Cell. Physiol.* **2016**, *231*, 15-24.

(5) Hikazono, N., Noguchi, M., Fuji, K., Urushibara, A., Yokoya, A. The Yield, Processing, and Biological Consequences of Clustered DNA Damage Induced by Ionizing Radiation. *J. Radiat. Res.* **2009**, *50*, 27 – 36.

(6) Becker, D., Adhikary, A., Tetteh, S. T., Bull, A. W., Sevilla, M. D. Kr-86 ion-beam irradiation of hydrated DNA: Free radical and unaltered base yields. *Radiat. Res.* **2012**, *178*, 524 – 537.

(7) Adhikary, A., Becker, D., and Sevilla, M. D. Electron spin resonance of radicals in irradiated DNA. In Applications of EPR in radiation research (A. Lund, M. Shiotani (Eds.)), Springer-Verlag, Berlin, Heidelberg, **2014**, 299 - 352.

(8) Raskazovskiy, Y., Debije, M., Bernhard, W. A. Direct Radiation to Crystalline DNA: What is the Source of Unaltered Base Release? *Radiat. Res.* **2000**, *153*, 436–441.

(9) Sevilla, M. D., Becker, D., Kumar, A., Adhikary, A. Radiation-Induced Free Radical Mechanisms in DNA. *Radiat. Phys. Chem.* **2016**, *128*, 60 – 74.

(10) Becker, D.; Adhikary, A.; Baumann, T.; Curran, K.; Hanson, C.; Jacobs, T.; Sevilla, M. D. Unaltered Base Release in Ion-Beam Irradiated DNA: Role of excited state phenomena. Presented at the 63rd Annual Meeting of the Radiation Research Society, Grand Fiesta Americana- Coral Beach- Cancun, Mexico, October 15-18, 2017.

(11) Adhikary, A., Malkhasian, A.Y.S., Collins, S., Koppen, J., Becker, D., and Sevilla, M. D. UVA-visible photo-excitation of guanine radical cations produces sugar radicals in DNA and model structures. *Nucleic Acids Res.* **2005**, *33*, 5553 – 5564.

CHARGE GENERATION, TRANSPORT AND TRANSFER IN DNA: MECHANISMS AND SOME APPLICATIONS

Yuri A. Berlin[1]

[1]*Department of Chemistry, Center for Nanofabrication and Molecular Self-Assembly, Northwestern University, 2145 Sheridan Road, Evanston, IL 60208, USA*

Charge transfer in DNA has been studied intensively for over two decades by both experimentalists and theoreticians.[1-4] Part of this attention finds its roots in the biological relevance of oxidative DNA damage, where charged species migrate over long distances. Additionally, there is a strong interest in exploiting the combination of the electronic properties of DNA with its programmable self-assembling properties to achieve self-organizing electronic components and circuits.

In this lecture I consider key processes governing the behavior of charge carriers in DNA molecules and assemblies, summarize approaches used to describe mechanisms of these processes, and analyze main factors affecting the efficiency and time scale of charge transport in such systems. Several recent applications based on progress in understanding charge motion across DNA oligomers will also be discussed.[5,6]

References

(1) Berlin, Y. A.; Kurnikov, I. V.; Beratan, D.; Ratner, M. A.; Burin, A. L. DNA Electron Transfer Processes: Some Theoretical Notions. *Top. Curr. Chem.* **237**, 1-36 (2004).

(2) Wagenknecht, H. A. *Charge Transfer in DNA* (Wiley-VCH, 2005).

(3) Genereux, J. C.; Barton, J. K. Mechanisms for DNA charge transport. *Chem. Rev*. **110**, 1642–1662 (2010).

(4) Lewis, F. D. Distance-dependent electronic interactions across DNA base pairs. Charge transport, exciton coupling, and energy transfer. *Israel J. Chem.* **53**, 350–365 (2013).

(5) Young, R. et al. Charge Transport across DNA-Based Three-Way Junctions.

(6) Shu, R. et al. Charge splitters and charge transport junctions based on guanine quadruplexes. *Nature Nanotechnology* in press (2018).

CAN A PRE-HYDRATED ELECTRON INDUCE A DISSOCIATIVE ELECTRON ATTACHMENT?

Mehran Mostafavi[1]

[1]*Laboratoire de Chimie Physique, CNRS/Université Paris-Sud, Bâtiment 349, 91405 Orsay, France*

Pulse radiolysis is a substantial tool to study the reactivity of the products of aqueous solution decomposition caused by ionizing radiation. Among the products of water radiolysis, we can find reducing and oxidizing species, however fate of the radicals formed under radiation at the very short time scale is still not fully understood. Reactions taking place are so fast that for a long time the information about primary events were unavailable. The solvation of the electron and the proton transfer by the water hole are fully accomplished at shorter time than 1 ps. However, in some conditions, reactions could take place even at shorter time than 1 ps.

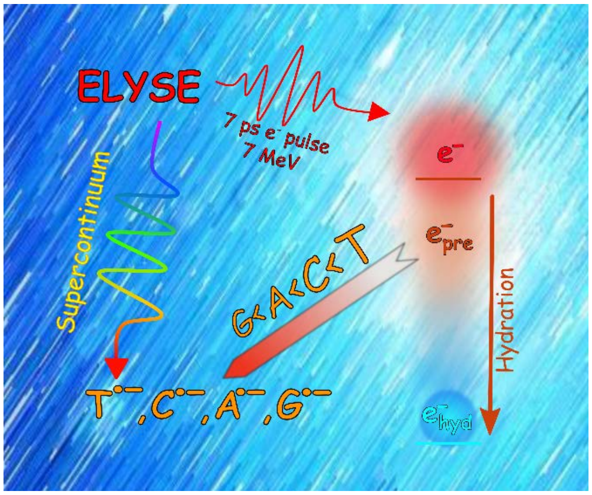

Scheme: Electron attachment on DNA-bases by the excess electron in water before its hydration completes.

For example, it was shown that the electron transfer reaction of the water hole competes with the known proton transfer reaction and the water hole can oxidize solute when it is at high concentration. For the excess electron also, the reaction can occurs before its solvation. Ultrafast electron transfer processes of prehydrated electron e_{pre}^{-} to several system such as silver ion, silver cyanide and DNA bases – G, A, C, T and nucleosides/tides is investigated by employing 7 ps electron pulse radiolysis coupled with pump-probe transient absorption spectroscopy. In this approaches, the objective was to observe the product of the reaction of the pre-hydrated electron with the solutes. In the pioneer works performed during 70's, only the amount of the remaining hydrated electron was observed, and the question if the product of the reaction of a solute with the hydrated electron and the pre-hydrated electron is the same was not addressed. Bases on our observations of the hydrated electron and also the product of the reaction between pre-hydrated electron and the solutes the dissociative electron attachment process induced by the pre-hydrated electron will be discussed

References

(1) Reactivity of prehydrated electrons toward nucleobases and nucleotides in aqueous solution. Ma, J.; Wang, F.; Denisov, S. A.; Adhikary, A.; Mostafavi, M., Science Advances, 2017, 3:e1701669

(2) Effect of the solvation state of electron in dissociative electron attachment reaction in aqueous solutions. Wang, F.; Archirel, P.; Muroya, Y.; Yamashita, S.; Pernot, P.; Yin, C.; El Omar, A. K.; Schmidhammer, U.; Teuler, J.; Mostafavi, M. Phys. Chem. Chem. Phys. **2017**, *19*, 23068−23077
(3) Unexpected Ultrafast Silver Ion Reduction: Dynamics Driven by the Solvent Structure. Balcerzyk, A.; Schmidhammer, U.; Horne, G.; Wang, F.; Ma, J.; Pimblott, S. M.; de la Lande, A.; Mostafavi, M. J. Phys. Chem. B, **2015**, *119*,10096–10101

THE INFLUENCE OF GEOMETRY AND CONFORMATION OF PEPTIDES CONTAINING SULFUR ATOMS ON THE TYPE OF THREE-ELECTRON BONDS INVOLVED IN THE STABILIZATION OF SULFUR RADICAL CATIONS

Krzysztof Bobrowski,[1] Gordon L. Hug,[2] Ireneusz Janik,[2] Piotr Filipiak,[3] Tomasz Pedziński,[3] Franciszek Kazmierczak,[3] and Bronislaw Marciniak[3]

[1] Institute of Nuclear Chemistry and Technology, 03-195 Warszawa, Poland
[2] Radiation Laboratory, University of Notre Dame, Notre Dame, IN 46556, USA
[3] Faculty of Chemistry, Adam Mickiewicz University, 60-780 Poznan, Poland

Oxidation of peptides containing sulfur atom(s) leads to a variety of interesting mechanistic pathways through neighboring group participation. Peptides containing methionine (Met) and S-methylcysteine (S-MeCys) are a case in point. There have been several studies on the $^{\bullet}$OH-induced oxidation of small peptides containing Met and S-MeCys residues.[1-8] Stabilizations, through neighboring group participation involving *2c-3e* three-electron bonds, of the resulting monomeric sulfur radical cations ($>S^{+\bullet}$) were seen when the Met residues were C- or N-terminal or were incorporated inside the peptide molecule. In the latter case, such stabilization occurs with involvement of heteroatoms located in the peptide bonds.

The aim of this study is to establish whether and to what extent conformational and geometric factors in peptides affect the stabilization of sulfide radical cations ($>S^{+\bullet}$) via the formation of intramolecular σ*-type 2*c*-3*e* S∴O, S∴N and S∴S-bonds.

A first set of peptide molecules was designed with the purpose of observing changes in their tendencies to form various intramolecular σ*-type bonds in linear dipeptides containing stereoisomers of Met as compared to these same tendencies observed in two previously studied cyclic dipeptide isomers containing Met: *c*-(*L*-Met-*L*-Met) and *c*-(*L*-Met-*D*-Met).[4-5,8] The newly synthesized molecules are three N-acetyl-methionyl-methionine amides substituted with the methyl group and with various combinations of *L*- and *D*-stereoisomers of Met residues. The side chains of Met-residues in *L*,*L*-configured linear dipeptides are forced to point in opposite directions in space which makes it more difficult for them to come into close contact. On the other hand, the side chains of Met residues in *L*,*D*/*D*,*L*-configured linear dipeptides tend to be both on the same side of the peptide backbone, and, for this reason, close contacts between side chains should be enhanced. The geometrical preferences are exactly reversed in cyclic dipeptides which should be manifested in different relative yields of the intramolecularly □*-type 2*c*-3*e* S∴O, S∴N and S∴S-bonded transients. Another aspect of these studies arises from the effect of differences in the steric constraints between analogous linear and cyclic dipeptides which influences the extent of *p*-orbital interactions involved in formation of intramolecular S∴S-bonds in sulfide radical cations.

A second set of peptide molecules was designed with the purpose of observing changes in their tendencies to form various intramolecular σ*-type bonds in cyclic dipeptides containing stereoisomers of S-MeCys as compared to these same tendencies observed in two previously studied cyclic dipeptide isomers containing Met: *c*-(*L*-Met-*L*-Met) and *c*-(*L*-Met-*D*-Met).[4-5,8] These newly synthesized molecules are *c*-(*L*-S-MeCys-*L*-S-MeCys) and *c*-(*D*-S-MeCys-*L*-S-

MeCys dipeptides. The two sets of peptides differ only in the lengths of their side chains Met vs S-Me-Cys (the shorter homologue of Met). It is of interest to see whether this difference (i) can effect the extent of *p*-orbital interactions involved in the formation of intramolecular S∴S-bonds or (ii) effect kinetic and thermodynamic preferences (a) for four- versus five-membered ring configuration in the formation of intramolecular S∴N-bonds or (b) for five- versus six-membered configuration in the formation of intramolecular S∴O-bonds in sulfide radical cations. The diverse behavior of these peptides will be discussed in terms of a change in spectral and kinetic parameters resulting from various preferences in the formation of three-electron bonded transients.

Nanosecond pulse radiolysis, coupled with the time-resolved spectrophotometric UV/vis and conductometric detection, was used to obtain the spectra and to follow the kinetics of the reaction intermediates.

References

(1) K. Bobrowski, J. Holcman, "*Formation and stability of intramolecular three-electron S∴N, S∴S and S∴O bonds in one-electron-oxidized simple methionine peptides. Pulse radiolysis study*", J. Phys. Chem. 1989, **93**, 6381.

(2) K. Bobrowski, Ch. Schöneich, J. Holcman, K.-D. Asmus, "*•OH radical induced decarboxylation of γ-glutamylmethionine and S-alkylglutathione derivatives: evidence for two different pathways involving C- and N-terminal decarboxylation*", J. C. S. Perkin Trans. 2. 1991, 975.

(3) Ch. Schöneich, D. Pogocki, G. L. Hug, K. Bobrowski „*Free radical reactions of methionine in peptides: mechanism relevant to β–amyloid oxidation and Alzheimer's disease*" J. Am. Chem. Soc. 2003, **125**, 13700.

(4) G. L. Hug, K. Bobrowski, D. Pogocki, G. Hörner, B. Marciniak „*Conformational influence on the type of stabilization of sulfide radical cations in cyclic peptides*" ChemPhysChem 2007, **8**, 2202.

(5) K. Bobrowski, G. L. Hug, D. Pogocki, B. Marciniak, C. Schöneich „*Stabilization of sulfide radical cations through complexation with the peptide bond: mechanisms relevant to oxidation of proteins containing multiple methionine residues*" J. Phys. Chem. B. 2007, **111**, 9608.

(6) K. Bobrowski, G. L. Hug, D. Pogocki, B. Marciniak, Ch. Schöneich "*Sulfur-radical cation-peptide bond complex in the one-electron oxidation of S-alkylglutathiones*" J. Am. Chem. Soc. 2007, **129**, 9236.

(7) G. L. Hug, K. Bobrowski, D. Pogocki, B. Marciniak, C. Schöneich, G. Hörner "*Factor analysis of transient spectra. Free-radicals in cyclic dipeptides containing methionine*" Res. Chem. Interm. 2009, **35**, 431.

(8) S. Barata-Vallejo, C. Ferreri, T. Zhang, H. Permentier, R. Bischoff, K. Bobrowski, C. Chatgilialoglu "*Radiation chemical studies of Gly-Met-Gly in aqueous solution*" Free Radical Res. 2016, **50**, S24-S39.

5-AZIDO-MODIFIED PYRIMIDINE NUCLEOSIDES: ELECTRON MEDIATED FORMATION OF π-TYPE AMINYL RADICAL AND ITS CONVERSION TO σ-TYPE IMINYL RADICAL

Zhiwei Wen[1], Jufang Peng[1], Paloma Tuttle[1], Dipra Debnath[2], Sunny Rishi[2], Cameron Hanson[2], Samuel Ward[2], Yaou Ren[1], Carol Garcia[1], Yuan Liu[1], Yanfeng Liu[3], Weixi Zhao[3], Peter M. Glazer[3], Anil Kumar[2], Michael D. Sevilla[2], Stanislaw F. Wnuk[1], and Amitava Adhikary[2]

[1]*Department of Chemistry and Biochemistry, Florida International University, Miami, Florida 33199, USA*
[2]*Department of Chemistry, Oakland University, Rochester, Michigan 48309, USA*
[3] *Department of Therapeutic Radiology, Yale University School of Medicine, New Haven, CT 06520, USA.*

The chemically stable 5-azidomethyl-2'-deoxyuridine (5-AmdU, **1**) has been utilized for metabolic labeling of DNA as well as fluorescent imaging of live cells. We have synthesized 5-azidomethyl-2'-deoxycytidine (5-AmdC, **2**). The 5-(1-azidovinyl)-2'-deoxyuridine (5-AvdU, **3)**, and 5-(1-azidovinyl)-2'-deoxycytidine (5-AvdC, **4**) has been prepared by the regioselective Ag-catalyzed hydroazidation of the 5-ethynyl substrates with $TMSN_3$. The 5-AmdU **1** was converted to its 5'-triphosphate using Yoshikawa protocol followed by coupling with pyrophosphate. Employing DNA replication and repair polymerases, the 5-AmdU-5-TP was enzymatically incorporated into a variety of DNA strands having random sequence, trinucleotide repeats and telomere sequences. Radiation-mediated pre-hydrated electrons which are formed in homogeneous aqueous glassy (7.5 M LiCl) systems in the absence of oxygen at 77 K, led to site-specific formation of neutral aminyl radical **5** from 5-AmdU. ESR spectrum of the π-type aminyl radical shows a prominent doublet of ca. 91 G resulting from the sum of two β-proton hyperfine couplings arising from the two hydrogens from CH_2 group.

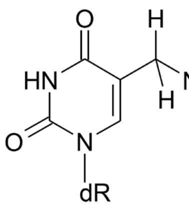

1

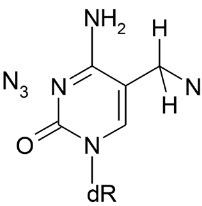

2

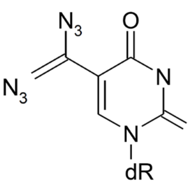

3

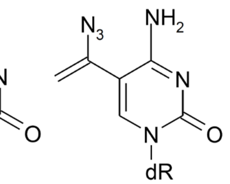

4

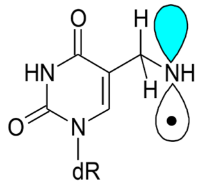

5

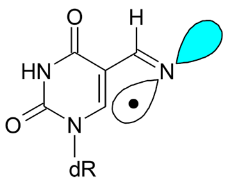

6

Radiation-produced electron-mediated site-specific formation of neutral aminyl radical was observed from 5-AvdU **3**, and from 5-AvdC **4** as well. Our ESR spectral studies and DFT calculations showed that the novel π-type neutral aminyl radicals generated from **1-4** undergo facile conversion to σ-type iminyl radicals (e.g., radical 5 converted to **6**). Our work provides the first evidence of π-type aminyl radical and σ-type iminyl radical formation in a modified nucleoside under a reductive environment. These aminyl and iminyl radicals are known to generate DNA damage via oxidative pathways. Furthermore, we present evidence that these azido-nucleosides can be successfully applied as radiosensitizers in cells under hypoxic conditions.

Supported by: NIH NCI R01CA045424; Research Excellence Fund and Center for Biomedical Research at Oakland University

ABSTRACTS of POSTER PRESENTATIONS

(in alphabetical order of presenter)

5-AZIDO-MODIFIED PYRIMIDINE NUCLEOSIDES: ELECTRON MEDIATED FORMATION OF π-TYPE AMINYL RADICAL AND ITS CONVERSION TO σ-TYPE IMINYL RADICAL

Zhiwei Wen[1], Jufang Peng[1], Paloma Tuttle[1], Dipra Debnath[2], Sunny Rishi[2], Cameron Hanson[2], Samuel Ward[2], Yaou Ren[1], Carol Garcia[1], Yuan Liu[1], Yanfeng Liu[3], Weixi Zhao[3], Peter M. Glazer[3], Anil Kumar[2], Michael D. Sevilla[2], Stanislaw F. Wnuk[1], and Amitava Adhikary[2]

[1]*Department of Chemistry and Biochemistry, Florida International University, Miami, Florida 33199, USA*
[2]*Department of Chemistry, Oakland University, Rochester, Michigan 48309, USA*
[3] *Department of Therapeutic Radiology, Yale University School of Medicine, New Haven, CT 06520, USA.*

The chemically stable 5-azidomethyl-2'-deoxyuridine (5-AmdU, **1**) has been utilized for metabolic labeling of DNA as well as fluorescent imaging of live cells. We have synthesized 5-azidomethyl-2'-deoxycytidine (5-AmdC, **2**). The 5-(1-azidovinyl)-2'-deoxyuridine (5-AvdU, **3)**, and 5-(1-azidovinyl)-2'-deoxycytidine (5-AvdC, **4**) has been prepared by the regioselective Ag-catalyzed hydroazidation of the 5-ethynyl substrates with $TMSN_3$. The 5-AmdU **1** was converted to its 5'-triphosphate using Yoshikawa protocol followed by coupling with pyrophosphate. Employing DNA replication and repair polymerases, the 5-AmdU-5-TP was enzymatically incorporated into a variety of DNA strands having random sequence, trinucleotide repeats and telomere sequences. Radiation-mediated pre-hydrated electrons which are formed in homogeneous aqueous glassy (7.5 M LiCl) systems in the absence of oxygen at 77 K, led to site-specific formation of neutral aminyl radical **5** from 5-AmdU. ESR spectrum of the π-type aminyl radical shows a prominent doublet of ca. 91 G resulting from the sum of two β-proton hyperfine couplings arising from the two hydrogens from CH_2 group.

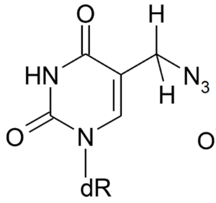

1

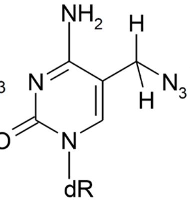

2

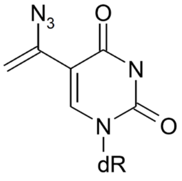

3

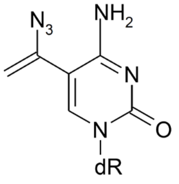

4

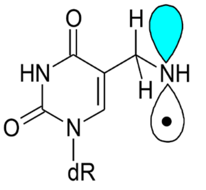

5

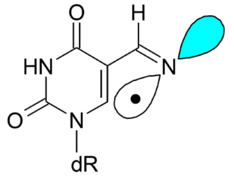

6

Radiation-produced electron-mediated site-specific formation of neutral aminyl radical was observed from 5-AvdU **3**, and from 5-AvdC **4** as well. Our ESR spectral studies and DFT calculations showed that the novel π-type neutral aminyl radicals generated from **1-4** undergo facile conversion to σ-type iminyl radicals (e.g., radical 5 converted to **6**). Our work provides the first evidence of π-type aminyl radical and σ-type iminyl radical formation in a modified nucleoside under a reductive environment. These aminyl and iminyl radicals are known to generate DNA damage via oxidative pathways. Furthermore, we present evidence that these azido-nucleosides can be successfully applied as radiosensitizers in cells under hypoxic conditions.

Supported by: NIH NCI R01CA045424; Research Excellence Fund and Center for Biomedical Research at Oakland University

RADIOLYTIC DEGRADATION OF 2,4-DICHLOROPHENOL AND CHEMICAL OXYGEN DEMAND DETERMINATION

Guadalupe Albarrán[1] and Edith Mendoza[1]

[1]Universidad Nacional Autónoma de México. Instituto de Ciencias Nucleares, Circuito Exterior, Cd. Universitaria. Cd de México, C.P. 04510

Chlorinated phenolic compounds can enter an aqueous medium through discharges of wastewater. There are several technological methods for wastewater treatments. The advanced oxidation processes (AOPs) promise to be one of the most efficient methods for the removal of non-biodegradable contaminants contained in surface and groundwater. Besides AOPs, radiation technologies have several advantages. 2,4-Dichlorophenol (2,4-DClP) is toxic and resistant to biodegradation. For the degradation of 2,4-DClP, some studies have been carried out using electron accelerators and γ ray sources.[1,2] This study identifies and quantifies the radiolytic products of 2,4-DClP and determines its radiolytic degradation in different concentrations (0.25, 0.50 and 0.7 mmol/L) and environments (air, without oxygen and under N_2O). The aqueous solutions of 2,4-DClP were analyzed immediately after irradiation by liquidchromatography. COD is a measure of the oxygen equivalent of the organic mattercontent of a sample that is susceptible to oxidation by a strong chemicaloxidant. This determination was carried out spectrophotometrically.

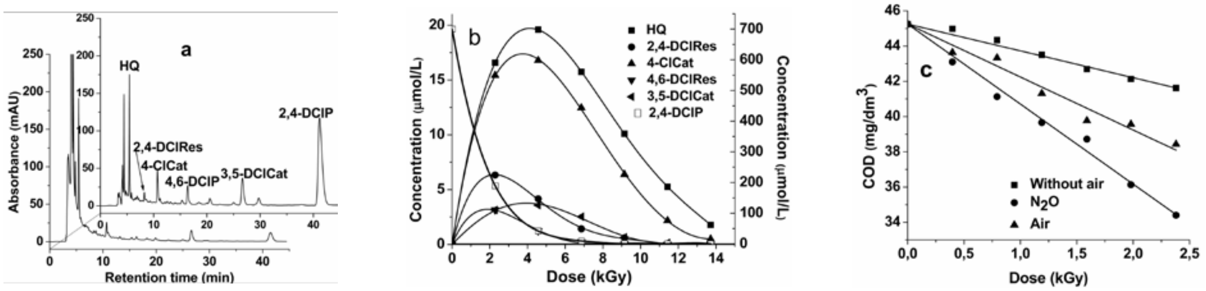

Chromatograms (a) show the five radiolytic products formed (rear plot at 2.5 kGy) and degraded (front plot at 6.3 kGy) for a 0.5 mmol/L 2,4-DClP solution, saturated with N_2O. Four compounds were produced by an addition reaction of $^{\bullet}OH$ to the free positions and one by a substitution reaction of one chlorine by attack of $^{\bullet}OH$. The formation of the radiolytic products (b) (sample of 0.7 mmol/L in air) showed that the largest product formed was HQ, which presented the greatest resistance to degradation. The 2,4-DClP (b) was easily degraded by 70 % at 2.3 kGy (the concentration is indicated on the right margin). COD (c) decreases as a function of dose for the three different environments at 0.25 mmol/L. The COD slope was the highest of the three concentrations studied when the sample contained N_2O because the $^{\bullet}OH$ present in the solution was two times that in air or without oxygen. Without oxygen and air in the solutions the free radicals participate in oxidation-reduction reactions and the degradation is slower.

In conclusion, 2,4-DClP degradation was more rapid in solutions containing N_2O and slower in those without oxygen or air.

References

(1) He, Y., Liu, J., Lu, Y., Wu. J. Gamma radiation treatment of pentachlorophenol, 2,4-dichlorophenol and 2-chlorophenol in water. *Radiat. Phys. Chem.***2002**, *65*, 565-570.

(2) Trojanowicz, M., Drzewicz, P., Panta, P.et al.Radiolytic degradation and toxicity changes in γ-irradiated solutions of 2,4-dichlorophenol. *Radiat. Phys. Chem.***2002***65*, 357-366.

ESR STUDIES OF GAMMA RADIATION AND MICROWAVE STERILIZED GRAFTS FOR PERIODONTOLOGICAL APPLICATIONS

Saharnaz Bargh[1], Mine Silindir-Gunay[1], A. Yekta Ozer[1], Seyda Colak[2] , Burak Kutlu[3], and Rahime Nohutcu[3]

[1]Hacettepe University, Faculty of Pharmacy, Department of Radiopharmacy, 06100, Sihhiye, Ankara, Turkey.
[2]Hacettepe University, Faculty of Engineering, Department of Physics Engineering, 06800, Beytepe, Ankara, Turkey.
[3]Hacettepe University ,Faculty of Dentistry, Department of Periodontology , 06100, Sıhhiye, Ankara, Turkey.

Periodontological grafts are used in dentistry to regenerate the lost tissue as gingival (soft tissue) or bone part. In this study, seven different periodontal dermal and bone grafts from human and animal sources (HBG1, HL1, MBG3, MDG2, PBG1, PDG1, PDG3) have been irradiated by gamma and microwave radiation for sterilization. The spectroscopic features of the radiolytic intermediates and radiation sterilization feasibility have been investigated by ESR. Unirradiated samples have indicated ESR signals with relatively low intensities while gamma irradiation caused an increase in the intensities of their ESR signals with increasing absorbed dose. Gamma irradiated samples exhibited complex ESR spectra consisting of 7, 5, 5, 4, 7, 5, and 2 resonance lines, respectively where g values for the central resonance lines of samples were found to be g = 2.0022, 2.0049, 2.0020, 2.0059,2.0021, 2.0043, 2.0054 and with peak-to-peak widths of the central resonance lines of the samples have been found to be ΔH_{pp} = 3.4 G, 11.6 G, 3.6 G, 12.3 G, 3.6 G, 12.0 G, 9.8 G for HBG1,HL1,MBG3,MDG2,PBG1,PDG1, PDG3 respectively. Microwave irradiation did not cause significant differences in ESR spectra. Long term stability tests performed for 25 kGy gamma irradiated samples have indicated that *8% of HBG1, 68% of HL1, 8% of MBG3, 38% of MDG2, 12% of PBG1, 75% of PDG1* and *33% of PDG3* decayed approximately during 1 month of storage process held at room temperature and atmospheric pressure. As conclusion, *HL1* and *PDG3* could be considered to be a good radiosensitive and radioresistive material, respectively.

Acknowledgment: Authors would like to acknowledge to Osteobiol ,Biohorizine and Botiss for valuable gifts of dermal and bone grafts. This study was supported by H.U. B.A.B. Project No: 12866.

IONIZING-RADIATION INDUCED SYNTHESIS OF POLY(VINYLPYRROLIDONE) NANOHYDROGELS AS DRUG DELIVERY SYSTEMS AND THE IMPLEMENTATION OF MRI CONTRAST AGENTS

Devyn Catterton[1], Zois Tsinas[1], Dianne L. Poster[2], David Grills[3], James Wishart[3], and Mohamad Al-Sheikhly[1]

[1] Department of Materials Science and Engineering, University of Maryland, College Park, MD, USA
[2] National Institute of Standards and Technology, Gaithersburg, MD, USA
[3] Brookhaven National Laboratory, Upton, NY, USA

Nanoparticles and especially nanohydrogels have been of interest to the scientific community as drug delivery agents due to their many potential benefits, including, targeted drug release, relatively low levels of toxicity, evasion of the reticulo-endothelial system, low shear modulus, and compatibility in aqueous systems making them ideal for intravenous administration. Further, by using ionizing-radiation, nanohydrogels can be synthesized without the use of any toxic chemicals and materials will be sterile, making them viable for *in vivo* applications. We are investigating the radiation induced synthesis of a biocompatible polymer, poly(vinyl)pyrrolidone (PVP), in dilute aqueous solutions using an electron beam. It has already been shown that at temperatures above 60˚C, PVP chains collapse due to the disruption of the polymer-water hydrogen bonding, resulting in an overall smaller hydrodynamic radius, R_h. By decreasing the overall R_h value, we aim to decrease the distances between the carbon-centered radicals, along the backbone of the chain. The formation of these c-centered radicals is a result of abstraction of H-atoms by the radiolytically produced OH from radiolysis of water. The intra crosslinking reactions between free radicals on the same polymer chain, leads to a decrease of R_h, and produces the nanogel structure. Dynamic light scattering (DLS) analysis to determine the hydrodynamic radius prior to and following irradiation of the PVP aqueous solutions was performed. Different conditions were studied using a low and high molecular weight PVP at various concentrations and temperatures. Additionally, irradiation conditions were optimized to enhance the intra-crosslinking versus the inter-crosslinking reactions. DLS results showed that low concentrations of PVP irradiated at low doses and dose rates, at temperatures above 60 °C, favors the intra-crosslinking reactions. Ultimately, scanning electron microscopy (SEM) analysis with the use of ionic liquid solutions was used to evaluate the DLS results and the size of the nanohydrogels when in solution. Current work aims to investigate the use of nanohydrogels as MRI contrast agents by incorporating gadolinium in the polymeric matrix. The overall methods and materials of this system will be presented, as well as a discussion of the role of temperature, molecular weight, and concentration in the formation of nanohydrogels.

EXCITED STATES AND ELECTRONIC COUPLING EXPLORED BY PULSE RADIOLYSIS

Andrew R. Cook[1], Anthony Grimonti, Paiboon Sreearunothai, Sada Asaoka, Michal Valášek,
Alison M. Funston, Pavel Poliakov, Josef Michl, J. R. Miller

[1]*Brookhaven National Laboratory, Bldg. 555 Chemistry, Upton NY 11973*

Pulse radiolysis provides powerful, and often unique, tools for the study of excited states and coupling of both closed and open shell molecules. These studies can provide important information on the nature of excited states and molecular structure. In this poster I will show two recent examples from our group.

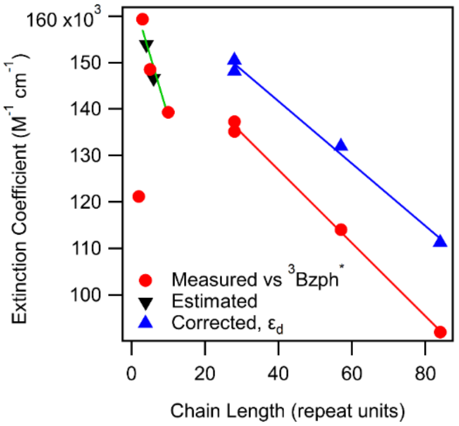

Triplet excited states of polyfluorenes were explored, determining spectra and extinction coefficients as a function of chain length. A common assertion is that conjugated polymer properties develop as chain length increases, becoming constant at long length. This was not found in the current case for the T_1-T_n extinction coefficient (see figure), though the integral of the absorption spectrum (oscillator strength) did increase linearly with length until 10 fluorene units. The decrease in ε with chain lengths exceeding 3 fluorene units is understood primarily by broadening of absorption spectra, but also by chain defects for chains longer than 16 units. The broadened spectra were unexpected, but provide insight into the nature of the polymer triplets. While it is natural to think of an excited state as a stationary object, the broadened spectra are best explained by motion of the triplet along the chain, which produces a larger range of geometries and absorption energies as chain length increases. A simple model was used to qualitatively explain these results, with a surprising conclusion that triplets move at nearly the same rate on polyfluorenes as singlets.

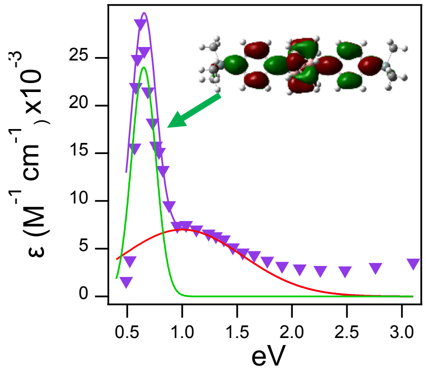

Electronic coupling, H_{ab}, through *p*-carborane spacers has been reported to be weak with singlet excited states. Our experiments with anions of 12-vertex oligomers (1-3 units) of carboranes, some with phenyl endgroups, paint a very different picture. Pulse radiolysis in THF produced radical anions, determined redox potentials by equilibria and measured their absorption spectra. One case (see figure), showed both Robin-Day class II (broad, 1.0 eV) and III (sharp, 0.6 eV) absorptions. The class III transition resulted from a fully delocalized excess electron across both benzene rings and the central carborane. In other cases with more than ~1/2 of the excess electron localized on a carborane, large cage distortions were triggered, resulting in class II transitions with massive reorganization energies. In both cases, H_{ab} ~ 0.5 eV between either a carborane cage and a phenyl ring or two carborane cages. Results provide evidence for effective "carborane conjugation" in radical anions that might be exploited in molecular wire materials or molecular electronics, which are classically composed of all π–conjugated molecules. Carboranes might be better considered as small resistors in π -conjugated chains, with coupling intermediate between alkane and π–conjugated bridge molecules. They also present a unique ability to maintain the magnitude of coupling as they rotate, while preserving the rigid-rod nature of conjugated polymers.

ION INDUCED STRUCTURAL CHANGES IN GRAPHITE

Lenore S. Miller[1], John Derek Demaree[2], Kristopher D Behler[2,3], Weigang Lu[1], Zhiping Luo[1], and Daryush Ila[1]

[1]Department of Chemistry and Physics, Fayetteville State University, Fayetteville NC 28301, United States
[2]Weapons and Materials Research Directorate, US Army Research Laboratory, Aberdeen Proving Ground MD 21005, United States
[3]SURVICE Engineering Company, Belcamp MD 21017, United States

We have studied changes in the surface of graphite before and after 1.45 MeV Au bombardment, to assess the effect of highly ionizing bombardment on the topography and atomic bonding of carbon in graphitic materials, using Atomic Force Microscopy (AFM), x-ray photoelectron spectroscopy (XPS), Raman spectroscopy, and 3D laser microscopy. The hexagonal carbon ring structure of graphene sheets in graphite were observed using AFM, to assess any changes in carbon bond length or distortion of the hexagonal lattice due to the passage of the heavily ionizing particles. Rutherford Backscattering Spectrometry (RBS) in conjunction with XPS were used to identify impurities in the material and at the surface, and their potential impact on graphite surface properties. RBS was used because most impurities are significantly heavier than carbon, and therefore they can be easily detected and quantified without any need for substrate background subtraction. XPS was used to confirm the RBS findings, and identify any differences in the distribution of impurities in the bulk and at the surface of the material before and after MeV implantation. Ion induced changes in carbon bonding, including the transformation of graphitic sp2 bonding to amorphous or diamond-like sp3 bonds were measured using Raman spectroscopy, a transformation which may be explained by rapid thermal quenching following ion-induced excitation.

AZO FUNCTIONALIZED, HYDROPHILIC FABRICS FOR THE EXTRACTION OF URANIUM FROM SEAWATER

Travis C. Dietz[1], ZoisTsinas[1], Ileana M. Pazos[2], Eli Fastow[1], Weixing Li[3], Fred Bateman[2], Dianne Poster[2], David Grills[4], Mohammad Adel-Hadadi[3], Aaron Barkatt[3], James Wishart[4], and Mohamad Al-Shiekhly[1]

[1]*Department of Materials Science and Engineering, Univ. of Maryland, College Park, MD;*

[2]*National Institute of Standards and Technology, Gaithersburg, MD;*

[3]*Department of Chemistry, The Catholic University of America, DC;*

[4]*Brookhaven National Laboratory, Upton, NY*

The world's oceans contain a relatively uniform uranium concentration of about 3 μg/L. While this appears to be an exceedingly small concentration, the total quantity of uranium throughout the world's oceans is on the order of 1000 times higher than presently known in terrestrial deposits. In order to take advantage of this immense resource to support the nuclear energy industry for years to come, a co-polymer system produced by attaching a monomer capable of extracting uranium from seawater to a durable polymer substrate has been developed. A class of azo monomers were chosen for extraction experiments due to their high affinity for uranium. This was shown in preliminary testing through the use of activated charcoal loaded with said compounds where they were shown to remove more than 90 wt. % of the total uranium in a 0.2 mg U/L solution. The fabrics were irradiated using an electron beam, wherein radicals were generated on the surface of the substrate to initiate radical polymerization. By themselves, the azo compounds could not be grafted using radiation directly; they had to be chemically attached to the surface of the fabrics after a chemical precursor, vinylbenzyl chloride (VBC), had been grafted. The fabrics were characterized with attenuated total reflectance Fourier transform infrared spectroscopy and energy dispersive X-ray spectroscopy in order to verify the attachment. These fabrics were then exposed to uranium-doped seawater solutions for a set period of time, after which the remaining solution was tested for the quantity of uranium left in solution using a spectrophotometric method and inductively coupled plasma mass spectrometry. Initially, the azo grafted fabrics extracted about 10 wt. % of uranium in solution. This was likely due to the hydrophobic nature of the azo groups, which prevented access of the uranium-carrying seawater to the azo binding sites. To correct for this, acidic monomers were co-grafted with the VBC precursor and then the co-grafted fabrics were chemically treated to attach the azo groups. The acid-azo functionalized fabrics were able to extract more than 70 wt. % of uranium in 0.2 mg U/L seawater solution after being rotated in the solution for nine days. This extraction efficiency is still lower than that achieved by the charcoal experiments, indicating that the fabrication of the adsorbents can be further optimized.

UNDERSTANDING GENERATION OF MULTIFUNCTIONAL NANOGELS IN CHEMICAL-FREE EBEAM IRRADIATION SYNTHESIS

Lorena Anna Ditta,[1] Björn Dahlgren[2], Maria Antonietta Sabatino[1], Mats Jonsson[2],
Clelia Dispenza[1]

[1] *Università degli Studi di Palermo, Viale delle Scienze, Edificio 6, 90128 Palermo, Italy*
[2] *KTH Royal Institute of Technology, SE-100 44 Stockholm, Sweden*

Radiation engineered nanogels are the core of very promising theranostic nanodevices.[1-3] They can be produced starting from aqueous solutions of chemically inert polymers by pulsed e-beam irradiation. Both size and functionality can be controlled by an appropriate choice of the ionising irradiation conditions, polymer concentration and gaseous atmosphere. Recent research activities have been devoted to investigate the mechanism that leads to the formation of poly(N-vinyl pyrrolidone) nanogels functionalised with carboxyl groups, primary amines and double bonds. Experimental syntheses with two different set-ups and the relative products characterisations have been combined with numerical simulations of the radiation chemistry of the aqueous systems exposed to the specific pulsed irradiations used in the experiments. The controlling reactions for functional group formation are discussed and mechanistic insights are derived.

A novel, simple and effective methodology for double bond quantification is also proposed.

References

(1) Dispenza, C, Spadaro G., Jonsson M. Radiation Engineering of Multifunctional Nanogels. Top Curr Chem (Z) **2016**, *374*, 69.

(2) Dispenza, C., Sabatino, M.A., Ajovalasit, A., Ditta, L.A., Ragusa, M., Purrello, M., Costa, V., Conigliaro, A., Alessandro, R. Nanogel-antimiR-31 conjugates affect colon cancer cells behaviour. RSC Adv. **2017**, *7(82)*, 52039-52047.

(3) Picone, P., Sabatino, M.A., Ditta L.A., Amato, A., San Biagio, P.L., Mulè, F., Giacomazza, D., Dispenza, C, Di Carlo M. Nose-to-brain delivery of insulin enhanced by a nanogel carrier. J Control. Rel. **2018**, *270*, 23-36.

Acknowledgments

This research is carried out as part of the IAEA CRP F22064 “Nanosized delivery systems for radiopharmaceuticals”.
The Authors wish to thank the Centre for Radiation Research and Technology, Institute of Nuclear Chemistry and Technology, Warsaw, Poland for their collaboration.

NEW EXPERIMENTS: NEUTRON/PROTON RADIOLYSIS OF WATER UP TO 350 °C

G. L. Draper[1], A. Baidak, S. M. Shubeita, H. E. Sims, R. M. Orr

[1]*University of Manchester, Oxford Rd, Manchester M13 9PL, UK*

A detailed understanding of the radiolysis of water under PWR operating conditions (280 to 325 °C; 200 bar) is vital for the successful modelling and control of PWR primary coolant chemistry. Water radiolysis yields the oxidising species OH and H_2O_2, which without proper control may enhance the corrosion of reactor components. The past fifty years have seen numerous groups researching high temperature water radiolysis; most efforts have focussed on the contribution of low LET radiation (gammas, electrons) to the observed yields of primary radiolysis products. Few have attempted to quantify the contribution of neutron radiolysis to the overall yields.

A group at the University of Manchester, UK is investigating numerous aspects of PWR chemistry. One facet of this project is the measurement of primary yields of radiolysis products arising from neutron radiolysis at temperatures up to 350 °C. Protons from the 5 MeV Pelletron accelerator at the Dalton Cumbrian Facility are used to simulate neutron radiolysis in a water sample. Yields are measured using scavengers to convert short-lived reducing radicals into stable gaseous products which can be detected by GC-MS. Initial experiments have concentrated on validating the preliminary yield results against established standards; the long term aim of this project is to measure yields as a function of both temperature and proton energy. We will showcase the method developed for these experiments, discuss the experimental challenges we have faced thus far, and present our newest results.

RADIOLYSIS OF WOOD SACCHARIDES, OLIGOSACCHARIDES, POLYSACCHARIDES AND LIGNIN

Mark S. Driscoll[1], Jay LaVerne[2], Mohamad Al-Sheikhly[3], Dianne Poster[4]

[1] *State University of New York College of Environmental Science and Forestry, Syracuse, NY, USA*
[2] *University of Notre Dame, Notre Dame, IN, USA*
[3] *University of Maryland, College Park, MD, USA*
[4] *National Institute of Standards and Technology (NIST), Gaithersburg, MD, USA*

Wood and other lignocellulosic materials are natural and renewable materials made of three main polymers; cellulose, hemicellulose and lignin. Cellulose is the most abundant natural polymer on earth with hemicellulose and lignin being 2nd and 3rd respectively. Cellulose and hemicellulose are both polysaccharides while lignin is a crosslinked phenolic polymer. While wood is very abundant it has little use outside the lumber and paper industries. This lack of use is due to the recalcitrance of the material, meaning wood is difficult to brake about into its individual useable components. Many different pretreatment techniques have be developed for wood but they are either highly energy intensive and/or require the use of toxic chemicals. Ionizing radiation has been studied as a pretreatment process for a wood based bio refinery for the production of fuels and chemicals. Ionizing radiation treatment of wood chips has been shown to increase the amount of hemicellulose and lignin removed from the chips by hot water extraction. Ionizing radiation treatment has also been shown to decrease the molecular mass of cellulose leading to more efficient hydrolysis to glucose. To try and better understand the process of wood irradiation, g-values were determined for cellulose, micro crystalline cellulose, cellulose oligomers, xylan, organosolv lignin, cottonwood, glucose and amylopectin. When possible both crystalline and amorphous versions of the compounds were studied. Also investigated was the "protective effect" that lignin has on cellulose and hemicellulose in wood.

INCREASED HIGHWAY LIFE VIA ELECTRON BEAM INITIATED POLYMER MODIFICATION

Slavica Grdanovska[1], Charlie Cooper[1], Ben C. Cox[2]

[1] *Illinois Accelerator Research Center, Fermi National Accelerator Laboratory*
[2] *Army Corps of Engineers, Engineering Research and Development Center*

Current roads, constructed of bituminous asphalt, require maintenance and repair that costs over $50 billion per year while still facing application and longevity issues. Efforts to improve roads by chemical modification have had only limited success because the resulting highways still suffer from rapid aging. Enhancing strength properties of bitumen by means of electron beam induced polymer modification could reduce or prevent crack initiation and propagation in pavements due to various weather conditions and heavy loads.[1,2] Using mobile electron beam accelerators mounted in trucks, to do in situ modification of bitumen to yield a material that is both strong and durable as well as resistant to cracking during thermal cycles, can double the lifetimes of some pavements.[3] This method will essentially increase the efficiency of road construction and future repairs. The advantages of extended life pavements include a substantial decrease in use of heavy machinery for repairs; decreased fuel usage and carbon footprint; and decreased energy use. For roadways specifically, increased road lifetime also means reductions in fuel use and commuter wait times in traffic due to highway repairs and increased workable lifetime of the hot mix asphalt.

Electron beam initiated crosslinking and polymerization of materials lead to increased strength and toughness. The amount of crosslinking and subsequent material properties can be precisely controlled by the electron beam exposure time. The electron penetration depth in the product is determined by its energy which in asphalt is around 2 cm. While the initial energy deposited is important, further electron interactions within the polymer would promote additional chemistry to be driven deeper in the system.

Figure 1 - Truck-Mounted Compact SRF Accelerator for Pavement Application

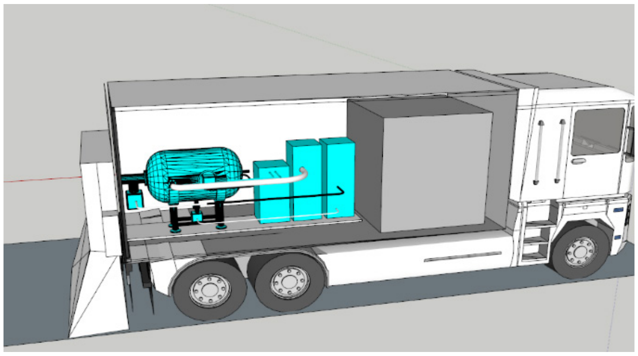

At present, electron beam processing is conducted using an accelerator in a fixed location. Development in accelerator technology allows for the construction of efficient, compact, high-power, high-energy and mobile electron linear accelerators. This work focuses on treating several bitumen-polymer formulations at various dose rates and total doses to improve material properties and produce feasible bitumen products for road use.

(1) Cardone, F.; Ferrotti, G.; Frigio, F.; Canestrari, F. Influence of Polymer Modification on Asphalt Binder Dynamic and Steady Flow Viscosities. *Construction and Building Materials* **2014**, *71*, 435–443.
(2) Becker, Y.; Méndez, M. P.; Rodríguez, Y. Polymer Modified Asphalt. *Vision Tecnologica* **2001**, 39–50.
(3) Kephart, R. Method and System for In-Situ Cross Linking of Polymers, Bitumen and Similar Materials to Increase Strength, Toughness and Durability via Irradiation with Electron Beams from Mobile Accelerators. *US 9,340,931 B2*, May 17, **2016**.

RADIOLYSIS OF HYDROGEN PEROXIDE ASSOCIATED WITH ALUMINUM OXIDE

Kazuhiro Iwamatsu[1], Jay A. LaVerne[1]

[1]*Radiation Laboratory, University of Notre Dame, Notre Dame IN 46556*

The reaction of water radiolysis species at metal oxide surfaces is a major problem in the nuclear field, such as reactor safety and the storage of nuclear waste materials. Radiation energy is absorbed not only by water but also by these metals that initiate reactions at the surface. Hydrogen peroxide (H_2O_2) is one of the important species in surface reactions, because it is a major water radiolysis product and the main species that causes corrosion of reactor surfaces. The surface reaction in the radiation field is complicated, therefore, more fundamental information should be obtained. This work examines the behavior of H_2O_2 associated with Al_2O_3.

Concentrations of H_2O_2 decreased as absorbed dose increased in all conditions. They reached steady state concentration at high dose without Al_2O_3, while they decreased to zero with any amount of Al_2O_3 as shown in the Figure. Formation of H_2O_2 was observed in the case of a mixture of 25 mM nitrate and Al_2O_3 in spite of no formation of H_2O_2 with ultra-pure water and Al_2O_3 shown in inset. Nitrate scavenges hydrated electrons preventing their reaction with H_2O_2 in neat water radiolysis. There is no difference in H_2O_2 formation with and without Al_2O_3, therefore "$H_2O_2 + e_{aq}^-$" is the main decay reaction of H_2O_2 in neat water and with a mixture of Al_2O_3. Decomposition reactions due to electrons were employed in a simulation model and a few surface reactions were scrutinized. Simulation results could not reproduce experimental results using only the surface reaction of H_2O_2. With considering the surface reaction of O_2^- which is derived from dissociation of $HO_2^\bullet$ due to its pKa value (pKa = 4.57), experimental results could be reproduced by the simulation result.

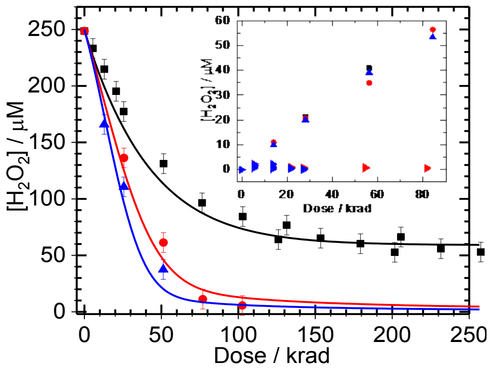

Concentration of H_2O_2 as a function of absorbed dose in the mixture of H_2O_2 and (■) 0 g, (●) 0.5 g, (▲) 1.0 g of Al_2O_3, (solid lines) model calculations. Inset: Evolution of H_2O_2 in the mixture of 25 mM Nitrate and (■) 0 g, (●) 0.5 g, (▲) 1.0 g of Al_2O_3, mixtuire of ultra-pure water and (▶) 0.5 g, (▶) 1.0 g of Al_2O_3

References

(1) Pastina, B. and aVerne, J.; *J. Phys. Chem.* A 2001, **105**, 9316.
(2) Hiroki, A. and LaVerne, J.; *J. Phys. Chem.* B 2005, **109**, 3364
(3) Iwamatsu, K., Sandin, S. and LaVerne, J.; *Radiat. Phys. Chem.*, 2018, **145**, 207

THE ROLE OF SURFACE-BOUND HYDROXYL RADICALS IN RADIATION INDUCED DISSOLUTION OF UO_2

Alexandre Barreiro Fidalgo[1], Yuta Kumagai[2], Björn Dahlgren[1] and Mats Jonsson[1]

[1]*Department of Chemistry, Applied Physical Chemistry, KTH Royal Institute of Technology, SE-100 44 Stockholm, Sweden*
[2]*Japan Atomic Energy Agency, Nuclear Science and Engineering Directorate, 2-4 Shirane Shirakata, Tokai-mura, Nakagun, Ibaraki 319-1195, Japan*

Radiation induced dissolution of UO_2-based nuclear fuel is a key-process in the safety assessment of geological repositories for spent nuclear fuel. It is essential that simulations carried out to support the safety assessment are based on correct descriptions of the reaction mechanisms. In recent years, one of the key-issues has been the mechanism of the reaction between the radiolysis product H_2O_2 and UO_2, in particular the role of surface-bound hydroxyl radicals proposed to be formed upon surface catalyzed decomposition of H_2O_2. In this work we have studied the nature of this proposed intermediate. Experiments were performed to study the kinetics of H_2O_2 consumption and uranium dissolution at different initial H_2O_2-concentrations. The kinetic analysis of the H_2O_2-consumption implies that the initial rate can be described by the Freundlich adsorption isotherm. Further analysis of the kinetics reveal that the consumption rates for a given H_2O_2 concentration were different depending on the initial H_2O_2 concentration. This is attributed to an alteration of the reactive interface, likely caused by blocking of surface sites by oxidized U/surface-bound hydroxyl radicals. The dissolution yield given by the amount of dissolved uranium divided by the amount of consumed hydrogen peroxide was used to compare the different cases. For all initial H_2O_2-concentrations the dissolution yield increases with reaction time. The final dissolution yield decreases with increasing initial H_2O_2-concentration. This is expected from the mechanism of catalytic decomposition of H_2O_2 on oxide surfaces. As the experiments were performed in solutions containing 10 mM HCO_3^- and a strong H_2O_2-concentration dependence was observed in the 0.2-2.0 mM H_2O_2-concentration range, we conclude that the intermediate hydroxyl radical is surface bound rather than free. In view of the results presented here, the possible difference in reaction mechanism between H_2O_2-decomposition on redox sensitive metal oxides and metal oxides where the metal ion is already in its highest oxidation state is discussed. The mechanistic findings are also included in numerical simulations of radiation-induced dissolution of UO_2. The impact of the updated mechanism on the kinetics of uranium dissolution is analyzed and discussed.

NOVEL SYSTEM FOR PULSE RADIOLYSIS WITH MULTIANGLE LIGHT SCATTERING DETECTION (PR-MALLS)

S. Kadłubowski[1], P. Sawicki, S. Sowiński, J.M. Rosiak, P. Ulański

[1]Lodz University of Technology, Institute of Applied Radiation Chemistry, Wroblewskiego 15,
93-590 Lodz, POLAND

Time-resolved pulse radiolysis, utilizing short pulses of high-energy electrons from accelerators, is an effective method for rapidly generating free radicals and other transient species in solution. Combined with fast time-resolved spectroscopic detection (typically in the ultraviolet/ visible/ near-infrared), it is invaluable for monitoring the reactivity of species subjected to radiolysis on timescales ranging from picoseconds to seconds. When used for polymer solutions, pulse radiolysis can be coupled with light-scattering detection, creating a powerful tool for kinetic and mechanistic analysis of processes like degradation or crosslinking of macromolecules. Changes in the light scattering intensity (LSI) of polymer solutions are indicative of alterations in the molecular weight and/or in the radius of gyration, i.e., the dimensions and shape of the macromolecules. In addition to other detection methods, LSI technique provides a convenient tool to study radiation-induced alterations in macromolecules as a function of time after the pulse. Prerequisite for the application of the LSI method is the property of a polymer to scatter light of a given wavelength much stronger than the neat solvent. First attempts to combine light scattering technique and pulse radiolysis were made by Schnabel et al. in 1970's.[1] Second system of this type has been built at the Institute of Applied Radiation Chemistry (IARC) in Lodz by Rosiak and co-workers.[2] Both of them were measuring intensity of light scattered at one (right) angle. Another setup, constructed at the Max-Planck-Institute for Radiation Chemistry, was able to detect scattered light at a single low angle.[3] Nowadays an advanced pulse radiolysis & multi-angle light-scattering-intensity system is being built at IARC. Idea of its operation and preliminary results will be shown. Implementation of the proposed system will provide a novel research tool, which is expected to contribute to the expansion of knowledge on free-radical reactions in monomer- and polymer solutions, by delivering precise kinetic data on changes in molecular weight and size, and thus allowing to formulate or verify reaction mechanisms. The proposed method is universal and can be applied for studying both natural and synthetic polymers. The developed system can be also valuable in studies of the border of biology and medicine, especially on radical reactions of biopolymers and their conformational transitions. Furthermore, capability to follow fast changes in mass and dimensions of nanoobjects may be of significant importance for nanoscience and nanotechnology.

References

(1) Tabata Y. Pulse Radiolysis; CRC Press, Boca Roton, 1991
(2) Lubis R.; Olejniczak J.; Rosiak J.; Kroh J. System for Measurements of Changes of LSI in Polymer Solution after Electron Pulse. Radiat. Phys. Chem. 1990, 36, 249-252.
(3) Adinarayana M.; Bothe E.; Schulte-Frohlinde D. Hydroxyl radical-induced strand break formation in single-stranded polynucleotides and single-stranded DNA in aqueous solution as measured by light scattering and by conductivity. Int. J. Radiat. Biol. 1988, 54, 723-737.

Acknowledgements. This project was supported by the National Science Centre, Poland (grant no. 2012/07/B/ST4/01429)

RADIATION GRAFTING OF IONIC LIQUIDS TO SYNTHESIZE POLYMER ELECTROLYTE MEMBRANES FOR FUEL CELL OPERATION ABOVE 100°C

Kevin Mecadon[1], Mohamad Al-Shiekhly[1], Fred Bateman[2], and Joseph Robertson[2]

[1] *Department of Materials Science and Engineering, University of Maryland,*
College Park, MD, USA
[2] *National Institute of Standards and Technology, Gaithersburg, MD, USA*

The purpose of this project is to design, synthesize and analyze innovative anhydrous fuel cell membranes that can operate at temperatures above 100°C. Operating at this higher temperature region improves performance and reliability of fuel cells: increasing proton mobility, enhancing reaction kinetics, increasing catalysis activity and reducing carbon monoxide poisoning. Traditional polymer electrolyte membrane fuel cells (PEMFCs) are not able to operate above 100°C because water is used as a proton conductive medium though the Grotthuss hopping mechanism. Through substituting water with protic ionic liquids we have developed a new proton conductive network solid state PEMs that can perform at high temperature by grafting ionic liquids systems into fluorocarbon thin films. Polymers were selected for grafting to develop membranes with the following properties: high proton conductivity, low electrical conductivity, high mechanical properties, high chemical resistance, and high temperature and humidity stability. The method used to synthesize anhydrous polymer electrolyte membranes (PEMs) was radiation grafting using heterocyclic protic ionic liquid monomers and fluorocarbon substrates. The goal was to produce solid state proton conducting PEMs that do not rely on water for proton conductivity and can operate at high temperatures. PEMs were synthesized at The Medical Industrial Radiation Facilities (MIRF) at the National Institute of Standards and Technology (NIST). MIRF is a 10 MeV electron beam accelerator, which was used to indirectly radiation graft heterocyclic protic ionic liquids onto fluorocarbon substrates to create PEMs. After samples were irradiated, free radicals were generated in the fluorocarbon substrates which acted as grafting sites. Then, ionic liquid monomers were added to the sample which grafted and polymerized at the free radicals sites. Samples were then placed in an oven for a post heat treatment to promote monomer diffusion and bulk grafting. This method produced PEM that had proton conductive ionic liquids solid state network grafted to a fluorocarbon backbone. After synthesis, the extent and uniformity of PEM composition was analyzed using FTIR microscopy, SEM/EDS, SANS and their proton conductivity measured using 2 point probe EIS.

Through this study we have shown that indirect radiation grafting can be used to successfully graft ionic liquids onto fluorocarbon substrates to synthesize PEMs. The resulting ionic liquid PEMs showed high proton conductivity above 100°C and behaved independent of humidity. Our ionic liquid PEMs also showed a positive correlation of increasing proton conductivity with temperature above 100°C even after the PEMs are completely dehydrated. The chemical properties and structure of the grafted ionic liquids greatly effects the proton conductive mechanisms present in the PEMs. These trends found through the course of this research will help the development of future anhydrous PEM with higher proton conductivity, performance, and reliability.

ION INDUCED STRUCTURAL CHANGES IN GRAPHITE

Lenore S. Miller[1], John Derek Demaree[2], Kristopher D Behler[3,4], Weigang Lu[1], Zhiping Luo[1], Daryush Ila[1]

(1)Department of Chemistry and Physics, Fayetteville State University, Fayetteville NC 28301, United States
(2)Weapons and Materials Research Directorate, US Army Research Laboratory, Aberdeen Proving Ground MD 21005, United States
(3)Weapons and Materials Research Directorate, US Army Research Laboratory, Aberdeen Proving Ground MD 21005, United States
(4)SURVICE Engineering Company, Belcamp MD 21017, United States

We have studied changes in the surface of graphite before and after 1.45 MeV Au bombardment, to assess the effect of highly ionizing bombardment on the topography and atomic bonding of carbon in graphitic materials, using Atomic Force Microscopy (AFM), x-ray photoelectron spectroscopy (XPS), Raman spectroscopy, and 3D laser microscopy. The hexagonal carbon ring structure of graphene sheets in graphite were observed using AFM, to assess any changes in carbon bond length or distortion of the hexagonal lattice due to the passage of the heavily ionizing particles. Rutherford Backscattering Spectrometry (RBS) in conjunction with XPS were used to identify impurities in the material and at the surface, and their potential impact on graphite surface properties. RBS was used because most impurities are significantly heavier than carbon, and therefore they can be easily detected and quantified without any need for substrate background subtraction. XPS was used to confirm the RBS findings, and identify any differences in the distribution of impurities in the bulk and at the surface of the material before and after MeV implantation. Ion induced changes in carbon bonding, including the transformation of graphitic sp2 bonding to amorphous or diamond-like sp3 bonds were measured using Raman spectroscopy, a transformation which may be explained by rapid thermal quenching following ion-induced excitation.

AU@TIO$_2$ FABRICATED THROUGH X-RAY RADIOLYSIS AND THEIR APPLICATION AS POTENTIAL RADIOSENSITIZERS

M.C. Molina Higgins[1]

[1]*Mechanical and Nuclear Engineering, Virginia Commonwealth University, 401 West Main St, Richmond, Virginia 23284-306730. molinahiggimc@vcu.edu*

Research on methods that enhance the absorbed dose in tumors are of valuable interest in radiotherapy as they may reduce the collateral damage to healthy tissue. One of these techniques is radiosensitization where nanomaterials are used to increase radiation effectiveness during treatment. This work aims to produce and evaluate gold-titania (Au@TiO$_2$) nanocomposites (NCs), for its use as potential radiosensitizers. Au@TiO$_2$ NCs were fabricated using X-rays, a method that departs from traditional synthesis and provides low by-product formation, which is fundamental for medical applications. Au NPs were supported on TiO$_2$ with either particle size distributions of 5-10 nm or 10-30 nm, using different ligands such as NaOH or urea and under different absorbed doses ranging from 0.1 KGy to 7.6 KGy, in order to determine the effects of these parameters in the final Au nanoparticle size and loading. The use of high absorbed doses (7.6 KGy) produced Au particles of 1.1 ± 0.1 nm, herein the size was not affected by the choice of ligand, meanwhile at low absorbed doses (0.72 KGy) the ligand affected the Au particle size, resulting in a size reduction of 20% when NaOH was used. The radiosensitization assessment of Au@TiO$_2$ NCs was made by monitoring the decomposition of a Methylene Blue (MB) solution under X-rays in the presence of Au@TiO$_2$ NCs. The dye containing the nanomaterial was irradiated at different operating voltages (50 KV and 225 KV) and results showed that the presence of Au@TiO$_2$ NCs increased MB decomposition rate by a factor of ~ 3.8.

DOSE RATE EFFECT ON THE DEPOLYMERIZATION OF CELLULOSE

Lisa Paulsen[1], Mark S. Driscoll[1*], Arthur J. Stipanovic[1], Fred B. Bateman[2] and Ileana Posaz[2]

[1]*State University of New York College of Environmental Science and Forestry, Syracuse, NY, USA*
[2]*National Institute of Standards and Technology (NIST), Gaithersburg, MD, USA*

In recent years, interest in using lignocellulosic biomass to produce renewable fuels instead of traditional corn-based ethanol has increased as the environmental concerns, socio-political disputes, and the 'food vs. fuel' debate for corn-based ethanol has risen. One type of fast growing lignocellulosic biomass is shrub willow (*Salix* spp.). Willow is of particular interest because of its ease of cultivation and harvesting, ability to grow in a variety of marginal lands, and especially its high net energy ratio due to the low input (pesticides, fertilizers, etc.) requirements for growth. Because of the recalcitrance of woody biomass, it is necessary to exploit a pretreatment method to increase the activity of enzymes in creating fermentable sugars. One measure of recalcitrance is the crystallinity of cellulose, a primary component of wood. We have shown that the crystallinity for pure isolated microcrystalline cellulose decreases with increasing EBI dose. In the present study, willow chips with bark were irradiated over a dose range of 100 - 500 kGy. Two extractions, mild hot-water and 1% NaOH, were completed on irradiated samples to identify which method was most effective in reducing the crystallinity of cellulose and removing hemicelluloses as determined by Thermogravimetric Analysis (TGA). Our work showed an increase in removal of hemicelluloses and a decrease in cellulose crystallinity with increasing EBI under both extraction conditions. Also, enzymatic hydrolysis results showed an increase in sugar yields with increased EBI dose. The effect of EBI on willow match the experimental data shown for sugar maple and purified components of wood, including increased solubility, decreased cellulose crystallinity, and increased fermentable sugar yields upon enzymatic hydrolysis. This suggests that EBI on wood samples is a promising pretreatment method.

EFFECT OF Β-DIKETO GROUP MODIFICATION OF CURCUMIN ON ANTIOXIDANT ACTIVITY AND FREE RADICAL REACTIONS: CORRELATED WITH COMPUTATIONAL STUDIES

Shaukat Ali M. Shaikh[1], Beena G. Singh[1], Atanu Barik[1], Gottumukkala V. Subbaraju[2], Devidas B. Naik[1], K. Indira Priyadarsini[3]

[1]Radiation & Photochemistry Division, Bhabha Atomic Research Centre, Trombay, Mumbai-400085, India
[2]Natsol Laboratories, J.N.Pharmacity, Visakhapatnam-531019, India
[3]Chemistry Division, Bhabha Atomic Research Centre, Trombay, Mumbai-400085, India

Curcumin (CU), a polyphenol from C*urcuma longa* shows diverse pharmacological activities. It has limited therapeutic utility due to low bioavailability and degradation in aqueous solution. To overcome this, isoxazole (CI) and pyrazole (CP) derivatives were synthesized by modifying its β-diketo moiety. Herein we report the effect of the β-diketo modification on the free radical reactions of CP/CI/CU with different oxidizing free radicals. Reaction of CU, CP and CI with azide ($N_3^{\bullet}$) and trichloromethyl peroxyl ($CCl_3O_2^{\bullet}$) radicals, studied by pulse radiolysis technique, showed formation of phenoxyl radicals absorbing at 490, 410 and 380 nm, respectively, with reaction rate constants in the order $k_{CP} > k_{CI} \approx k_{CU}$. Similarly, the reaction with 2,2-diphenyl-1-picrylhydrazyl ($DPPH^{\bullet}$) radical showed IC_{50} value following the order of CU < CI ≈ CP. To address the differential antioxidant activity, the reaction was carried out in acidic medium, where the IC_{50} values showed a reverse trend and increased in the order CP < CI < CU. This differential antioxidant behaviour of CP/CI/CU was explained by molecular descriptors like adiabatic ionization potential (AIP), highest occupied molecular orbital level and spin population. The results indicated that reactions of CP, CI and CU with $N_3^{\bullet}$ and $CCl_3O_2^{\bullet}$ radicals was controlled by AIP values, while the reactivity with $DPPH^{\bullet}$ radicals was controlled by anionic concentration of the polyphenol and pK_a of the radicals. The study thus provides a new route for designing novel curcumin derivative with desired properties.

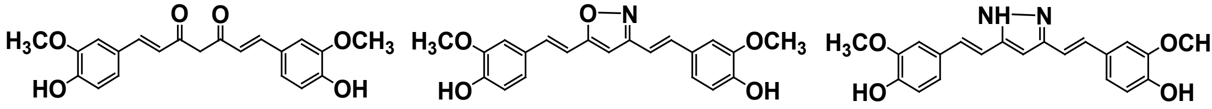

Curcumin
[CU]

Curcumin isoxazole
[CI]

Curcumin pyrazole
[CP]

Scheme - The chemical structures of CU, CI and CP

References

(1) Meo, F. D.; Lemaur, V.; C, Jerome; Lazzaroni, R.; Duroux, J.; Olivier, Yoann.; Trouillas, P. *J. Phys. Chem. A* **2013**, *117*, 2082-2092.

(2) Shaikh, S. M.; Barik, A.; Singh, B. G.; Modukuri, R. V.; Balaji, N. V.; Subbaraju, G. V.; Naik, D. B.; Priyadarsin, K. I. *Free Rad. Res.* **2016**, *50*, 1361-1373.

RADICAL PROCESSES INVOLVING QUINOXALIN-2-ONE DERIVATIVES RELEVANT TO THEIR PHARMACOLOGICAL APPLICATIONS

K. Skotnicki[1], K. Bobrowski[1], J. De la Fuente[2], A. Cañete[3]

[1]*Institute of Nuclear Chemistry and Technology, Warsaw, Poland*
[2]*Universidad de Chile, Santiago de Chile, Chile*
[3]*Pontificia Universidad Católica de Chile, Chile*

Quinoxaline derivatives gained a great deal of attention, mostly due to their biological activity. They are concerned as a potential anticancer, antimicrobial, antifungal and anxiolytic drugs as well as inhibitors of enzymes activity.

In the first stage, spectral and kinetic properties of quinoxalin-2-one one-electron oxidation and reduction products have been characterized. In the context of potential quinoxalin-2-one interactions with protein receptors the second stage of research have focused on elucidation of radical processes involving quinoxalin-2-ones and selected amino acids. I have confirmed that tryptophan and tyrosine can be oxidized by products of quinoxalin-2-ones $N_3^\bullet$ oxidation products, yielding tryptophyl and tyrosyl radicals respectively. On the other hand 3-methylquinoxalin-2-one can be reduced by α-aminoalkyl radicals produced by means of $^\bullet$OH oxidation of methionine. Second order reaction rates have been measured for aforementioned reactions with several C7-substituted quinoxalin-2-one derivatives.

In the final stage I have for the first time characterized spectral and kinetic properties of caroverine hydrochloride derived radicals. What is more, second-order rate constants have been measured for their reactions with Trp and Tyr. I have also confirmed the possibility of caroverine hydrochloride reduction by α-aminoalkyl radicals from Met.

In this work I have utilize pulse radiolysis technique based on linear electron accelerator, combined with UV-Vis spectrophotometry.

DEXTRAN-BASED HYDROGELS FOR BIOMEDICAL APPLICATIONS – RADIATION-INITIATED SYNTHESIS AND CHARACTERIZATION

Kamila J. Szafulera[1], Radoslaw A. Wach, Piotr Ulanski

[1]Lodz University of Technology, Institute of Applied Radiation Chemistry, Wróblewskiego 15,
90-001 Łódź, Poland

Current scientific literature reports a number of applications for polysaccharides in biomedical field. Biopolymers are known for excellent biocompatibility and biodegradability. Many of them are able to support biological processes making polysaccharides a component of bioactive wound dressings. Additionally, submicron-size polysaccharide hydrogels can be considered as drug delivery systems (DDS).

The current work was aimed to synthesize a dextran derivative having substituents capable of covalent crosslinking (Dex-MA – dextran methacrylate), and to develop conditions suitable for formation of macroscopic and nano/microgels using ionizing radiation. Unquestionable advantage of using radiation is possibility of processing materials in any physical state, typically with no use of additional chemicals. Dex-MA has been synthesized by coupling glycidyl methacrylate with dextran. A series of Dex-MA solutions (degree of substitution - DS ~ 0.1–1) was treated by electron beam at different concentration and wide range of doses. Crosslinking of Dex-MA in aqueous solutions was found to be an efficient process. The effect of crosslinking (intra- or intercrosslinking) is dependent on the DS and concentration. Synthesized macroscopic hydrogels were thoroughly characterized – the gel fraction and the equilibrium degree of swelling were determined. Irradiation at lower concentrations resulted in intracrosslinked nano- and microgels. Moreover, cytotoxicity tests were performed. Cytocompatibility of Dex-MA of DS below 1 was demonstrated.

The collected results suggested that radiation processing of Dex-MA is very promising and the obtained final forms of hydrogels are expected to find applications as biomaterials used either in regenerative medicine or as DDS.

SPECTRAL SHIFT OF SOLVATED ELECTRONS IN A MIXTURE OF IONIC LIQUIDS AT LOW TEMPERATURES

Kenji Takahashi[1], Surajdevprakash B. Dhiman[2], Koji Osawa[2], and James F. Wishart[2]

[1]*Kanazawa University, Kanazawa 920-1192, Japan*
[2]*Brookhaven National Laboratory, New York 11973-5000, USA*

The solvated electron in room temperature ionic liquids has been the subject of several investigations and several reports exist on its nature and absorption spectrum. Here we report on the behavior of the excess electron in a 1:1 mole ratio mixture of the ionic liquids 1-butyl-1-methylpyrrolidinium bis(trifluoromethylsulfonyl)imide (P_{14} NTf_2), and 1-decyl-1-methylpyrrolidinium bis(trifluoromethylsulfonyl)imide (P_{110} NTf_2), using picosecond pulse radiolysis with 2-ns detection. We used this ionic liquid mixture with two different sizes of cations in order to suppress the freezing point below the glass transition temperature so that we could investigate solvation dynamics at quite low temperatures. We also measured the yields of solvated electrons at several low temperatures. Temperature-dependent studies reveal that the yield of the solvated electron decreases with decreasing temperature, due to a highly reactive pre-solvated electron and slow solvation dynamics. These low temperature investigations also grant access to the solvation dynamics of the electron in the ionic liquids. These findings provide new information that will guide a new generation of ionic liquids applications.

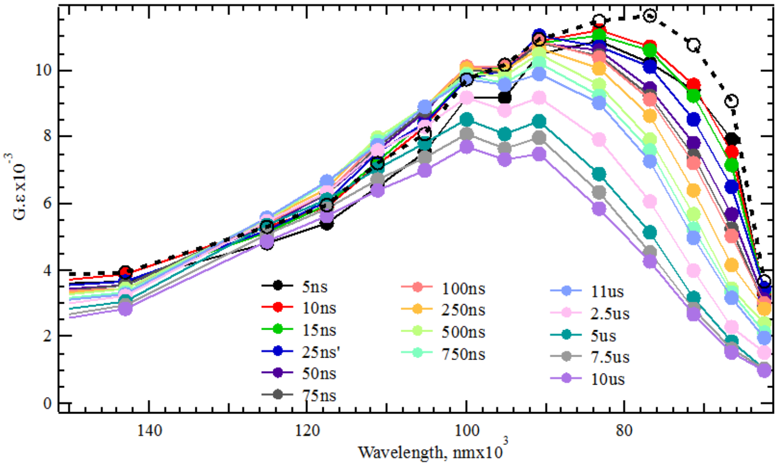

Figure 1 - Time-resolved absorption spectra of the solvated electron at -50 ˚C.

GAMMA RADIATION FOR THE DEVELOPMENT OF MICROSTRUCTURED PVA/GELATIN BASED SCAFFOLDS FOR CONTROLLED RELEASE OF PLATELET RICH PLASMA

Justine P. R. O. Varca[1], André Ferrari[1], Caroline S. A. de Lima[1], Kamila M. Nogueira[1], Gustavo H. C. Varca[1], Monica B. Mathor[1], Ademar B. Lugão[1]

[1]*Nuclear and Energy Research Institute – IPEN-CNEN/SP, Brazil*

Gelatin is a natural polymer originated from the collagen and presents poor mechanical properties. However, it is a natural and biocompatible polymer which is the main component of the extracellular matrix.[1] Polyvinyl alcohol is an artificial polymer with interesting mechanical properties and biocompatibility. Such polymers have been largely studied for biomedical applications.[2] Platelet Rich Plasma (PRP) has been widely explored in many medical fields over the last decades especially in orthopedic area and for athletic treatments.[3] Based on the PRP applications for tissue regeneration, the present work aimed the development of a scaffold for the controlled release of PRP for wound treatments, as well as study the influence of different radiation doses on the scaffold formation. The scaffold was prepared based on two formulations, one composed by gelatin (7%, w/w) and PVA (5%, w/w), and the second by gelatin (10%, w/w) and PVA (5%, w/w). The formulations were separately solubilized in distilled water and heated up to 80 ºC under constant stirring for 1 hour. Posteriorly, both blends were disposed in circular glass moulds. The samples were cooled at 4 ºC for at least 24 h and then irradiated at 15, 25 and 50 kGy using a 5 $kGy.h^{-1}$ dose rate. After irradiation the samples were frozen and freeze dried. The scaffold was characterized in terms of structure and morphology by mechanical assays, differential scanning calorimetry, scanning electron microscopy, optical coherence tomography and infrared spectroscopy. In addition, platelet adhesion and release, and cytotoxic assays were also performed. Samples irradiated at 15 kGy presented pore size diameter of around 1.4 µm and porosity of 54%, while samples irradiated at 25 kGy, presented pore size diameter of around 1.1 µm and porosity of 49%. Optical coherence tomography showed that gelatin control samples presented more superficial degradation as irradiation dose increased, while PVA control sample presented higher integrity, indicating that this polymer is less sensitive to gamma radiation. The system presented suitable mechanical properties and the platelet adhesion and release assays showed that the scaffold presented adequate pore size range to host and release the platelets, and non-cytotoxic to platelets, featuring adequate properties to be applied as dressing for wound treatments.

Key words: scaffold, polymers, pore size, gamma radiation, platelet rich plasma.

(1) X. Wu, Y. Liu, X. Li, Y. Zhang, Y. Long, X. Wang, Y. Guo, F. Xing, J. Gao. Preparation of aligned porous gelatin scaffolds by unidirectional freeze-drying method. Acta Biomat., **2010**, 6, 1167-1117.

(2) M. Ye, P. Mohanty, G. Ghosh. Morphology and properties of poly vinyl alcohol (PVA) scaffolds: Impact of process variables. Mat. Sci. and Engin. C, **2014**, 42, 289-294.

(3) A. Rienzi, A. Miller, I. Cuevas. Plasma rico en plaquetas – Indicaciones en lesiones deportivas. Tend. en Med., **2016**, 48, 111, 145-151.

REACTIONS INDUCED ON THE RADIATION IN TRIBUTYL PHOSPHATE STUDIED BY PICOSECOND PULSE RADIOLYSIS

Furong Wang[1], Gregory P. Horne[2], Pascal Pernot, Pierre Archirel and Mehran Mostafavi[1]

[1]*Laboratoire de Chimie Physique, CNRS/Université Paris-Sud, Bâtiment 349, 91405 Orsay, France*

[2]*Idaho National Laboratory, 1955 N. Fremont Ave., Idaho Falls, Idaho 83415, United States*

Tributyl phosphate (TBP) is the key extractant used in current spent nuclear fuel solvent extraction reprocessing schemes for the recovery of uranium and plutonium.[1–4] Under process conditions, TBP is exposed to a high intensity multi-component radiation field, undergoing radiolytic degradation. As TBP is typically used as a 30 vol. % solution diluted by a suitable organic diluent (e.g. dodecane or odourless kerosene), it is subject to both direct and indirect radiation effects, ultimately liberating a number of detrimental degradation products.[5,6]

The behavior of neat Tributyl phosphate (TBP) under ionizing radiation was studied with 7 ps electron pulse of 7 MeV kinetics energy. The solvated electron in neat TBP exhibits a very broad absorption band in visible and near IR (NIR) and its maximum is beyond t 1500 nm. Nitromethane and biphenyl are used to scavenge e_s^- to determine the absorption spectra and he molar extinction coefficient of the absorption band of e_s^- in TBP, respectively. The time dependent yield of e_s^- has been determined from 7 ps to 7 ns and compared with that in water, THF and Diethyl carbonate. Another absorption band in found in the visible range. The kinetics analysis shows that this species, in contrast to e_s^-, is stable up to 7 ns. The DFT calculations showed that the absorption in visible is due the triplet state of TBP* formed by the electron pulse.

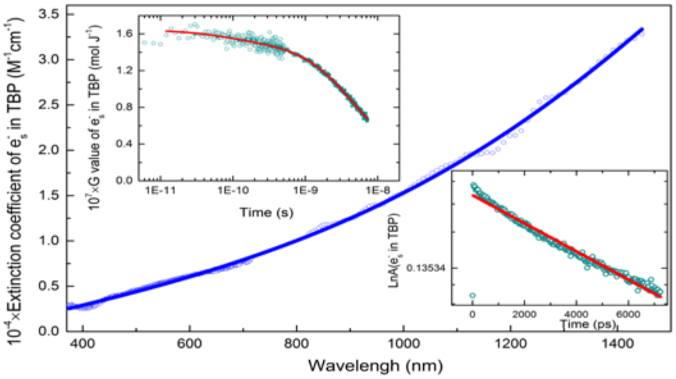

***Figure 1** - Molar extinction coefficient of e_s^- in TBP. The insets are time dependent radiolytic yield of e_s^- in TBP (upper-left) and the the kinetics of e_s^- in logistic (bottom-right).*

References

(1) Schulz, W. W.; Navratil, J. D.; Talbot, A. E. *Science and Technology of Tributyl Phosphate Volume 1*; CRC Press: Bosa Roca, United States, 1984.
(2) Schulz, W. W.; Navratil, J. D. *Science and Technology of Tributyl Phosphate Volume 2*; CRC Press: Bosa Roca, United States, 1987.
(3) Schulz, W. W.; Navratil, J. D. *Science and Technology of Tributyl Phosphate Volume 3*; CRC Press: Bosa Roca, United States, 1990.
(4) Wick, O. J. *Plutonium Handbook, A Guide to the Technology – Volumes 1 & 2*; The American Nuclear Society, 1980.
(5) MOYER, B. A. *Ion Exchange and Solvent Extraction: A Series of Advances, Volume 19*; CRC Press, 2017.
(6) Mincher, B. J.; Modolo, G.; Mezyk, S. P. Review Article: The Effects of Radiation Chemistry on Solvent Extraction: 1. Conditions in Acidic Solution and a Review of TBP Radiolysis. *Solvent Extr. Ion Exch.* **2009**, *27* (1), 1–25.

RADIOLYTIC HYDROGEN PRODUCTION FROM THE WATER RADIOLYSIS IN CSH

YIN, C.[1], DANNOUX-PAPIN, A.[1], HAAS, J.[1], NGONO-RAVACHE, Y.[2], RENAULT, J-P.[3]

[1]CEA, DEN, MAR, DE2D, SEAD, Laboratoire d'études des Ciments et Bitumes pour le Conditionnement, 30207 Bagnols sur Cèze Cedex, France
[2]CIMAP, UMR CEA-CNRS-ENSICAEN-USBN, BP5133, 14070 Caen Cedex 5, France,
[3]CEA, DRF, IRAMIS, NIMBE, Université Paris Saclay, 91191 Gif-sur-Yvette Cedex, France

Water radiolysis is one of the consequences of the interaction between a cementitious matrix and low or intermediate-level radioactive wastes that are encapsulated within this matrix.[1] Thus, for safety assessment, the hydrogen released from the cementitious packages must be limited and quantified.

Up to now, the hydrogen production was thought to arise solely from the water trapped in the cement porous network.[3,4] However, recent experimental and theoretical indication suggest that the cement paste itself can play a significant role in H2 production.[2]

Calcium silicate hydrate (C-S-H) is the main hydrate (70%) of Portland cement. This present work is focused on the interactions between water and C-S-H, a nanocrystallized product with a layered chemical structure. The aim of this study is to understand the radiolytic mechanisms of the hydrogen production in hydrated C-S-H.

Therefore, after characterization by several techniques (nitrogen gas adsorption-desorption, X-ray diffraction, thermogravimetric analysis, infrared and Raman spectroscopies, small-angle X-ray scattering), C-S-H with different chemical composition and cured at different controlled relative humidities were submitted to gamma radiation and heavy ions beams to determine their H_2 radiolytic yield, $G(H_2)$[i]. The results show the H_2 production is strongly modified in highly confined system in comparison to the bulk water.

The EPR spectroscopy experiments using trapping molecules are in progress to reveal the reaction mechanisms involved. The present work would help us to understand the radiation effects in confined media and particularly in cements.

References

(1) Spinks, J. W. T.; Woods, R. J., An introduction to radiation chemistry. **1990**.

(2) Le Caër, S.; Dezerald, L.; Boukari, K.; Lainé, M.; Taupin, S.; Kavanagh, R. M.; Johnston, C. S. N.; Foy, E.; Charpentier, T.; Krakowiak, K. J.; Pellenq, R. J. M.; Ulm, F. J.; Tribello, G. A.; Kohanoff, J.; Saúl, A., Production of H2 by water radiolysis in cement paste under electron irradiation: A joint experimental and theoretical study. *Cement and Concrete Research* **2017,** *100* (Supplement C), 110-118;

(3) Bouniol, P.; Bjergbakke, E., A comprehensive model to describe radiolytic processes in cement medium. *Journal of Nuclear Materials* **2008,** *372* (1), 1-15;

(4) Bouniol, P.; Muzeau, B.; Dauvois, V., Experimental evidence of the influence of iron on pore water radiolysis in cement-based materials. *Journal of Nuclear Materials* **2013,** *437* (1), 208-215.

---

[i] *$G(H_2)$ represents the amount of H_2 produced per energy unit deposited in the system. It is expressed in $mol.J^{-1}$.*

HIGH RESOLUTION DOSIMETRY FOR STERILIZATION OF SENSITIVE ELECTRONICS

Vu Le, Byron Lambert, Johnathan Manion, Dom Patel, Scott Dalton

Healthcare innovation has led to a growing number of combination products which can introduce complexities for sterilization if one or more components or products within the package are sensitive to radiation sterilization. The next generation of medical devices will include a large market for wearables. Electronic components for these wearables will be the biggest challenge for the radiation sterilization process. The assessment of maximum acceptable doses of each electronic component must be determined within a much smaller footprint of the device. This requires a high resolution dosimetry process.

A distribution of dose can be measured to a single pixel through a scanned image of a dosimeter film using the Risoscan software.[1] Each pixel represents a dose in the cross section of the dosimeter in both x and y axis as seen in Figure 1. This capability combined with known maximum acceptable doses of components and unique load configurations can optimize the likelihood of using radiation sterilization for combination devices with sensitive electrical components.

An assessment of radiation sensitivity of thermistors, capacitors, and integrated circuits was performed. Thermistors and resistors saw no change when irradiated at doses between 0.2 to 49 kGy. The integrated circuits were irradiated at a target dose of < 1 kGy and the results demonstrated increased variability in performance. The total budget of drift was monitored across several parameters to identify a max dose of approximately 0.13 kGy accounting for uncertainty from process development of dosimetry films. Sensitive components can be shielded or re-located to a distance away from the source where less dose is delivered and maximum acceptable dose can be managed to maximize product performance.

Figure 1.

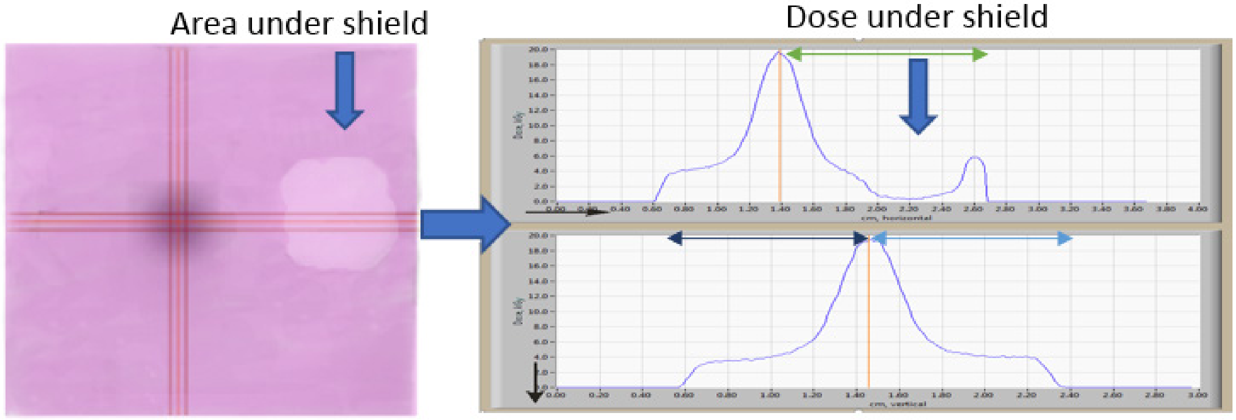

References

(1) Helt-Hansen, J., Miller A. 2004. RisoScan – a new dosimetry software. Radiat. Phys. Chem.71, 359-362.

ICIP-2018 List of Participants

Amitava Adhikary adhikary@oakland.edu
Oakland University
318 Meadow Brook Rd, Rochester, MI 48309

Abimbola Oluseyi Akinbuwa-Onwueme lagosstate.government@yahoo.com
Lagos State Ministry of Health
Unity Road, Ikeja, Lagos, Nigeria

Guadalupe Albarrán albarran@nucleares.unam.mx
Universidad Nacional Autónoma de México
Av Universidad 3000, Cd. Universitaria, Coyoacán,
04510 Ciudad de México, CDMX, Mexico

Mohamad Al-Sheikhly mohamad@umd.edu
University of Maryland College Park
4418 Stadium Drive, College Park, MD 20742

Saharnaz Bargh saharnaz_gil@yahoo.ca
Hacettepe Universitesi Eczacilik Fakultesi,
Radyofarmasi ABD
Hacettepe, 06230 Altındağ/Ankara, Turkey

David Bartels bartels.5@nd.edu
Notre Dame Radiation Laboratory
Notre Dame, IN 46556

Fred Bateman fbb@nist.gov
National Institute of Standards and Technology
100 Bureau Dr, Gaithersburg, MD 20899

David Becker dbecker@oakland.edu
Oakland University
318 Meadow Brook Rd, Rochester, MI 48309

Yuri Berlin berlin@northwestern.edu
Northwestern University
633 Clark St, Evanston, IL 60208

Matthew Bird mbird@bnl.gov
Brookhaven National Laboratory
98 Rochester St, Upton, NY 11973

Krzysztof Bobrowski kris@ichtj.pl
Institute of Nuclear Chemistry and Technology
Dorodna 16, 03-195 Warszawa, Poland

Devyn Catterton dcatt@terpmail.umd.edu
University of Maryland, College Park
4418 Stadium Drive, College Park, MD 20742

Andrzej Chmielewski A.Chmielewski@ichtj.waw.pl
Instytut Chemii i Techniki Jądrowej
Dorodna 16, 03-195 Warszawa, Poland

David Close closed@etsu.edu
East Tennessee State University
1276 Gilbreath Dr, Johnson City, TN 37614

Andrew Cook acook@bnl.gov
Brookhaven National Lab
98 Rochester St, Upton, NY 11973

Xavier Coqueret xavier.coqueret@univ-reims.fr
Universite de Reims Champagne-Ardenne
9 Boulevard de la Paix, 51100 Reims, France

Gustavo Henrique Costa Varca varca@usp.br
Nuclear and Energy Research Institute - IPEN-CNEN/SP
Jardim Universidade Pinheiros, de, Av. Prof. Lineu Prestes, 2242 - Butantã, São Paulo - SP, 05508-000, Brazil

Benjamin Coughlin benjamin.coughlin@tufts.edu
Tufts University
419 Boston Ave, Medford, MA 02155

Fred Currell f.j.currell@qub.ac.uk
The University of Manchester
Oxford Rd, Manchester M13 9PL, UK

John Demaree
john.d.demaree.civ@mail.mil
US Army Research Lab
2800 Powder Mill Rd, Adelphi, MD 20783

Travis Dietz
tcdietz@umd.edu
University of Maryland College Park
4418 Stadium Drive, College Park, MD 20742

Clelia Dispenza
clelia.dispenza@unipa.it
Università degli Studi di Palermo
Piazza Marina, 61, 90133 Palermo PA, Italy

Gemma Draper
gemma.draper@postgrad.manchester.ac.uk
University of Manchester
Oxford Rd, Manchester M13 9PL, UK

Mark Driscoll
mdriscol@esf.edu
State University of New York College of
Environmental Science and Forestry
1 Forestry Dr, Syracuse, NY 13210

Brendan Dromey
b.dromey@qub.ac.uk
Queen's University Belfast
University Rd, Belfast BT7 1NN, UK

Amanda Forster
amanda.forster@nist.gov
National Institute of Standards and Technology
100 Bureau Dr, Gaithersburg, MD 20899

Sara Goldstein
sara.goldstein1@mail.huji.ac.il
Hebrew University
Givat Ram, Jerusalem, 91904 Israel

Slavica Grdanovska
slavica@fnal.gov
Fermilab
Pine Street and, Kirk Rd, Batavia, IL 60510

David Grills
dcgrills@bnl.gov
Brookhaven National Laboratory
98 Rochester St, Upton, NY 11973

Weiyao Gu State University of New York College of Environmental Science and Forestry 1 Forestry Dr, Syracuse, NY 13210	wgu100@syr.edu
Noel Guardala George Washington University 2121 I St NW, Washington, DC 20052	nguardala76@gwu.edu
Dirk Guldi University of Erlangen Schloßplatz 4, 91054 Erlangen, Germany	dirk.guldi@fau.de
Alexander Harris Brookhaven National Laboratory 98 Rochester St, Upton, NY 11973	alexh@bnl.gov
Gregory Horne Idaho National Laboratory 2525 Fremont Ave, Idaho Falls, ID 83402	gregory.horne@inl.gov
Christopher Howard Nordion University Endowment Lands, BC, Canada	chris.howard@nordion.com
Reggie Hudson NASA Goddard Space Flight Center 8800 Greenbelt Rd, Greenbelt, MD 20771	reggie.hudson@nasa.gov
Patricia Huestis University of Notre Dame Notre Dame, IN 46556	phuestis@nd.edu
Liam Isherwood University of Manchester Oxford Rd, Manchester M13 9PL, UK	liam.isherwood@postgrad.manchester.ac.uk
Kazuhiro Iwamatsu University of Notre Dame Notre Dame, IN 46556	iwamatsu.1@nd.edu

Mats Jonsson
matsj@kth.se
KTH Royal Institute of Technology
Brinellvägen 8, 114 28 Stockholm, Sweden

Slawomir Kadlubowski
slawekka@mitr.p.lodz.pl
Lodz University of Technology
Stefana Żeromskiego 116, 90-924 Łódź, Poland

Eaman Karim
etakarim@umd.edu
University of Maryland College Park
4418 Stadium Drive, College Park, MD 20742

Byron Lambert
byron.lambert@abbott.com
Abbott Vascular
26531 Ynez Rd, Temecula, CA 92591

Jay LaVerne
laverne.1@nd.edu
University of Notre Dame
Notre Dame, IN 46556

Sophie LE CAER
sophie.le-caer@cea.fr
Paris Saclay University
CEA SaclayDRF/IRAMIS/NIMBE UMR
3685/LIONS, Bâtiment 546, F-91191 Gif-sur-Yvette
Cedex France

Richard Livingston
rliving1@umd.edu
University of Maryland College Park
4418 Stadium Drive, College Park, MD 20742

Jun MA
ma.jun.26m@st.kyoto-u.ac.jp
Kyoto University
Yoshidahonmachi, Sakyo Ward, Kyoto, Kyoto
Prefecture 606-8501, Japan

Eric Maimon
emymon1@gmail.com
Nuclear Research Center Negev
POB 9001, Beer-Sheva, 84190, Israel

Stuart Maloy
maloy@lanl.gov
Los Alamos National Laboratory
New Mexico 87545

Bronislaw Marciniak
marcinia@amu.edu.pl
Adam Mickiewicz University
Wieniawskiego 1, 61-712 Poznań, Poland

Kevin Mecadon
kmecadon@gmail.com
University of Maryland College Park
4418 Stadium Drive, College Park, MD 20742

David Meeker
dsm17d@my.fsu.edu
Florida State University
600 W College Ave, Tallahassee, FL 32306

Dan Meyerstein
danm@ariel.ac.il
Ariel University & Ben-Gurion University
Ariel University, Ariel 40700 Israel

Stephen Mezyk
Stephen.Mezyk@csulb.edu
California State University
1250 Bellflower Boulevard, Long Beach, CA 90840
USA

John Miller
jrmiller@bnl.gov
Brookhaven National Lab
98 Rochester St, Upton, NY 11973

Lenore Miller
lmille16@broncos.uncfsu.edu
Fayetteville State University
1200 Murchison Rd, Fayetteville, NC 28301

Maria Molina Higgins
molinahiggimc@vcu.edu
Virginia Commonwealth University
Richmond, VA 23284

Kim Morehouse
kim.morehouse@fda.hhs.gov
U.S. Food and Drug Administration
57 New Hampshire Ave, Silver Spring, MD 20993

mehran mostafavi
mehran.mostafavi@u-psud.fr
Université Paris-Sud
15 Rue Georges Clemenceau, 91400 Orsay, France

Justine Paula Oliveira Varca justinepaula@usp.br
Nuclear and Energy Research Institute
Jardim Universidade Pinheiros, de, Av. Prof. Lineu
Prestes, 2242 - Butantã, São Paulo - SP, 05508-000,
Brazil

Asuman Yekta Ozer yktzer@yahoo.com
Hacettepe Universitesi Eczacilik Fakultesi,
Radyofarmasi ABD
Hacettepe, 06230 Altındağ/Ankara, Turkey

Lisa Paulsen ltpaulse@syr.edu
State University of New York College of
Environmental Science and Forestry
1 Forestry Dr, Syracuse, NY 13210

Gary Pertmer pertmer@umd.edu
University of Maryland College Park
College Park, MD 20742

Dean Peterman dean.peterman@inl.gov
Idaho National Laboratory
2525 Fremont Ave, Idaho Falls, ID 83402

Alejandro Ramos-Ballesteros alejandro.ramos@correo.nucleares.unam.mx
National Autonomous University of Mexico
Av Universidad 3000, Cd. Universitaria, Coyoacán,
04510 Ciudad de México, CDMX, Mexico

Joey Robertson joey.robertson@nist.gov
National Institute of Standards and Technology
100 Bureau Dr, Gaithersburg, MD 20899

Jessika Rojas jvrojas@vcu.edu
Virginia Commonwealth University
Richmond, VA 23284

Christian Schoneich schoneic@ku.edu
University of Kansas
1450 Jayhawk Blvd, Lawrence, KS 66045

Benjamin Schwartz
schwartz@chem.ucla.edu
University of California, Los Angeles
Los Angeles, CA 90095

Shaukat Ali Shaikh
shaukatali.shaikh92@gmail.com
Bhabha Atomic Research Centre
Radiation and Photochemistry Division, Trombay,
Mumbai, Maharashtra, 400085 India

Konrad Skotnicki
k.skotnicki@ichtj.waw.pl
Institute of Nuclear Chemistry and Technology
Dorodna 16, 03-195 Warszawa, Poland

Marisa Smith
marisa.smith@manchester.ac.uk
The University of Manchester
Oxford Rd, Manchester M13 9PL, UK

Sebastian Sowiński
ssowinski@mitr.p.lodz.pl
Institute of Applied Radiation Chemistry, Faculty of
Chemistry, Lodz University of Technology
Wróblewskiego 15, 90-001 Łódź, Poland

Steven Swarts
sgswarts@ufl.edu
University of Florida
Gainesville, FL 32611

Kamila Szafulera
kszafulera@mitr.p.lodz.pl
Lodz University of Technology, Institute of Applied
Radiation Chemistry
Wróblewskiego 15, 90-001 Łódź, Poland

Kenji Takahashi
ktkenji@staff.kanazawa-u.ac.jp
Kanazawa University
Japan, 〒920-1192 Ishikawa Prefecture, Kanazawa,
角間町

Fuh-Wei Tang
fuh-wei.tang@abbott.com
Abbott Vascular
26531 Ynez Rd, Temecula, CA 92591

Maria Eugenia Toimil Molares
m.e.toimilmolares@gsi.de
GSI Helmholtz Center for Heavy Ion Research
Planckstr. 1, Darmstadt, 64342 Germany

Ronald Tosh
rtosh@nist.gov
National Institute of Standards and Technology
100 Bureau Dr, Gaithersburg, MD 20899

Zois Tsinas
zstsinas@hotmail.com
University of Maryland College Park
College Park, MD 20742

Furong WANG
furong.wang@u-psud.fr
Laboratoire de Chimie Physique, Université Paris Sud
310 Rue Michel Magat, 91400 Orsay, France

Mei Wang
mwang122@umd.edu
University of Maryland College Park
College Park, MD 20742

James Wishart
wishart@bnl.gov
Brookhaven National Laboratory
98 Rochester St, Upton, NY 11973

Taylor Woehl
tjwoehl@umd.edu
University of Maryland College Park
College Park, MD 20742

Chengying Yin
ycying0229@gmail.com
French Alternative Energies and Atomic Energy Commission
Marcoule, Bagnols-sur-cèze, 30200 France

Yoichi Yoshida
yoshida@sanken.osaka-u.ac.jp
Osaka University
1-1 Yamadaoka, Suita, Osaka Prefecture 565-0871, Japan

	Sunday, July 22nd	Monday, July 23rd	Tuesday, July 24th	Wednesday, July 25th	Thursday, July 26th	Friday, July 27th
07:00		Breakfast	Breakfast	Breakfast	Breakfast	
07:15						
07:30						
07:45						
08:00		S. Mezyk	M.E. Toimil-Molares	D. Demaree	A. Chmielewski	Breakfast
08:15						
08:30		B. Dromey	D. Guldi	M. Nasef	C. Howard	
08:45						
09:00		S. Le Caër	G. Horne	J. Rojas	J. Robertson	K. Bobrowski
09:15						
09:30		D. Meyerstein	D. Grills		T. Woehl	A. Adhikary
09:45						
10:00		Coffee break	Coffee break	Coffee break	Coffee break	Coffee break
10:15		X. Coqueret	J. Miller	Young Investigator Presentations 2	K. Morehouse	Closing Remarks
10:30						
10:45		G. Varca	Y. Yoshida		F. Bateman	
11:00						
11:15		B. Schwartz	S. Goldstein		D. Peterman	
11:30						
11:45			F. Currell		M. Bird	
12:00						
12:15		Lunch on your own	Lunch on your own	Lunch on your own	Lunch on your own	
12:30						
12:45						
13:00						Airport Shuttle Departs for IAD
13:15						Airport Shuttle Departs for DCA
13:30						Airport Shuttle Departs for BWI
13:45						
14:00		Free Time	Poster Session	R. Livingston	C. Schoneich	
14:15						
14:30				F. Tang	D. Becker	
14:45						
15:00	Registration (will be open through Monday)			R. Tosh	Y. Berlin	Airport Shuttle Departs for IAD
15:15						Airport Shuttle Departs for DCA
15:30		Coffee break	Coffee break	Coffee break	M. Mostafavi	Airport Shuttle Departs for BWI
15:45		S. Maloy	Young Investigator Presentations 1	Poster Session		
16:00					Coffee break	
16:15		J. Weaver			ICIP Business Meeting	
16:30						
16:45		E. Karim			Poster Session	
17:00						
17:15		N. Guardala				
17:30					Proceed to Buddy's for the Banquet	
17:45						
18:00	Welcome Reception	Dinner on your own	Dinner on your own	Dinner on your own	Banquet Dinner at Buddy's (provided)	
18:15						
18:30						
18:45						
19:00						
19:15						
19:30						
19:45						
20:00	D. Bartels					
20:15						
20:30	A. Forster					
20:45						
		Fundamental Processes	Radiation Chemistry in Service of Energy Applications	Synthesis of Materials with Radiation	Radiation Effects on Biological Systems	
		Interfaces and Nuclear Applications	Consequences of Highly Mobile Transient Species	Advances in Methods and their Applications		